CZECH TECHNICAL UNIVERSITY IN PRAGUE

Faculty of Civil Engineering

Department of Architectural Engineering

Translucent composite slabs from high-performance concrete with optical fibers - technical solution and analysis

DOCTORAL THESIS

Nikola Štochl

Doctoral study programme: Civil Engineering

Branch of study: Building Engineering

Doctoral thesis tutor: prof. Ing. Petr Hájek, CSc., FEng.

Prague, 2023

CZECH TECHNICAL UNIVERSITY IN PRAGUE
Faculty of Civil Engineering
Thákurova 7, 166 29 Praha 6

DECLARATION

Ph.D. student's name: Nikola Štochl

Title of the doctoral thesis: Translucent composite slabs from high-performance concrete with optical fibers - technical solution and analysis

I hereby declare that this doctoral thesis is my own work and effort written under the guidance of the tutor prof. Ing. Petr Hájek, CSc., FEng.
All sources and other materials used have been quoted in the list of references.

The doctoral thesis was written in connection with research on the project: -

In Prague on 30. 3. 2023

signature

Acknowledgements

The work with measurement results was created as part of the doctoral thesis at the Czech Technical University. This experiment was materially supported by Czech construction companies Metrostav a.s. and TBG Metrostav s.r.o. The study is partially funded by institutional research at the Czech Technical University. I want to thank the Faculty of Civil Engineering CTU in Prague for co-financing instruments for measuring illumination and for the leasing of them. My main thanks go to Prof. Ing. Petr Hájek, CSc., FEng. for his professional guidance during my studies and for the preparation of my doctoral thesis. I would like to thank Ing. Tomáš Vlach, Ph.D. for his expert guidance during the work in the laboratory and Ing. Bc. Jaroslav Vychytil, Ph.D. for his expert support and guidance during the measurement of light parameters of light-transmitting slabs. Special thanks go to my colleague Ing. Kateřina Horníková, who helped me with the production of samples.

https://doi.org/10.14311/dis.fsv.2023.004

Abstract in Czech

Průsvitný beton jako stavební materiál již existuje v mnoha podobách, ale jeho světelné vlastnosti a možnosti jeho využití pro zlepšení osvětlení vnitřních prostorů nebyly dosud podrobně prozkoumány. Tato práce se zaměřuje na osvětlení vnitřních prostorů a prostupu světla pomocí konstrukcí ze světlo-propustného betonu. Provedená experimentální měření jsou rozdělena do dvou modelových situací s využitím zmenšených modelů místností. První část práce se zaměřuje na osvětlení místnosti prostřednictvím prostupu denního světla skrze stropní konstrukci ze světlo-propustného betonu. Druhá část práce zkoumá přenos světelné informace z umělého zdroje světla z jedné místnosti do druhé přes nenosnou dělící konstrukci složenou z unifikovaných desek ze světlo-propustného betonu. Pro experimenty bylo vytvořeno několik modelů a vzorků pro porovnání. Prvním krokem experimentu bylo vytvoření desek ze světlo-propustného betonu. Ačkoli existuje mnoho možností, jak takovou desku vyrobit, nejlepší variantou je použití vysokohodnotného betonu s výztuží ze skleněných vláken, která zlepšují vlastnosti přenosu zatížení, a plastových optických vláken pro přenos světla. Přidáním optických vláken můžeme dosáhnout přenosu světla mezi libovolnými dvěma prostory. Pro obě části experimentů jsme použili zmenšené modely místností. Desky o rozměrech 250x250x20 mm a 250x250x30 mm byly použity ve třech variantách: betonové desky s optickými vlákny, betonové desky se vzduchovými otvory a plné desky. V rámci experimentu byla měřena a porovnávána úroveň osvětlení v několika bodech modelu při průchodu každou ze tří různých desek. Na základě výsledků těchto experimentů byl učiněn závěr, že úroveň osvětlení interiéru jakéhokoli prostoru lze zlepšit použitím betonu propouštějícího světlo, zejména těch, které nemají přístup k přirozenému světlu. V rámci experimentu byly rovněž posouzeny pevnostní vlastnosti desek ve vztahu k jejich zamýšlenému použití a porovnány s vlastnostmi kamenných desek standardně používaných jako obklad.

Keywords in Czech

Světlo-propustný beton; plastová optická vlákna; světlo-propustná konstrukce; průsvitný beton; světlo-vedoucí beton; skleněná vlákna, vysokohodnotný beton

Abstract in English

Light transmitting concrete as a building material already exists in many forms, but its light properties and the possibilities of using it to improve the lighting of interior spaces, have not been investigated in detail yet. This work focused on the illumination of interior spaces using constructions made of light-transmitting concrete, which will allow light to pass between individual spaces. The experimental measurements carried out are divided into two typical situations using reduced room models. The first part of the work measured the light parameters of the room through the penetration of daylight through the ceiling from light-transmitting concrete. The second part of the work investigated the transmission of artificial light from one room to another through a non-load-bearing dividing structure composed of unified slabs of light-transmitting concrete. For the experiments, several models and samples were created for comparison. The first step of the experiment was to create slabs of light-transmitting concrete. While there are many options to produce such a slab, the best option is to use high-performance concrete with glass fibers reinforcement, which improve the load transfer properties, and plastic optical fibers for light transmission. By adding optical fibers, we can achieve the transmission of light between any two spaces. For both parts of the experiments, we used reduced scale models of rooms. Slabs with dimensions of 250x250x20 mm and 250x250x30 mm were used in three versions: concrete slabs with optical fibers, concrete slabs with air holes and solid slabs. The experiment measured and compared the level of illumination at several points in the model as it passed through each of the three different slabs. Based on the results of these experiments it was concluded that the interior level of illumination of any space can be improved by using light-transmitting concrete, especially those without access to natural light. The experiment also assessed the strength properties of the slabs in relation to their intended use and compared them with the properties of stone slabs used as cladding.

Keywords in English

light-transmitting concrete; plastic optical fibers; light-transmitting construction; translucent concrete; light-permeable concrete; glass fibers; high performance concrete

List of Acronyms

Abbreviation	*Expression*
CTU	Czech Technical University in Prague
FCE	Faculty of Civil Engineering
HPC	High-performance concrete
UHPC	Ultra high-performance concrete
LTC	Light Transmitting Concrete
POF	Plastic optical fiber
GOF	Glass optical fiber
GF	Glass fiber
MDF	Medium density fiber board
AM	Air mass
TC	Translucent concrete
AR	Alkali-resistant
ASR	Alkali silica reaction
HP	High Performance
PMMA	Polymethylmethacrylat
CIE	Commission Internationale de l'Eclairage
mPOF	Micro-structured polymer optical fibers
EIS	Etem Integrated Solution
TRC	Textile reinforcement concrete

Contents

1 Motivation and goals of the thesis

This doctoral thesis was developed based on several ideas, that I have been contemplating for the last years. The main objective of this work is to comprehensively create and assess samples of a material capable of improving the illumination of interior spaces with daylight and at the same time to bring daylight into communal spaces (like lobbies, corridors, stairwells) through walls made of light-transmitting concrete. In addition, this thesis focuses on different constructions made of light permeable concrete and the use of this material to create light comfort in indoor environments. My other criteria were aesthetic impression and architectural intent, which necessitated creating a screen or simple raster image out of a conventional concrete structure. During the day, this concrete allows daylight into the interior spaces and appears to be a regular concrete structure, but at night, it transforms to create visual effects on the façade, producing an extraordinary architectural experience. An additional objective is the use of the material for the signage system of the building (exit signs, parking space markings, etc.), as shown from the Figure 33 to Figure 35.

This thesis also deals with the technical analysis of the material and its production. The experiment was conceived from several perspectives, the first being the use of light-transmitting concrete in the construction industry. I began by considering the shape and design of the samples, how to produce them, and then how they would be technically analyzed. I decided to compare my samples to stone slabs, which are commonly used in construction, to demonstrate their equality of strength and their compatibility with cladding systems. The next step was to select light-translucent elements capable of transmitting light through the structure. Several options were considered such as glass and various types of plastic. However, glass and plastic optical fibers were the best light-transmitting materials for my purposes. I then needed to create the ideal concrete mixture, due to the density of the network of optical fibers required to create a raster image. It had to be a workable concrete mixture that compacted well and could get in between the individual optical fibers without creating air bubbles. Air bubbles negatively affect the resulting strength and aesthetic appearance of the concrete.

It was necessary to experimentally verify the individual properties of the samples. The Chapters in this thesis focus on each of the properties of the light translucent concrete. Chapter one measures and evaluates the light engineering parameters of the material. Chapter two measures its ability to resist individual loads in conjunction with its intended use. For the consideration of use, the compressive and tensile flexural strength of the material was measured using a three-point bending device. In the next chapter, I was measuring the thermal-physical properties of the material by determining the heat transfer coefficient through the structure. Finally, the last chapter of my thesis, focuses on implementation, how the slabs can be practically used in lightweight perimeter cladding. I compared my light transmitting concrete slabs to stone cladding slabs currently used in most installations of this kind, as well as the different anchoring options. If I use type of a lightweight envelope on the

building, then it creates a gap between the cladding and the supporting structure perfect for the placement of an artificial light source which can create a unique architectural effect. The experimental study which is the subject of this doctoral thesis has been conceived in a comprehensive way, beginning with the design of the light translucent concrete slab's shape and dimensions, the selection and analysis of the perfect light transmitting elements, the composition of the concrete mixture, the measurements of the sample's light properties and their compressive and tensile flexural strength, as well as their thermal-physical properties. Last but not least, the practical usage of LTC slabs for construction has been examined including its aesthetic contribution.

2 Introduction

The construction industry today offers a huge range of building materials that can be combined in various ways to create an entirely new material for a specific purpose as the need demands. This is how light-transmitting concrete came to be created [1]. Light is a very important factor that affects a person's mental and physical health. But today its abundance is diminished in cities where construction is spreading to the borders of already built-up areas, and where the buildings are designed to utilize every square meter possible within the boundaries of the building codes. So, concrete that could transmit light is a practical solution to these problems. Translucent concrete is already in existence and has been evaluated from many different angles [2]. One example is LiTraCon, which consists of a bundle of optical fibers placed in a block and then separated into the slabs [3]. Civil engineering companies Lucem and Luccon also manufacture light-permeable concrete, but the fibers are placed more precisely in the matrix [4] [5]. The design company Gravelli, which created the material LiCrete, takes a different approach by using a plastic matrix [6].

The main objective of this research was to measure the improvements of light conditions inside a building using light-permeable structures. This paper is an analysis of how those experimental measurements were conceived of and carried out, as well as the results of those experiments. The data supports the desired increase in the amount of visible electromagnetic radiation in building interiors when using light-transmitting concrete. The other part of the study is to comprehensively create and assess samples of a material capable of improving the illumination of interior spaces with daylight and at the same time to bring daylight into communal spaces (like lobbies, corridors, stairwells) through walls made of light-transmitting concrete. The originality of this study is in the measurements of light properties of light transmitting concrete slabs and of their effect on interior lighting conditions, as well as measurements testing their strength for purposes of use.

This study also deals with the technical analysis of the material and its production, as its properties have not been assessed in this way before. There are several processes for making light-transmitting concrete. The design of slabs made of light-transmitting concrete is a very difficult and complex task, which must take into consideration an analysis of numerous parameters [7]. These include ultimate bearing capacity, the ratio of the components of the concrete mixture, the type of reinforcement for the chosen purpose of use, the composition of the mixture in relation to the use of optical fibers and the prevention of their damage. The strength of the concrete mixture itself is already well known, but for my application case, the commonly used mixture in construction had to be modified due to the addition of optical fibers and air holes. The composition of the concrete mixture was influenced, for example, by the aggregate fraction, its chemical composition, its workability, and color. The concrete mixture designed for our purposes was tested by standard procedures and on test samples. The correct composition of the concrete mixture, volume ratio, the choice of optical fibers and their distribution in the structure

significantly influenced the measurement results. The ratio of optical fibers to the compound is very important. A larger amount of optical fibers increases the light gains, but at the same time increases the cost of the product itself [8] [9]. It may seem that the placement of optical fibers in concrete would not significantly affect the quality of illumination within the indoor spaces, but the measurements we made show that the light values are several times higher than when used a same size sample and the same concrete mixture, but in which the optical fibers were replaced by only continuous holes of the same dimension. Light radiation moves through the circular air penetrations of the slab at a significantly lower intensity than through optical fibers. Unsurprisingly, when using a solid slab, the light does not spread between the two spaces at all.

Experimental test measurements were performed on several concrete slabs from the same concrete mixture using the same type of glass fibers reinforcement. For the purpose of these experiments, three types of concrete slabs were chosen: a) solid slabs b) slabs with the addition of optical fibers of thickness 3 mm in exact grid and behind c) slabs with air holes of the same diameter and grid as optical fibers. The experimental study had to be divided into two parts. The individual phases define the type of material, such as the composition of the concrete mixture, its reinforcement, and the use of the type of optical fibers. Next, the production of unified slabs and the various light parameters used in the measurements were factored into the final conclusions. This research focuses on the possibility of using light-permeable concrete in places where daylighting is not possible using standard structures such as windows, skylights, etc. Regulations specify a minimum daylight factor value that we were able to achieve using light-transmitting concrete in locations where this would not otherwise have been possible. Because the purpose of this study was to measure the light properties of LTC slabs and their possible use in improving the lighting conditions inside a building, that goal has been achieved as this thesis demonstrates. It cannot be overlooked that the improvement of interior lighting has a positive effect on the wellbeing of human health. The other objective of this thesis was to measure the structural strength of light transmitting concrete slabs in comparison them with well-known stone slabs, such as travertine or granite. This comparison is useful to show that they can be safely substituted for traditional stone cladding.

3 Theoretical part - history, properties, and definitions

3.1 Theory of light-transmitting concrete

The first mention of light-transmitting concrete dates back to 1922, when a German scientist Paul Liese filed a patent application on the subject in the United States. Mr. Liese was involved in the development of concrete panels and blocks for vertical and horizontal structures. He was finally granted a patent in 1925 [2]. LTC was also mentioned in a Canadian patent from 1935. Since that time numerous studies and scientific researchers have been involved in the development of light-permeable concrete. The first to invent light-transmitting concrete, as we know it today, was the Hungarian architect Aron Lasonczi. In 2001 he used optical fibers randomly mixed into a concrete mixture to create a larger block of concrete, which was then cut into individual slabs of specified dimensions. One of the most important sources of information and inspiration for this project Lasonczi's material LiTraCon (Light Transmitting Concrete), its properties can be found in the Table 1. He invented it with his colleagues at the Technical University of Budapest. The material was registered as a trademark in 2001. In 2004, architect and inventor Aron Lasonczi founded the company LiTraCon Bt, located in the city of Csongrád, Hungary, which is only distributor of LiTraCon. Lasonczi's light-transmitting panels are what we know today under the brand name Litracon [10]. His method not the only one. In 2009, Mexican scientists Gutiérrez J. S. and Cázares S. O. G. filed for patent approval for translucent concrete that lets trough 80% of light and weight only 30% of standard concrete [11]. There are several other ways to create light-transmitting concrete, for example, one scientific team made it by to randomly places the optical fibers straight into a long beam-shaped sample and then cuts them into individual slab, other one already produces individual slabs directly with the placement of fibers in individual precise positions, later they published a paper how they did it [12] [13] [14] [15]. There are already several companies that are engaged in the production of translucent concrete. In addition to the Hungarian company Litracon, it is, for example, the German company Lucem or the Austrian company Luccon [16] [3] [4] [5]. One such option is adding a light enabling element throughout the concrete mixture. Usually, this element is placed into a precisely spaced matrix. Elements that can be considered for use include plastic forms, glass elements (which must be alkali-resistant), photosensitive materials or, in optimal case, optical fibers (glass or plastic) [17]. Research done using plastic pipes or rods concluded, that a large amount of money could be saved by using the plastic optical fibers [18] [19]. Further research has shown that the amount of light that optical fibers are able to transmit is significantly greater than plastic pipes or rods [20]. The above-mentioned elements allow for the transmission of the entire light spectrum. Including the transmission of infrared radiation, which provides heats losses and gains [21]. One of the most famous and spectacular structures using light transmitting concrete is the Italian Pavilion for EXPO 2010 in Shanghai. It was built by the Italcementi Group using a material created known as i.light [22]. I.light is a special concrete mixture to which a plastic matrix has been added, enabling the transmission of light from the exterior to the interior [23] [24].

3.2 Properties of light transmitting concrete

Translucent concrete (or light-transmitting concrete) is made from a concrete mixture plus light-optical elements such as glass or plastic optical fibers, which provide the necessary light-transmitting properties. Light information must pass through the entire structure from one end to the other. The passage of this light is influenced by the surface of the fiber. In addition any dust or dirt on the surface of the optical fiber reduces the passage of light. The shadows created on one side will appear on the other as contours on the surface of the structure. Translucent concrete is used in architecture, as a facade, for non-load-bearing interior structures, or for cladding in the interior. Light-transmitting concrete is also applied to various design accessories, like lamps or table desks. There are several ways to make translucent concrete. However, all methods are based on the use of fine-grained concrete (approx. 95%) and light-conducting elements (only 4-5%), which are added during the mixing process. When the translucent solid concrete element is created, it is separated into individual segments using machinery.

It is also important to work with natural daylight, which must be sufficient for the transmission of light between two spaces in order to be successful. If we wish to create a unified visual aesthetic on the structure, then light must be distributed evenly across the entire area. The mounting systems that we would use for the light-transmitting concrete slabs is similar to those for fixing stone slabs. Commonly used mechanisms for the façade are cut-in, or façade anchors and perforated slabs with visible screws.

Because of the bends in the optical fibers and the irregularities in the cut surfaces of the fibers, the light transmission is generally a little less than half of the light incident on the cross-sectional surfaces. Therefore, using five percent of the fibers in the mixture, the transmission is close to 2% of the total surface area of the element. Although 2% may seem negligible, because the human eye's reaction to light is non-linear, the optical fibers provide sufficient daylight in the interior.

Prefabricated building materials and panels of various sizes can be produced using this type of concrete, and thermal insulation can also be embedded in them. Optical fibers have almost no negative effect on compressive strength, thus, concrete with GOF or POF can be used for some load-bearing structures as well. Between the two main surfaces of each block of translucent concrete, run thousands of parallel optical glass fibers that form a matrix. The small amount of fibers in the material (approximately 4% of the total volume) and their small size enable them to mix perfectly with concrete and only minimally contributes to the formation of air bubbles, an inherent problem whenever mixing concrete. The result is a smooth and homogenous surface.

By combining self-compacting concrete or glass-cement mixtures with optical fibers, many visual effects can be achieved that depend only upon the method of laying the fibers in the formwork. They can give off specific figural, abstract geometric, or decorative motifs.

The translucency of the material is created by the GOF a POF that guide the light through the mass of concrete illuminating the opposite surfaces of the structure. Because the fibers are arranged in parallel formation, the light pattern on the dark side is the same as that on light side. That is, to say a sharp outline of shadows falling on the dark side are displayed equally on the light side. At the same time, the color of the light is preserved.

Translucent concrete opens up completely new possibilities for the construction industry, and at the same time, presents new opportunities and challenges for architects and designers. Positive reviews of the new material have been published in The New York Times, Wall Street Journal, The International Design Magazine, Der Spiegel, The Architectural Review, and others.

Table 1: LiTraCon – technical properties

LiTraCon -Technical properties	
Form	prefabricated panels/blocks
Ingredients	concrete mixture and optical fibers
Fiber content	from 3 to 5 % by volume
Translucency at 4% fiber optic	3%
Volumetric weight	2400 kg/m^3
Compressive strength	from 32 to 49 MPa (depending on the direction to pressure)
Tensile flexural strength	7.7 MPa (when used, e.g. As a walking pavement)
Thickness	from 20 to 3000 mm
Current maximal block size	300 x 600 mm
Surface	polished
Thermal insulation	possible
Color and texture	gray, beige, black, porous

3.3 Examples of existing construction

Translucent concrete was first used in 2002 for the surface pavement of a city square in central Stockholm. During the day the 350x350x50 mm blocks form a seemingly simple concrete pavement, but after sunset they glow thanks to the light sources placed beneath them. In complete darkness, a fascinating light pattern is created around the center of the city square.

In 2004, the new material was used in the construction of a private house in Budapest. A concrete block measuring 400x1200x60 mm was built into the south-facing dining room wall in place of window. During the day, the sun shines through the block window, and at night, the internal light sources pass through it.

Another example of this interesting material being used for a home interior can be seen in the German village of Sittelsen, located between Hamburg and Bremen. Here an experimental concrete house was built based on suggestions from readers of the

German magazine Schöner Wohnen (Nice Living). One wall of the house is made of white translucent concrete located in one of the most frequented areas of the house, which was completed in 2005.

But perhaps the finest example of LTC used for its aesthetic purposes in creating public art, is the European Gate in Komárno, Hungary. It is a 4 m tall sculpture made of LiTraCon blocks built in 2004 to celebrate Hungary's entry into the European Union. The European Gate won the German "Red Dot 2005 Design Award" for its high design quality. According to the inventor Áron Losonczi, it is theoretically possible to create a similar wall several meters thick from the same translucent concrete, because the fibers are able to transmit light without significant loss of light up to a thickness of 20 m.

The previously mentioned most well-known Hungarian company that produces translucent concrete is LiTraCon, which has several major projects that include HIPO reception desk (2015) in Budapest, Hungary, in the Figure 8; Garden Pavilion (2013) in Zurich, Switzerland, in the Figure 10; Erzsebet Square Benches (2013) in Budapest, Hungary, in the Figure 11; ON Club (2011) in Prague, Czech Republic, in the Figure 12; Studio Hibiya Wall (2011) in Tokyo, Japan, in the Figure 13; Europe Point (2010) in Budapest, Hungary, in the Figure 14; Private Flat (2010) in Budapest, Hungary, in the Figure 15; Iberville Parish Veterans Memorial (2008) in Baton Rouge, USA, in the Figure 18; Halifax Monument (2007) in Halifax, Canada, in the Figure 19 or Cella Septichora (2006) in Pécs, Hungary, in the Figure 20. Other examples of LTC used for aesthetic construction was presented by German company Lucem Lichtbeton, which included Hansa Carrée Lobby (2021) in Hamburg, Germany, in the Figure 1; Urban Star Sculpture (2020) in Augsburg, Germany, in the Figure 2; Capital Bank (2017) in Amman, Jordan, in the Figure 5; retail LUXX Living (2016) in Berlin, Germany, in the Figure 6 or Wahat Al Karama (2016) in Abu Dhabi, UAE, in the Figure 7. Other constructions that are worth mentioning are Altar in Church (2018) in Chrudim, in the Figure 3; Reception Desk and Kitchen Island (2018) in Prague, in the Figure 4 and Translucent Partition Bathroom (2015) in Slivenec, in the Figure 9, all in Czech Republic from design company Gravelli, which invented LiCrete blocks. Finally, it is important to mention famous Italy EXPO Pavilion (2010) in Shanghai, China, in the Figure 16 and Figure 17, from i.light material, which was invented by Italcementi Group.

In addition to the ability to transmit light, products made of transparent concrete are widely used thanks to their extremely favorable physical and technical properties. The material is constantly being reinvented with improvements, which is why it is possible to produce prefabricated elements of different sizes and colors.

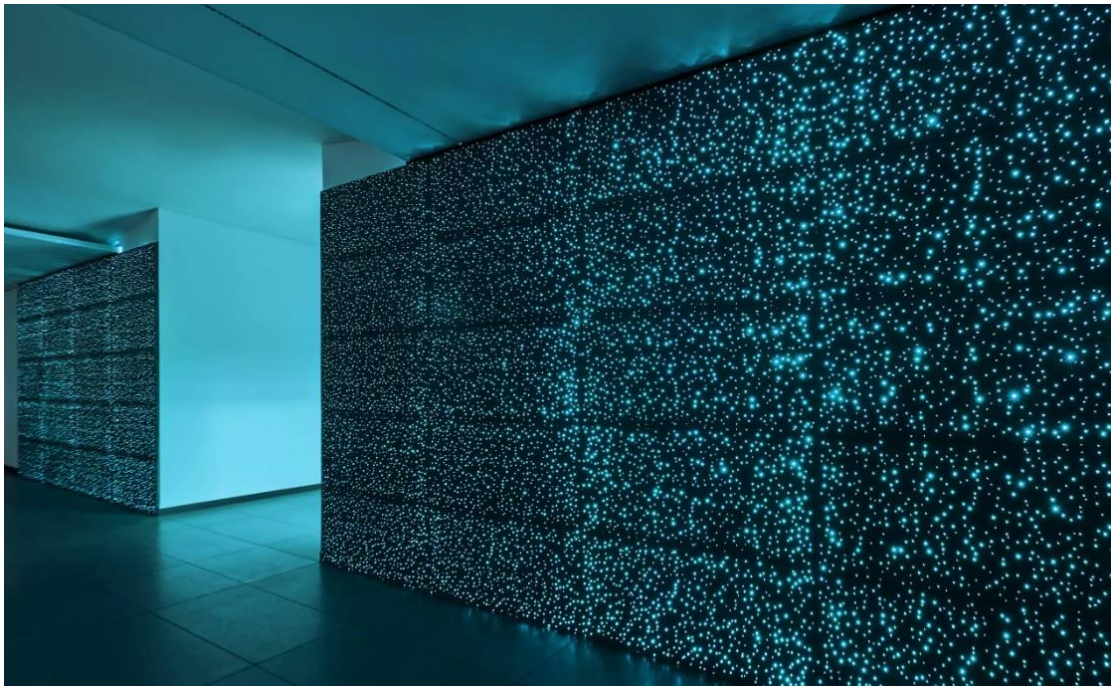

Figure 1: Hansa Carrée Lobby, Hamburg, Germany, 2021 [25]

Figure 2: Urban Star Sculpture. Augsburg, Germany, 2020 [25]

Figure 3: Altar made of translucent concrete, Chrudim, Czech Republic, 2018 [26]

Figure 4: Trask Solutions reception desk and kitchen island, Prague, Czech Republic, 2018 [26]

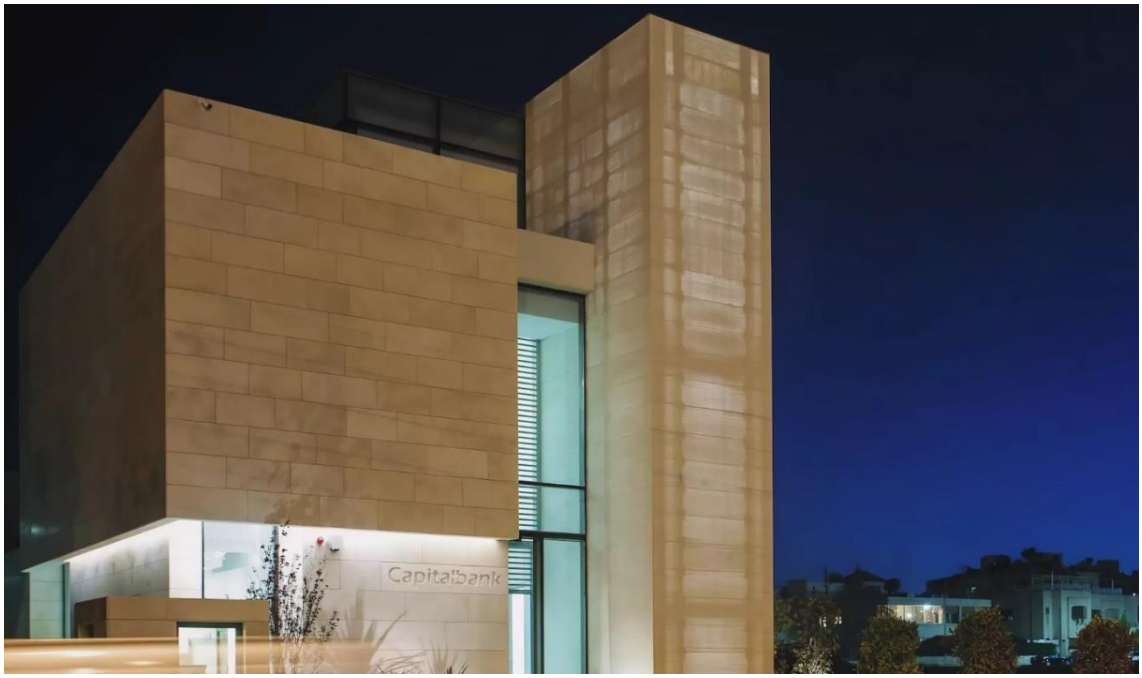

Figure 5: Capital Bank, Amman, Jordan, 2017 [25]

Figure 6: LUXX Living, Berlin, Germany, 2016 [25]

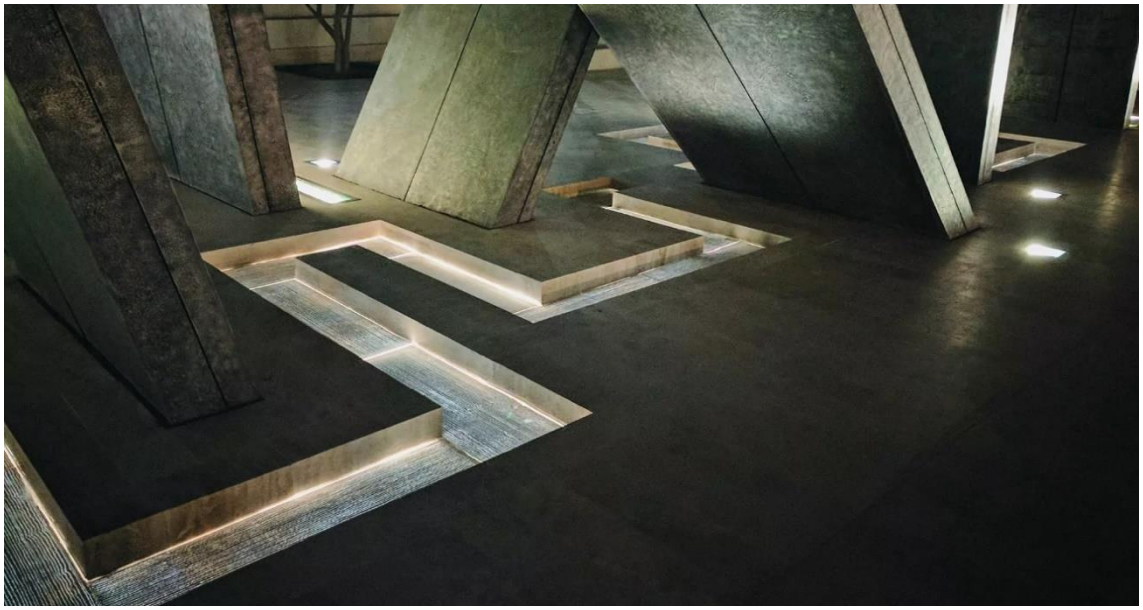

Figure 7: Wahat Al Karama, Abu Dhabi, UAE, 2016 [25]

Figure 8: HIPO reception desk, Budapest, Hungary, 2014 [27]

Figure 9: Translucent Partion Bathroom, Slivenec, Czech Republic, 2014 [26]

Figure 10: Garden Pavilion, Zurich, Switzerland, 2013 [27]

Figure 11: Erzsebet Square Benches, Budapest, Hungary, 2013 [27]

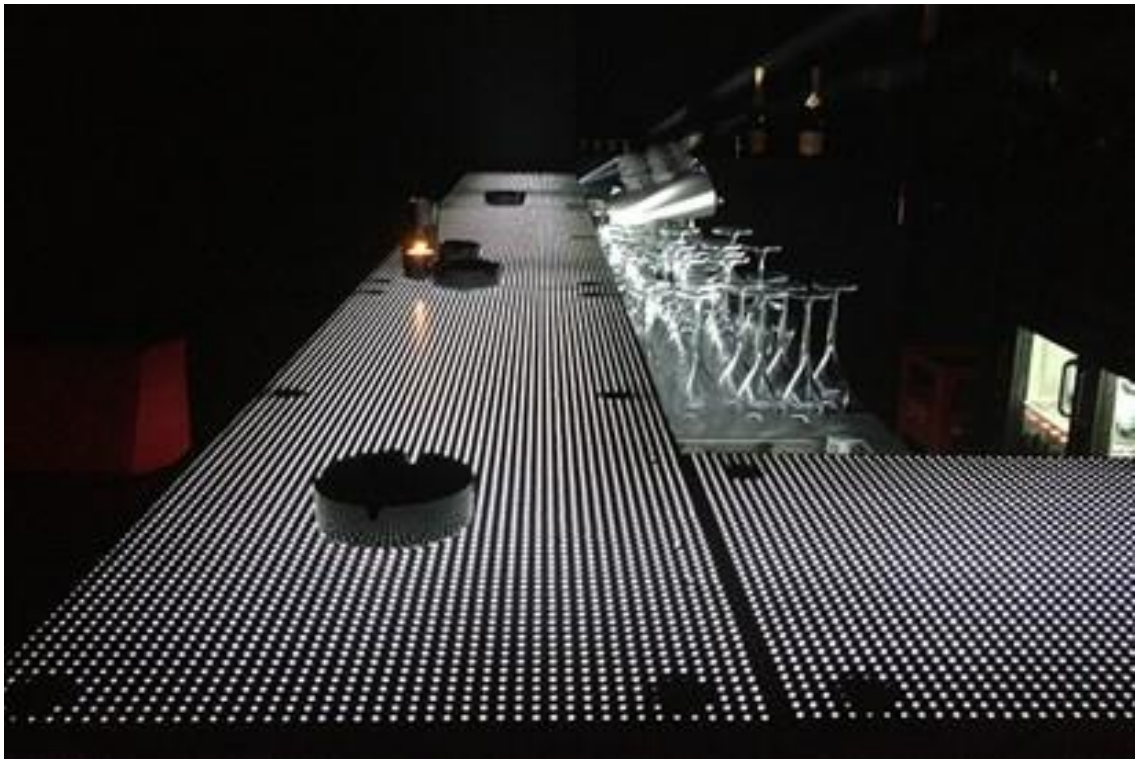

Figure 12: ON Club, Prague, Czech Republic, 2011 [27]

Figure 13: Studio Hibiya Wall, Tokyo, Japan, 2011 [27]

Figure 14: Europe Point, Budapest, Hungary, 2010 [27]

Figure 15: Private Flat in Budapest, Budapest, Hungary, 2010 [27]

Figure 16: Italy EXPO Pavilion, Shanghai, China, 2010 [28]

Figure 17: Italy EXPO Pavilion, Shanghai, China, 2010 [28]

Figure 18: Iberville Parish Veterans Memorial, Baton Rouge, Louisiana, USA, 2008 [27]

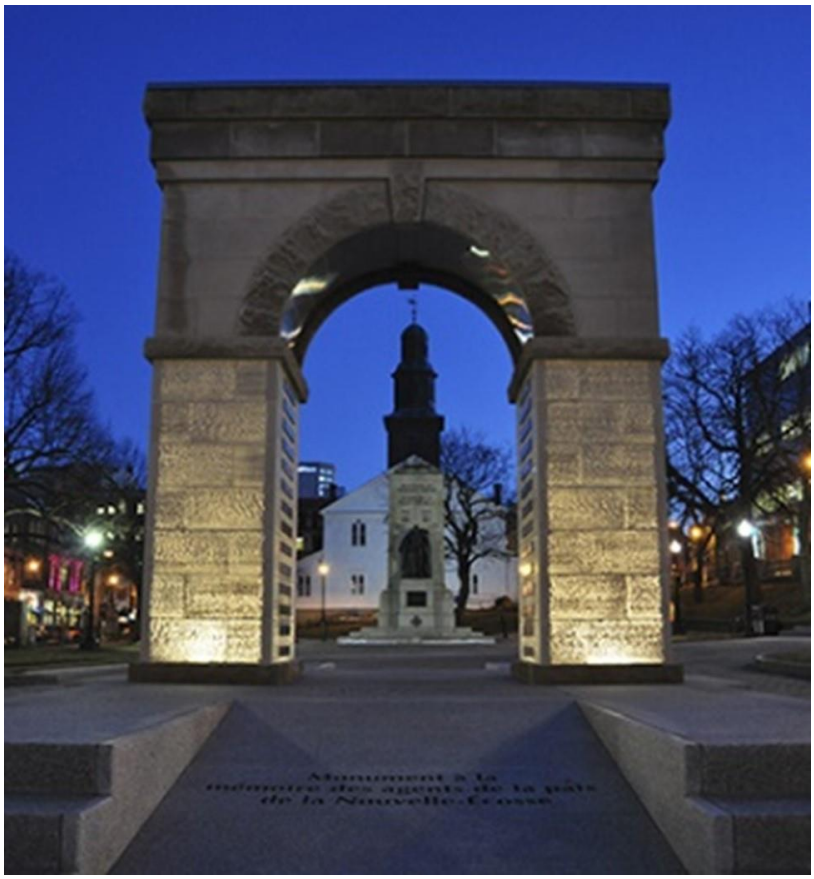

Figure 19: Halifax Monument, Halifax, Canada, 2007 [27]

Figure 20: Cella Septichora, Pécs, Hungary, 2006 [27]

3.4 Possibilities of using translucent concrete

The light-transmitting slabs are both practical and decorative. Unified slabs can be used for wall surfaces, partitions, floors or as a cladding material for interior structures and facades. The elements can be illuminated by a single light source, by several separate artificial light sources or by LED matrix shown in the Figure 26. The lights illuminating the surfaces can be stationary, like in the Figure 22, or moving to create interesting lighting effects. We can also hang the panels on the support structure and place a light source behind them, like in the Figure 21, which is part of my experiment. Ideal examples would be lightweight building envelopes or wall cladding in interior spaces. For example, we could create evacuation signage for buildings, parking systems or building signage (floors, numbering, etc.) in this way as shown in the Figure 33 and Figure 34. We can use light-permeable concrete panels for perimeter structures where we need to ensure at least minimal daylighting. The possible prefabrication of the slabs with embedded optical fibers could make the material more affordable. By placing the prefabricated translucent elements at the exterior-interior interface, we can achieve daylight transmission to the interior while acting as a rigid perimeter structure. Thanks to the properties of optical fibers, by attaching them to a light source, it is possible conduct electromagnetic radiation, of different colors from the light spectrum, through the material to its surface, creating unusual light patterns, like from the Figure 27 to the Figure 30, which all based on my research. The combination of a light source and a simple raster graphic pattern created with optical fibers precisely positioned in the prefabricated material opens up completely new possibilities and non-standard solutions. [29]

As mentioned above, it is possible to install fiber optic thread and light sources in building structures such as walls, ceilings, partitions, and floors, but we have to accept that it's complicated and expensive. If we are able to bring natural light into spaces where it could not be achieved by design, it is well worth the effort in producing this material. It is also worthwhile if we want to create an original look or design of the building. The work is very lengthy and demanding, whether it is because of the precise laying of the fibers or the implementation of a large number of holes. In all these cases, prefabricated structures with embedded optical fibers are the solution. In addition to practical solutions to natural light problems, the material can be used in a wide range of design applications.

In the implementation of unified panels, the amount of optical fiber placed in the structure is influenced by the dimensions of the panel, the graphic grid, the architectural intent, and the strength of the structure must not be affected. The optical fibers are evenly distributed in the block and carefully encased in the concrete mixture. The slab has a homogeneous structure with high strength. To achieve uniform illumination of the element, it is necessary to select the correct light source and to ensure that all the optical fibers are illuminated at the correct angle. For large sample sizes, it is important to ensure a sufficient number of light sources, their correct positioning in relation to the optical fibers.

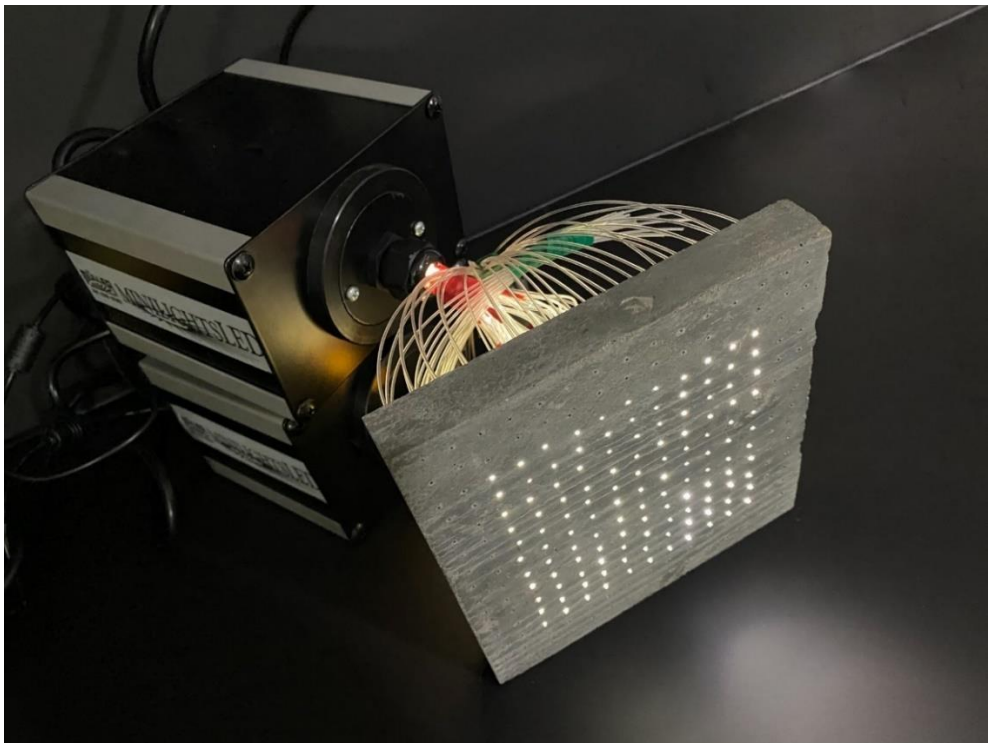

Figure 21: Slab with optical fibers connected to an artificial light source

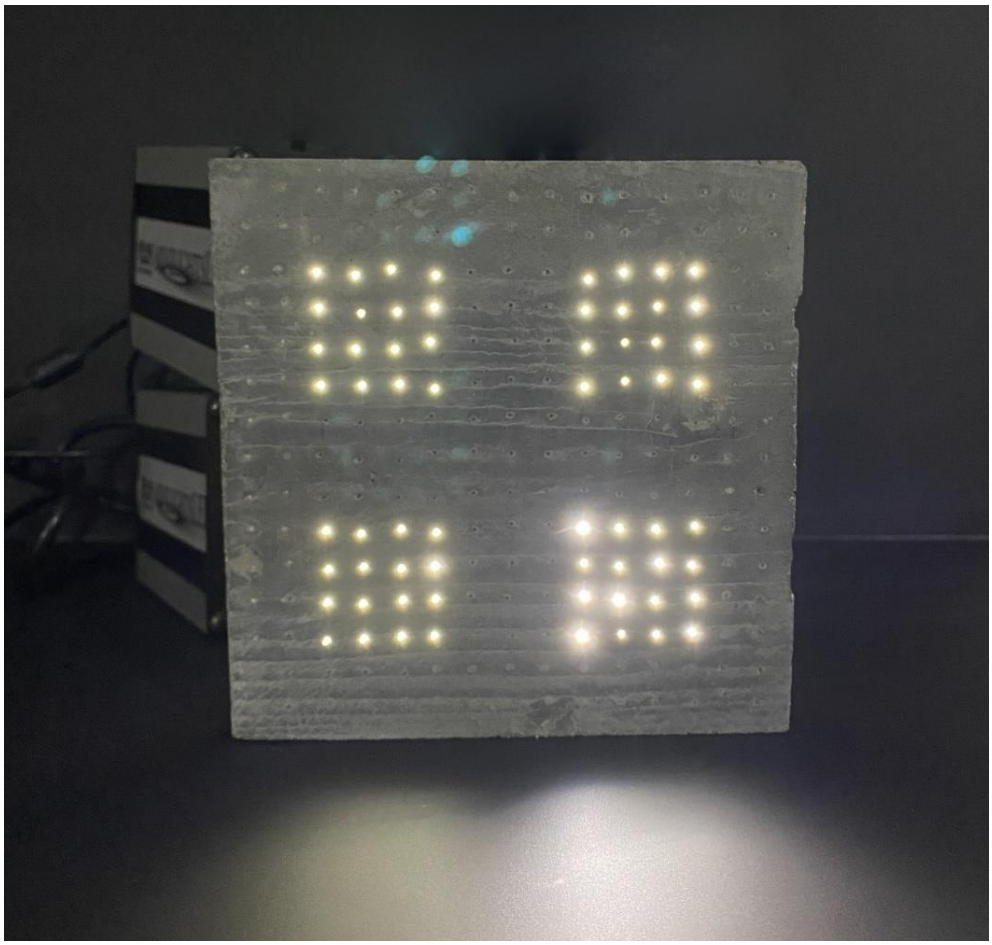

Figure 22: Slab with optical fibers connected to an artificial light source

If the distance between pixel pitch is smaller (the distance between each optical fiber), the higher the resolution and the closer the viewer can view the raster image or screen like in the Figure 23. Because light-transmitting concrete panels can be manufactured in any module and optical fiber spacing, we have greater flexibility to create screens of any size for example in the Figure 25 shown it. The intention at the start of the work was to use slabs of light-transmitting concrete on the façade or as cladding in the interior, to create a screen when the lights are switched on, and a concrete structure when they are switched off. The example was stone cladding and its use, both indoors and outdoors, to which we compare the concrete slabs. We could create an architecturally unique work. When the artificial sources were turned on could create any image and bring the building to life with special effects, like in the Figure 31. Conversely, when they were turned off the building would look like an ordinary concrete structure as in the Figure 32.

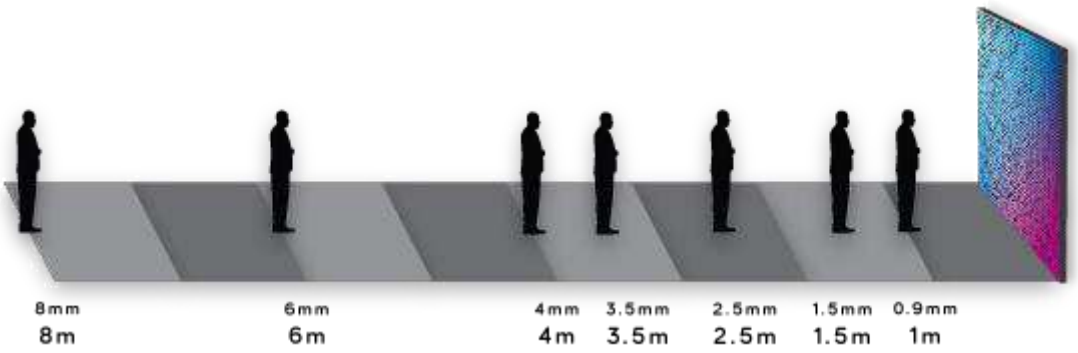

Figure 23: Examples of distance for image observation to the distance of individual points of the image [30]

The relative viewing distance is the ratio of the distance of the critical detail from the observer's eye and the dimension of the critical detail, the relationship is shown in the Figure 24. It is expressed as the ratio of the viewing distance P and the critical detail dimension d, as we can see in the Equation 1 below:

$$\rho_v = \frac{P}{d}\ (-) \tag{1}$$

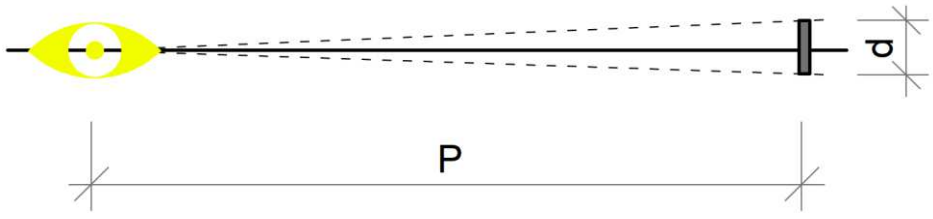

Figure 24: The Relative viewing distance diagram

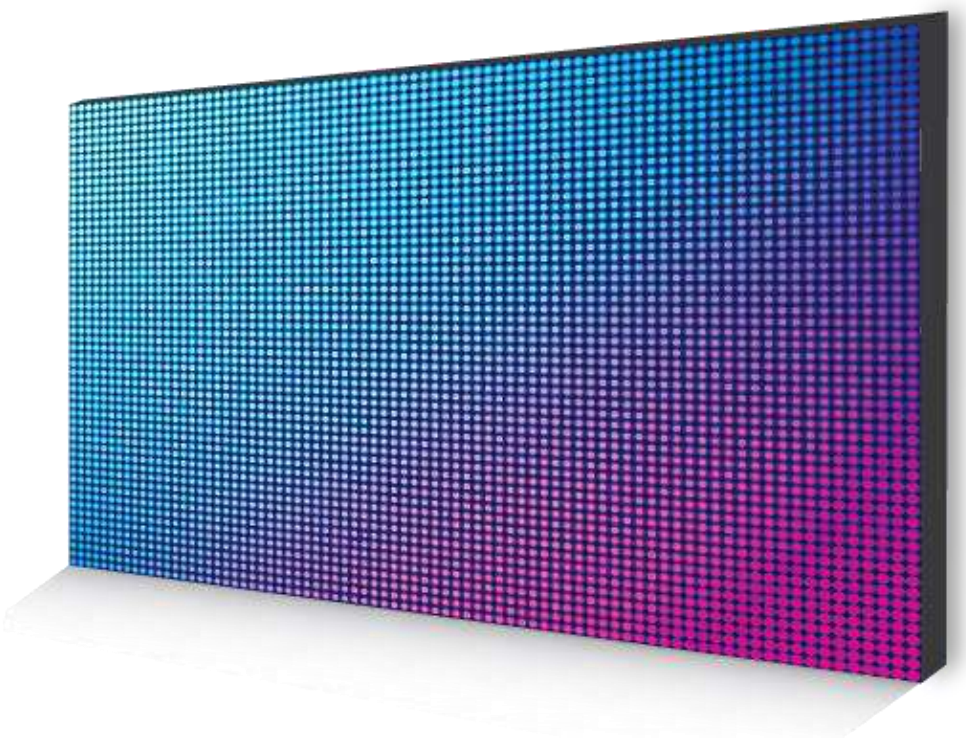

Figure 25: LED screen pattern [30]

Figure 26: LED RGB matrix 16x16 used for demonstration of slabs lighting on the façade [31]

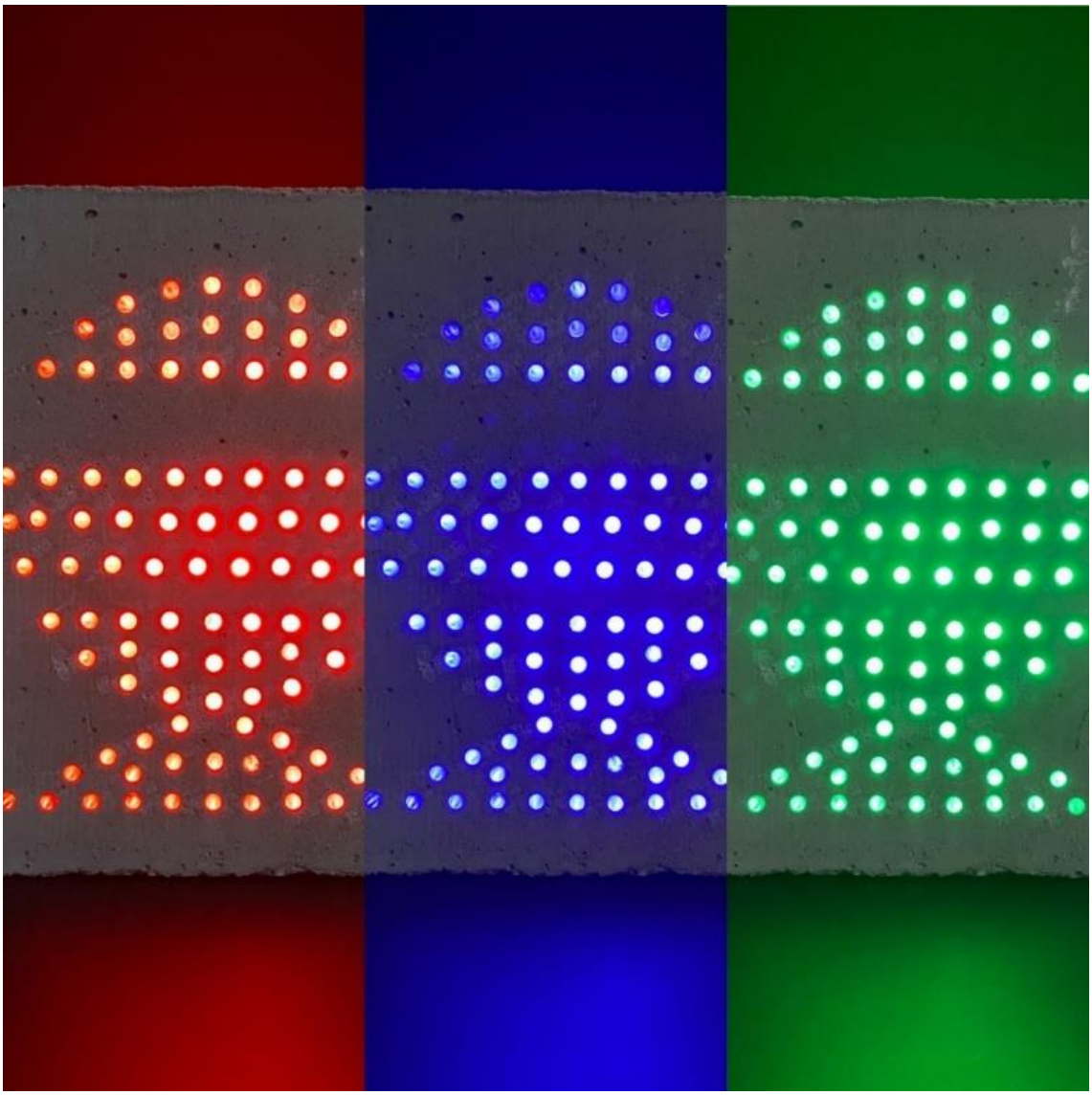

Figure 27: Examples of applications and lighting of light-permeable concrete slabs

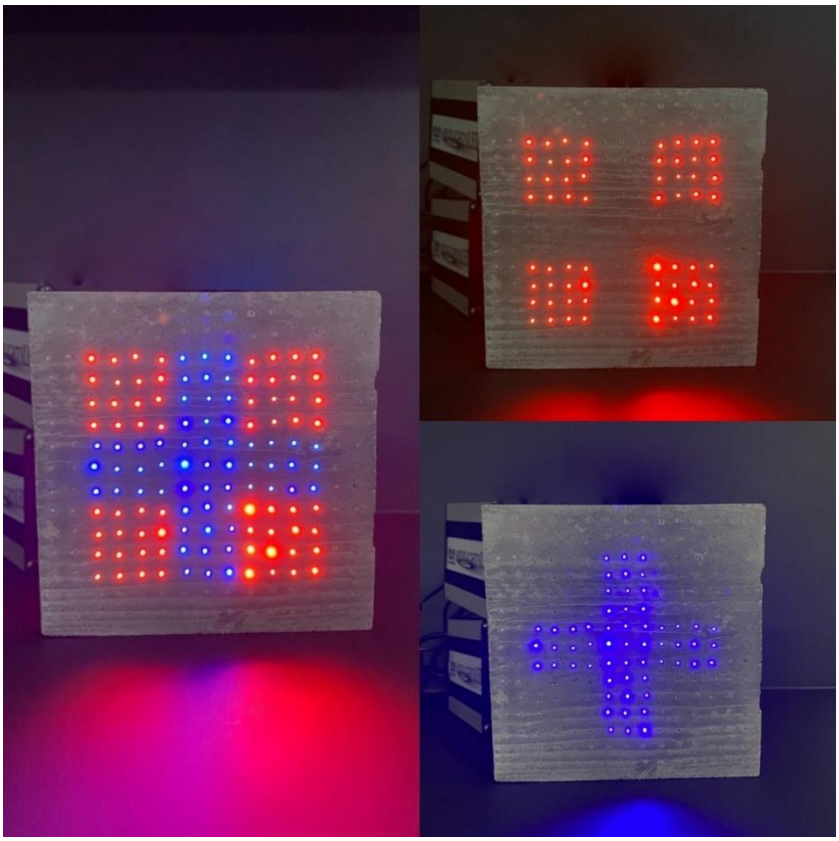

Figure 28: Examples of applications artificial light source to light-permeable concrete slabs

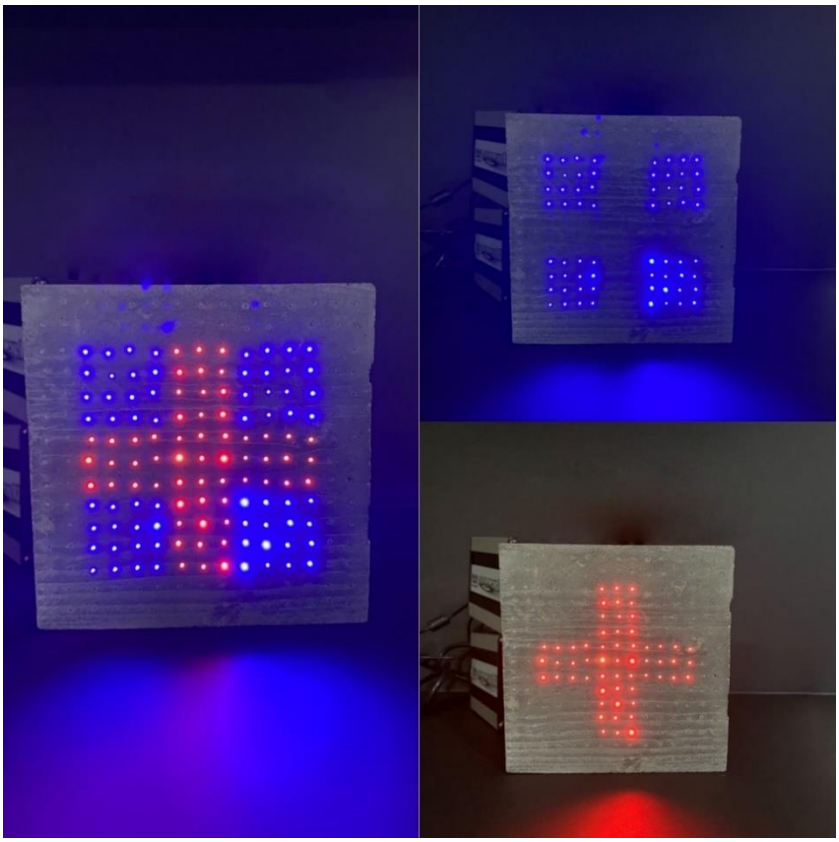

Figure 29: Examples of applications artificial light source to light-permeable concrete slabs

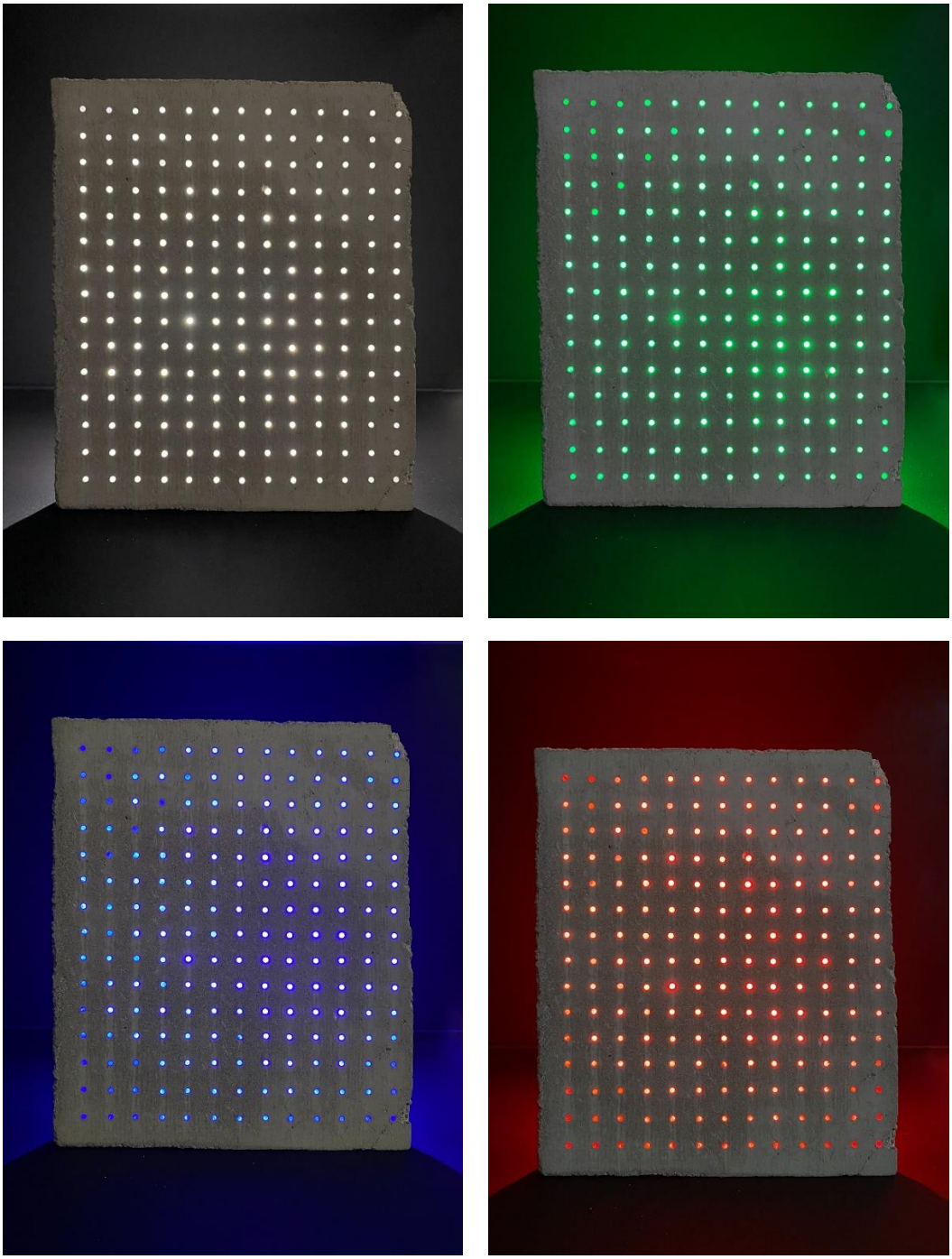

Figure 30: Examples of colored light transmittance

Figure 31: Example of façade cladding for our purpose [32]

Figure 32: Example of façade cladding for our purpose [32]

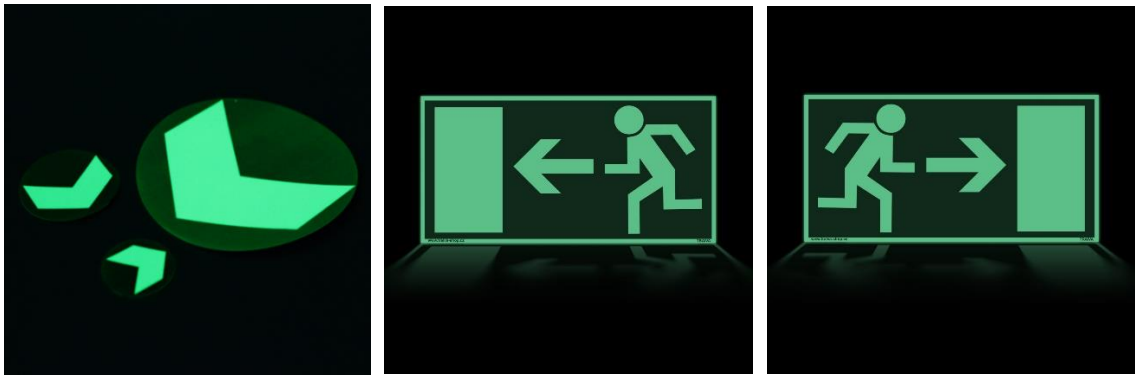

Figure 33: Samples of tables for the building escape plan [33]

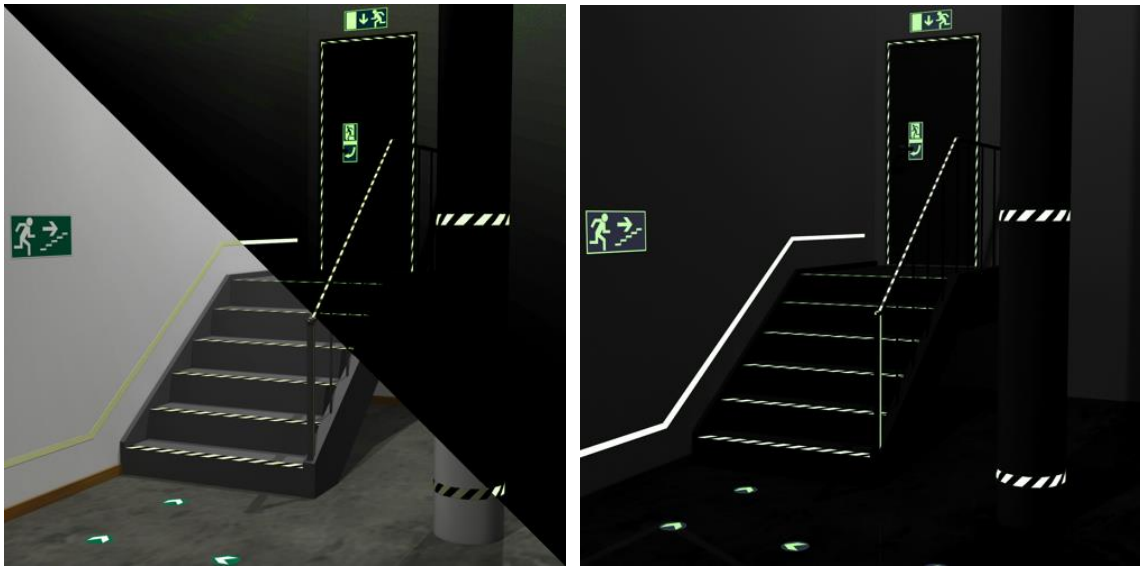

Figure 34: Examples of using tables for a building escape plan [33]

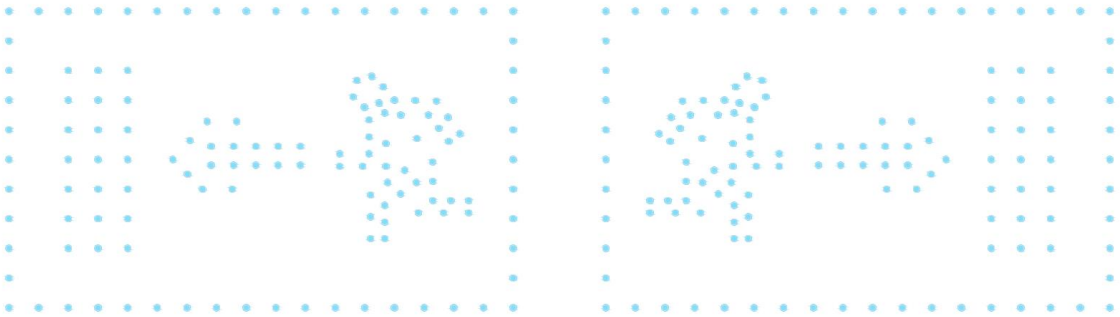

Figure 35: An example of how an escape signage might look like using optical fibers in concrete

4 Materials and Elements

4.1 Concrete mixture

Water is one of the main components of the concrete mixture, which contributes to hydration process and affects its workability. After mixing water with cement, a chemical reaction called hydration begins, which results in the concrete beginning to solidify and harden after a few minutes. The minimum water requirement for hydration is a range of 25-35% of the cement weight. The higher dose of water improves workability, which is needed to better distribute the concrete mixture with glass fibers between the precisely placed optical fibers. But at the same time, we must think about the negative factor of a larger amount of water. However, it must be taken into consideration, that the larger dose of water can create a larger number of pores and capillaries, which reduce its strength and resistance to environmental influences. The water coefficient *w* is therefore absolutely essential for the optimal consistency of the mixture for light-transmitting concrete. *W* is the ratio of the weight of the effective water content to the weight of cement in fresh concrete. Normally, the water coefficient ranges from 0.3 to 0.6. Concrete with a lower water content exhibits better mechanical properties such as strength, modulus of elasticity and resistance to pressure water seepage. Portland cement, which was used for the production of samples, is one of the most widely used types of cement [34]. It is a finely ground inorganic material that is used in the mixture as a hydraulic binder that hardens in air and under water. The proportions of the ingredients in the mixture can vary depending on the intended use of the concrete, which is why in my research changed the proportions for each sample. It will also be important to assess the type of cement in terms of its chemical properties and aggressiveness towards optical fibers added to concrete. The mixture should not be chemically aggressive, so as not to damage the optical fibers. It is also possible to use various additives and admixtures in the concrete mixture for light-transmitting concrete, either for faster solidification or hardening, but it is necessary to ensure that the chemical composition of these substances does not damage the optical fibers and therefore the resulting effect of the entire structure. The concrete mixture used in this study is PZ-HPC-53 with a bulk density of 1892 kg/m^3, its specification is in the Table 2 and the mixture itself is shown in the Figure 37. Both the compressive and tensile flexural strength of our mixture was determined by standard concrete test. The resulting measurement determined a compressive strength of 59.8 MPa and a tensile flexural strength of 10.7 MPa. Size of the aggregate should not be greater than 4mm [35]. Instead of aggregate, recycled materials such as waste glass from the flat glass industry can be used to improve light transmission, but the strength of the resulting element would be reduced. [36]. Because of that, we did not use waste glass for our samples. Glass inclusions have been classified as non-reactive in the accelerated alkali-silica reaction test [37]. For the production of concrete slabs with dimensions of 250x250x20(30) mm, white Portland cement of class 52.5 R is used. Aggregate passing through a sieve with a diameter of 4 mm was used in the concrete. When specifying a mixture for light-permeable concrete, it is important that the mixture is

highly workable and that the slabs have the required strength properties. These requirements are primarily influenced by the water ratio *w/C*, which could improve workability but also negatively affect the strength of the final product. Therefore, we have to choose a suitable superplasticizer with regard to the water ratio. Light microsilica and a water coefficient of 0.29 were used. The samples with optical fibers, which were evaluated in our experiment, have a ratio of optical fibers to concrete mixture 1:10. The volume of optical fibers in the sample is 10.2% (~120 kg/m^3) of the total volume. One of the studies investigated the production of translucent panels using a resin-concrete mixture, which could be used as an alternative mixture [38].

Table 2: Components of HPC mixture

Components of HPC mixture	
Components:	***Approximately (kg/m³):***
Aggregate 0-4mm	*~926*
White Cement I 52.5 R	*~608*
Light microsilica	*~101*
Superplasticizer	*~29.5*
Glass fibers - Anticrack HP 12	*~20*
Water	*~207*
TOTAL	***~1891.5***

The manufacturing process of the unified slabs is divided into several steps. The first step is to create a form of the given dimensions including prepared holes for optical fibers. In the second step, the form is precisely impregnated with a removal oil so that the sample can be removed from the form without damage and like a visual concrete structure. In the third step, glass fibers are added to the form and mixed into the concrete mixture, like in the Figure 36. In the fourth step, the optical fibers are placed in the form and arranged regularly in the transverse direction of the form. In the fifth step, the form is subjected to mechanical pressure or vibration so that the layers of optical fibers are uniformly cast, and the concrete mixture reaches all points of the form. In the sixth step, it is necessary to provide sufficient moisture for the specimen to cure. In the seventh step, the form is uncapped, and the sample is removed. If the slabs are used for a façade system, in the eighth step it is necessary to apply fabric reinforcement to the slab on the non-visible side and coat it with epoxy resin and drill holes for the stone screws that are screwed to the anchors.

The LTC block contains embedded optical fibers implemented in a concrete mixture that allow light to pass through the translucent block, thus creating a completely new material with optical properties. The optical fibers are arranged and embedded in the concrete mixture from the surface of one side of the block to the opposite side of the LTC block, wherein an end of the optical fibers is arranged to terminate at a respective

position on the first side surface, and at the other end the optical fibers are arranged in the same manner so as to also terminate at a respective position on the side surface. The material is characterized in that the fibers embedded in it form a LTC block with a homogeneous structure that can carry loads. The plurality of fibers is distributed substantially evenly over the entire lateral surface, whereby light can be emitted from the evenly distributed ends of one side through the rigid material to the other lateral surface.

One end of the fiber is positioned to be in a 90° position to the first lateral surface and the other end of the fiber is positioned to be in a 90° position to the second lateral surface. The plurality of individual thread is arranged in parallel in the longitudinal direction of the translucent block. The fibers are evenly distributed in the block and the ends of the fibers thus terminate on the side surfaces. The fibers allow light to be transmitted through the building block from one surface of the translucent block to another, or from the exterior to the interior, and the light is emitted from the evenly spaced ends of the fibers over substantially the entire illuminated surface.

The light-transmitting concrete panels are characterized in that the volume ratio of the cast material to the optical fiber's ranges from about 1:15 to about 1:8.

The concrete mixture for light-transmitting concrete is composed of high-strength cement, water, fine aggregate with a fraction of 0-4 mm and optical fibers.

Figure 36: Concrete mixture for samples

Figure 37: Concrete mixture for samples

4.2 Glass fibers - reinforcement

The use of glass fibers is necessary, because of the purpose of usage of the slabs and to increase their strength, which is weakened by the raster network of optical fibers or air holes. Anti-Crak® HP (62.4) fibers were used to produce light transmitting concrete samples, with optical fibers. These Anti-Crak® HP (High Performance) glass fibers, its specification is in the Table 3, are technologically perfect high-strength, high-modulus chopped strands from Cem-FIL alkali-resistant (AR) glass fibers intended for reinforcing cement-based materials. The strands of Anti-Crak® HP fibers have an optimized special surface treatment guaranteeing the resistance of the strand against abrasion while also maintaining the integrity of the strand during the mixing of the concrete. These integral strands are made up of 100 pieces of individual fibers with a low longitudinal weight equal to 45, and therefore their reinforcing effect is very high even at low weight doses [39]. Reinforcing glass fibers have approximately the same bulk density as concrete and therefore do not sink to the bottom of the mixture or float to the surface, their shape is in the Figure 38. They enable a very homogeneous dispersion of the strands throughout the volume of concrete. This type of fiber was designed to improve the mechanical properties of concrete mixtures, especially its tensile strength, impact strength, and ductility. They can replace steel reinforcement nets or wires and prevent cracking. They do not corrode and do not need cover layers. At the same time, they do not negatively affect the workability of the concrete mixture, which is essential to produce slabs with optical fiber distribution in a very dense grid arrangement. It is critical that the GF used, or the material from which they are made, be alkali-resistant [40]. Safe and easy handling in combination with their excellent mixability is another positive feature of glass fibers.

The basic components of my translucent or transparent concrete are glass or polymer fibers and fine-grained concrete. In previous attempts to produce translucent or TC, translucent elements made of glass or other light-conducting materials were mechanically inserted into the concrete mixture. The resulting product is not just a concrete mixture created by mixing several materials, but a completely new material that is homogeneous not only in its internal structure, but also on the surface. The material is produced in prefabricated blocks of various dimensions and is subsequently cut into precise shapes using, for example, a water jet.

Table 3: Technical Parameters - Anti-Crack HP (62.4) – Glass Fibers

Anti-Crak® HP (62.4) – Technical Parameters (Glass Fibers)

Fiber length (mm)	*Filament diameter (µm)*	*Tex*	*Lubricant content (%) ISO 1887 : 1980*	*Humidity (%) ISO 3344 : 1977*
6	14	45	0.08	0.3 max
12	14	45	0.08	0.3 max

- Electrical conductivity: very low
- Specific weight: 2.68 g/cm³
- Material: alkali-resistant glass
- Softening point: 860 °C
- Chemical resistance: very high
- Modulus of elasticity: 72 GPa
- Spring tensile strength: 1700 MPa
- Dosing of thin-walled prefabs up to 70 kg/m³

Figure 38: Glass Fibers [41]

Glass fibers suppress and control the formation of cracks in the concrete (multiple thin evenly distributed cracks). Reduce plastic settlement and crack formation during concrete settlement. Also improve the toughness of concrete, increase resistance to impact and mechanical damage an increase the resistance of concrete to fire. Could

increase the segregation resistance of fresh concrete and reduce concrete bleeding. GF are non-magnetic, corrosion resistant and resistant to alkaline environments. They must be evenly dispersed throughout the concrete volume. Glass fibers improve the concrete's ability to resist tensile stresses and improve the toughness of the concrete. They could reduce the negative effects of volume changes, especially shrinkage. Different types of fibers are different in properties, chemical composition, length, and shape.

4.3 Optical fibers – light transmission

An optical fiber is a cylindrical dielectric waveguide in which electromagnetic waves (usually light or infrared radiation) propagate in the direction of the fiber axis using the principle of total reflection at the interface of two media with a different refractive index [42]. The inner part of the fiber is called the core, around the core is the sheath, its primary protection. To couple the optical signal to the core, the refractive index of the core must be higher than that of the cladding [43]. Although both glass and plastic are transparent at particular wavelengths, allowing the fiber to guide light efficiently, major differences exist between the two materials when it comes to making the optical fiber.

Plastic core fibers are more flexible and inexpensive than glass ones. They are easier to install and can withstand greater stresses and weigh 60 % less than glass fibers [10]. Plastic Optical Fiber (POF), shown in the Figure 40, is a plastic fiber that transmits signals in the direction of its longitudinal axis by means of visible electromagnetic radiation. Most POFs in use are 1000 μm in diameter, of which the core itself is up to 980 μm. Thanks to this diameter, transmission is possible even if the ends of the fibers are slightly dirty or damaged, or if the axis of the beam is slightly bent. The optical properties of POF are of course related to the properties of the plastics themselves [15].

In our experiment we used fibers from PMMA (Polymethyl methacrylate), a synthetic polymer with thermoplastic properties, which is used for the fiber core with refractive indices around 1.49 and 1.59 [44]. The outer shell however is made of silicone resin with a refractive index of 1.46. It can be seen that a relatively large difference in refractive indices is introduced between the core and the mantle [45]. The light transmittance of PMMA is about 92 % in the entire range of the spectrum (this extends up to the UV region). At the same time, PMMA has good mechanical and electrical insulating properties, and is resistant to water, diluted alkalis and acids [42]. The most characteristic feature of PMMA is its clarity and complete lack of color even in thick layers. This allows not only for perfect transparency, but also for easy coloring. PMMA surpasses all conventional thermoplastics in its resistance to weathering [46]. Even after many years of exposure in a tropical climate, it was found to have only minimal changes in its clarity and color. POFs also have a high numerical aperture. Plastics that have useful optical properties typically have a much lower density than optical glasses. POF fiber is also immune to electrical interference and at the same time they are not electrically conductive [47]. POF fibers made of PMMA material with technical

parameters specified in the Table 4 and shown in the Figure 41 were used for our experimental measurements of light properties and the production of concrete slabs with optical fibers. It is important that the optical fibers used, or the material from which they are made, be alkali-resistant.

The development of optical glass fibers and plastic optical fibers is on a dramatic rise today due to their use in telecommunication technologies. Therefore, the optical fibers and cables that were used in the past cannot be compared with those of today. In earlier times, optical fibers, specifically GOF glass optical fibers, were used more for methods of crack detection in structures, and thanks to this, valuable inventions were created that influenced the development of statics and the quality of structures. At the beginning of the 90s, the first forms of translucent concrete were created, which led to the invention of today's modern form with the use of thin optical fibers arranged in a regular grid and with the precise laying of horizontal layers of fibers in the structure.

Light transmission through the unified slabs works with both natural and artificial light. By means of the ends of the fibers, which end on the side surfaces, it is therefore possible to achieve light effects evenly distributed over essentially the entire side surface of the slab, which alternatively emits light. The advantage is that the light-transmitting fibers are completely integrated with the cast material, while the strength of the building block is almost unaffected. Unified slabs create a homogeneous structure with the ability to carry large loads. Fibers that conduct electromagnetic radiation (which are light rays) are used, such as glass fibers, optical fibers, transparent plastic fibers, and the like. The thickness of the fiber can range from a few tenths of a millimeter to several millimeters. The light transmittance of the building block depends on the number of fibers, but a ratio of about 1:10 is suitable. This means that one-tenth of the light emitted to the surface of the slab is emitted by the fibers to the other side of the slab. The volume ratio of cast material and optical fibers ranges from approximately 1:15 to approximately 1:8.

Optical fibers are flexible and can be bundled like cables. They are particularly advantageous over long distances because the light passes through the fiber with little attenuation. The fiber is also immune to electrical interference. Although fibers can be made of transparent plastic, glass, or a combination of both, for long distances glass fibers are always used because of lower optical attenuation. Both multimode and singlemode fibers are used for telecommunications, with multimode fiber being used predominantly for shorter distances up to 550 m (600 yards) and singlemode fiber being used for longer distances.

Sideglow is a filament that emits light both at the end of its section and along its entire length. It can be either soft, hard, or glittery. Endglow is a filament that emits light at the end of its cross-section. It can be either soft or hard. Glass optical fibers are almost always made of quartz, but some other materials, such as chalcogen glasses, are used for longer wavelengths. Like other glasses, these glasses have a refractive index of about 1.5. Plastic optical fibers (POF) are commonly fibers with a core diameter of 0.5 mm or larger. POFs typically have higher attenuation than glass

fibers (1 dB/m or higher), and this high attenuation limits the range for POF-based systems.

There are three basic types of optical fibers, like we can see in the Figure 39:

1) Multimode - Step-index fiber
2) Multimode - Graded-index fiber
3) Monomode - Single mode fiber

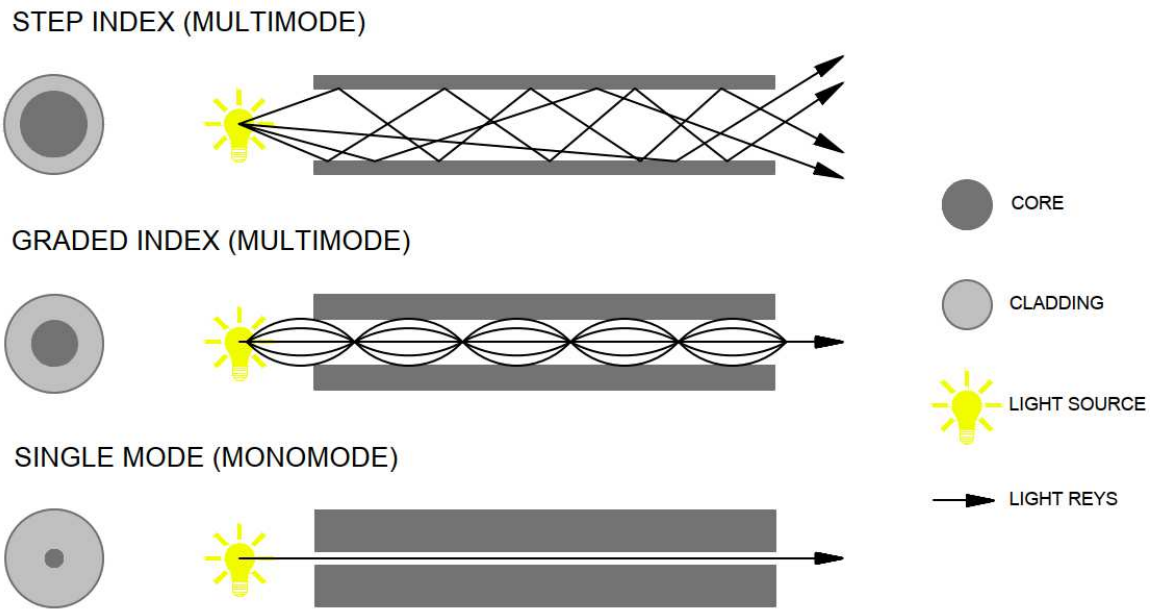

Figure 39: Types of optical fibers

Since the singlemode fibers propagate light in one clearly defined path, intermodal dispersion effects are not present, allowing the fibers to operate at larger bandwidths than a multimode fiber [48]. On the other hand, multimode fibers have large intermodal dispersion effects due to the many light modes of propagation they can handle at one time. The most interesting form of this phenomenon is probably the sharp display of shadows on the opposite side of the wall. Moreover, the color of the light also remains the same. A multimode fiber can propagate hundreds of light modes at one time while singlemode fibers only propagate one mode as shown in the Figure 39 above [49].

For our experimental measurement of light properties and the production of concrete slabs with optical fibers we used POF type fibers made of PMMA, singlemode endglow, as sideglow fibers lose their advantage in this case and would be unnecessarily expensive. For a description of the specifications, see in the Table 4 below:

Table 4: Plastic Optical Fibers (POF) – Multimode – Technical Parameters

POF - Multimode – Technical Parameters (Plastic Optical Fibers)	
Material:	***Optical loss (dB/km)***
PMMA - polymethylmethacrylate	200
The greatest angle of incidence (°)	***External refractive index:***
75	n1 = 1.402 (glass n = 1.5-1.9)
Operating temperature (°C)	***Refractive index of the core layer:***
-10~ + 70	n2 = 1.516
Range of wavelengths:	***Minimum bending radius:***
380-780	8xD

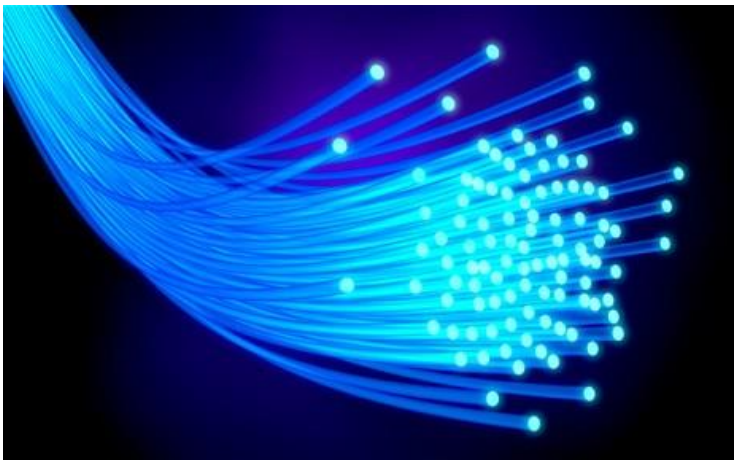

Figure 40: Optical Fibers [50]

Figure 41: Used optical fibers POF

Plastics with useful optical properties typically have much lower density than optical glass. They are lighter and so contribute to consumer pleas. These main reasons have contributed to the expanding use of plastic optics, and probably the biggest goal for the future is the development of the fabrication and replication process, creating opportunities for the production of unique optical components, which could create more possibilities for light transmitting concrete. Greater options in material parameters and manufacturing process principles have allowed engineers to achieve significant reductions in cost (price) in mass production. If the price of optical fibers goes down, the price of translucent concrete will go down too.

The POF is divided into three basic parts: a core consisting of an amorphous transparent polymer, an outer shell consisting of a transparent polymer having a refractive index less than that of the core. The transparent amorphous core polymer is composed of a large group of polymeric substances, namely PMMA (acrylic), polystyrene, polycarbonate (all also in the deuterated state), an alkyl methacrylate copolymer and at least one monomer. The outer shell of the POF contains fluorinated polymers such as polyvinyl fluoride. Polymers used for the outer core shell are thermoplastic (e.g., polyamides, polystyrene or polyacetal) and thermoset (e.g., polyester resins, phenolic resins, or epoxy resins).

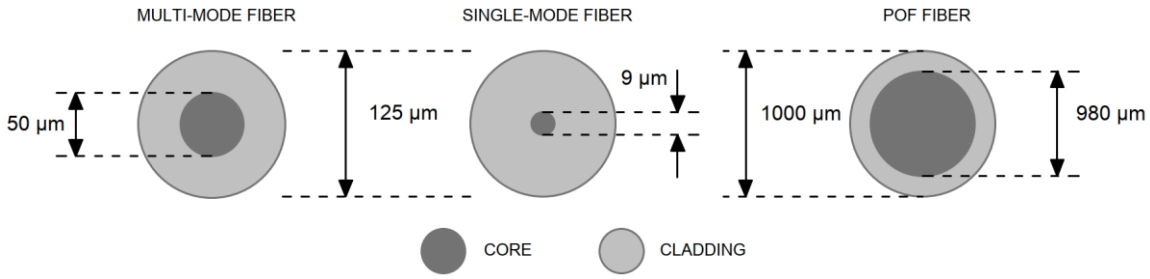

Figure 42: Diagram of comparison of glass and plastic optical fiber

There are two types of optical plastics used, which are referred to as thermoplastics and thermosets. Thermoplastics can be repeatedly softened without changing their chemical composition. This implies that thermoplastics are flowable at elevated temperatures, but some thermoplastics do not flow even at elevated temperatures and others flow without elevated temperatures only due to mechanical pressure. In contrast to thermoplastics, thermosets change their properties due to higher temperature and once cured, the material cannot be melted again by heat. A better understanding of the difference between these two types of plastic requires a better understanding of their molecular structures. The basic and key difference is their linearity or non-linearity. In contrast, thermoplastics are linear, and thermosets are cross-linked [51]. One of the most exciting advances in polymer fibers is the development of micro-structured polymer optical fibers (mPOF), a type of photonic crystal fiber. In larger diameter POFs, 96% of the cross-sectional area forms the core. Similar to traditional glass fibers, light is guided through the core of the fiber. The size of the POF core is in some cases up to 100 times larger than in glass fibers. [42]

4.3.1 Differences between POF and GOF

Many POFs have minimal attenuation for wavelengths located in the visible part of the spectrum and in the near-infrared region (<1.3μm) when using perfluorinated polymers. In contrast, glass optical fibers have minimal attenuation in the >1.5μm region and some GF even at longer wavelengths.

Typical POFs have large propagation attenuations - typically 50 to 100 dB/km, while glass optical fibers can achieve very small attenuations - around 1 dB/km for multi-mode fibers or even well below 1 dB/km for single-mode fibers. This is the reason why POFs are mainly used for light transmission over shorter distances.

POFs are mostly threads with a large core diameter of around 1 mm and a large numerical aperture (e.g., 0.4), which allows POFs to carry a large number of vids. This can be useful when light-emitting diodes are used as light transmitters. In the same way as for glass optical fibers, intermodal scattering can be minimized when using profiles with a graded refractive index. Thus, POFs are not suitable candidates for single-mode lines like glass optical fibers. The differences between the POF and GOF fibers can be seen in the Figure 42.

POFs are mechanically stronger and more flexible. Their multifilament conductors with large cores and high numerical aperture allow them to fit within the tolerances for connectors, and so simple plastic parts are used for which almost no prior knowledge is required. For these reasons (and not because of the cheaper material), they allow POFs offer significant financial savings in many applications.

4.3.2 Polymethylmethacrylate (PMMA)

It is commonly known as plexiglass or acrylic glass is a transparent synthetic polymer with thermoplastic properties. It is prepared by block polymerization, but also by suspension, possibly in emulsion or solution [52]. Block polymerization simultaneously shapes the product (it is done in formworks that have the shape of the future product) [51]. Polymethyl methacrylate is sold under several names (Perspex, Umaplex, Plexiglas, Acron, Acrylon) [53]. It is used for the production of so-called organic glass and various products for domestic and technical use.

Polymerization of methacrylic acid esters for plastics production is usually block or suspension. Of the esters used, methyl methacrylate is the most important. Several block polymerization technologies are used in industrial practice, differing mainly in the shape of the polymerization form (to produce slabs, tubes and rods). The product is often referred to as organic glass.

Block polymerization produces an uncross linked product (average molar mass 0.5 × 106 to 1.5 × 106) or a partially crosslinked product with very good properties. Commercial materials tend to be about 54% syndiotactic, 37% atactic, and 9% isotactic and completely amorphous [51].

The most characteristic property of PMMA is its purity and complete colorless even in thick layers. This allows not only its perfect transparency but also its easy coloring.

PMMA outperforms all conventional thermoplastics in terms of weather resistance. Even after many years of exposure to tropical climates, we find little change in its clarity or coloration.

PMMA is rubbery and easy to form at 130 - 140 °C (which makes it suitable for the manufacture of complex parts of devices). It also has excellent shape memory, which is manifested by the return of the formed plate to its original flat shape when heated to T_m. The light transmittance of PMMA is about 92% over the entire spectral range (extending into the UV region). PMMA has good mechanical and electrical insulating properties and resists water, dilute alkalis, and acids. It does not resist more concentrated acids and hydroxides. It dissolves in aromatic and chlorinated hydrocarbons, esters, ketones, ethers. Can be well machined. Heat resistance without load is about 80 °C. It is not harmful to health and also has the advantage of easy bonding of PMMA by adhesive bonding. Its disadvantage is its low surface hardness [51].

In an oxygen atmosphere, the ignition temperature of PMMA is about 460 °C; when burned, it decomposes without residue [53]. into carbon dioxide and water. It is stable in nature, but readily dissolves with a variety of solvents.

Block PMMA is a relatively expensive plastic, and its use is appropriate where its advantageous properties apply.

PMMA is used in many cases as a substitute for glass; another alternative is polycarbonate. The advantages of PMMA over glass are low production costs, ease of bending, lower weight, and greater impact resistance. The disadvantages are, on the other hand, its lower chemical resistance, and its hardness, which makes it easy to scratch.

4.4 Alkali-Silica Reaction

ASR is a chemical reaction that occurs in concrete when the following three components are present: alkali, water, and amorphous silicon, visual explanation is shown in the Figure 43.

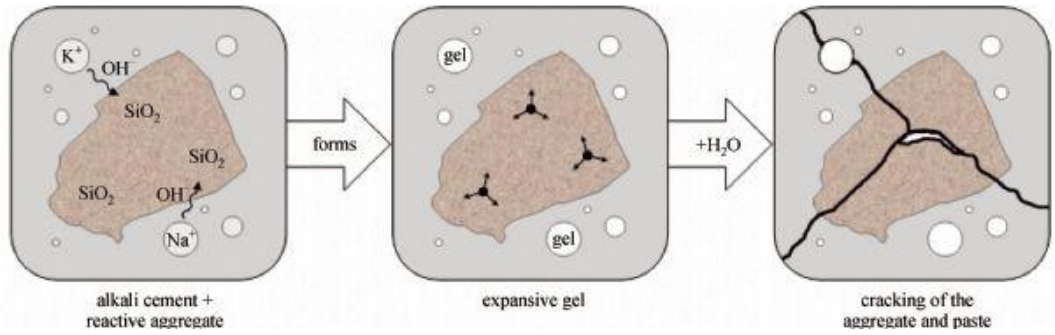

Figure 43: Alkali-Silica Reaction – explanation [54]

Alkalis get into the concrete with cement, or the concrete is so-called doped with alkalis from the environment (part of CHRL). Except for exceptional cases, water is always contained in concrete. Amorphous silicon is part of the aggregate from some quarries. The product of ASR in concrete are gels, the volume of which is greater than the volume of the original components. This can lead to the disintegration (tearing) of the concrete during long-term and intensive exposure.

5 Production Part - Samples

5.1 Production of translucent concrete slabs

The experimental production and measurement of light properties on the samples from high performance concrete mixture with embedded optical fibers or air holes were carried out by a team of technical staff from TBG Metrostav and researchers from Czech Technical University in Prague. The research is focused on unified slabs containing light-transmitting optical fibers embedded in the concrete mixture. The work also deals with the method of manufacturing slabs with light-transmitting optical fibers. The slabs are both practical and decorative. Unified slabs can be used for wall surfaces, floors or as cladding material for interiors and facades. The elements can be illuminated by a single light source or several separate light sources. The lights illuminating the surfaces can shine stationary or they can move and thus create interesting lighting effects.

We can also build the slabs into structures and place a light source in them. In this way, we could create, for example, evacuation markings for buildings, parking systems or object markings (floors, numbering, etc.). We can also use them for perimeter constructions for rooms where we need to provide at least minimal daylight illumination, replace them with prefabricated elements with built-in optical fibers, by placing prefabricated elements with optical fibers at the interface of the exterior with the interior, thus they will transmit daylight into the interior and at the same time, they will function as a rigid perimeter structure. Thanks to the properties of optical fibers, by connecting them to a light source, it was possible to emit electromagnetic radiation of various colors from the light spectrum, through the material onto its surface and thus create unusual light patterns. The combination of a light source and a simple raster graphic image created using optical fibers precisely placed in the prefab opens up completely new possibilities and non-standard solutions.

As mentioned above, it is possible to place optical fibers and light sources in building structures such as walls, ceilings, and floors. However, if we are dealing with larger surfaces with a large number of elements, we have to optimize or robotize the production, because the standard production process is time-consuming and expensive. If we are able to bring natural light into spaces where it was impossible to achieve it by design, it will pay off despite the high costs associated with production.

The production is complex and must be precise, whether it is due to the precise laying of the fibers or the realization process of a large number of holes in the MDF formworks. In all these cases, the solution of prefabricated constructions with embedded optical fibers is offered. In addition to practical solutions to problems with natural light, we can use the material in a wide range of design applications. In the implementation of unified slabs, the number of optical fibers placed in the structure is influenced by the dimensions of the slab, the graphic grid, the architectural plan

and the fact that the strength of the implemented element is not affected. The optical fibers are evenly distributed in the block and carefully filled with a concrete mixture, which must be perfectly compacted. The slab has a homogeneous structure with high strength. If we want to achieve uniform illumination of the element, it is necessary to choose the right light source and ensure the illumination of all optical fibers at the right angle. When creating large samples, it is important to ensure a sufficient number of light sources, their location and correct position in relation to optical fibers. The thickness of unified slabs made of translucent concrete can range from 2 to 5 cm. Since the research was very complex, the whole process was divided into several stages in the following order.

5.2 Design of the sample

The shape of the sample that we constructed for our experiment was determined based on several factors: 1) the dimensions of the sample in relation to its particular use; 2) sample price; 3) sufficient strength; 4) transmission of light information and creation of a simple raster image. The dimensions were chosen to simulate standard construction practice. I tried to copy the dimensions of stone and ceramic cladding as much as possible. For that reason, I chose samples with dimensions of 250x250 mm with thicknesses of 20 mm a 30 mm for comparison. One of the main goals was to make samples for an acceptable price with sufficient strength and light transmitting properties, which would then allow me to create a simple raster image. For the sake of comparison, I used the compressive and tensile flexural strength values of travertine and granite stone.

The definition of a raster image, or two-dimensional matrix of points (pixels), is when each point takes on certain values according to a simple image and forms a continuously filled area (taster). The bit depth defines the maximum number of shades. If I had wanted to achieve the greyscale shade, I would have need 8 bits. But for my purposes I wanted to achieve the color space, so we needed three RGB channels (red, green, blue), which is 24 bits. To succeed I had to place the optical fibers in as dense a grid as possible, while still optimizing the costs of the production of the slabs. Another factor was the compaction of the concrete mixture with the glass fibers, so that it would spread evenly between the individual optical fibers and would not create air gaps that weaken the strength of the slabs. Viewing distance is also very important. The further we are, the clearer the image will seem to us, and the closer we are, the more unclear it will appear. Thus, I chose an observation distance of 2 m the light-transmitting slabs and adapted a grid of optical fibers of 3 mm thickness. The optimal distance of optical fibers in the sample grid, which is dependent upon the clarity of the image, the price of the slabs, and the feasibility of the construction is 15x15 mm. One end of the fiber is positioned to be at 90° to the first side surface and the other end of the fiber is positioned to be also at 90° to the second side surface. The number of individual fibers is arranged parallel in the longitudinal direction of the building block. The fibers are evenly distributed in the block and the ends of the fibers are polished for better light transmission. The fibers allow the light to be transmitted by the building block from the light source from one

surface to the other, or from the exterior to the interior, whereby the light is emitted from the evenly spaced ends of the fibers over essentially the entire illuminated surface. The number of fibers is uniformly distributed over substantially the entire side surface, whereby light can be emitted from the uniformly distributed ends of one side through the rigid material to the other side surface.

5.3 Samples specification

Three types of samples of the same dimensions and two different widths were chosen to produce unified slabs and subsequent experimental measurements. Slabs for my experiment are shown in the Figure 44 . All unified slabs were created from the mixture specified in article 2.2 using 3 mm diameter multimode POF made of PMMA, and Anti-Crak HP (62.4) glass fibers, which improve the mechanical properties of the boards, especially for carrying loads. All slabs were of unified dimensions, namely 250x250 mm with a thickness of 20 and 30 mm, specified in the Figure 45. The samples were divided into the following categories:

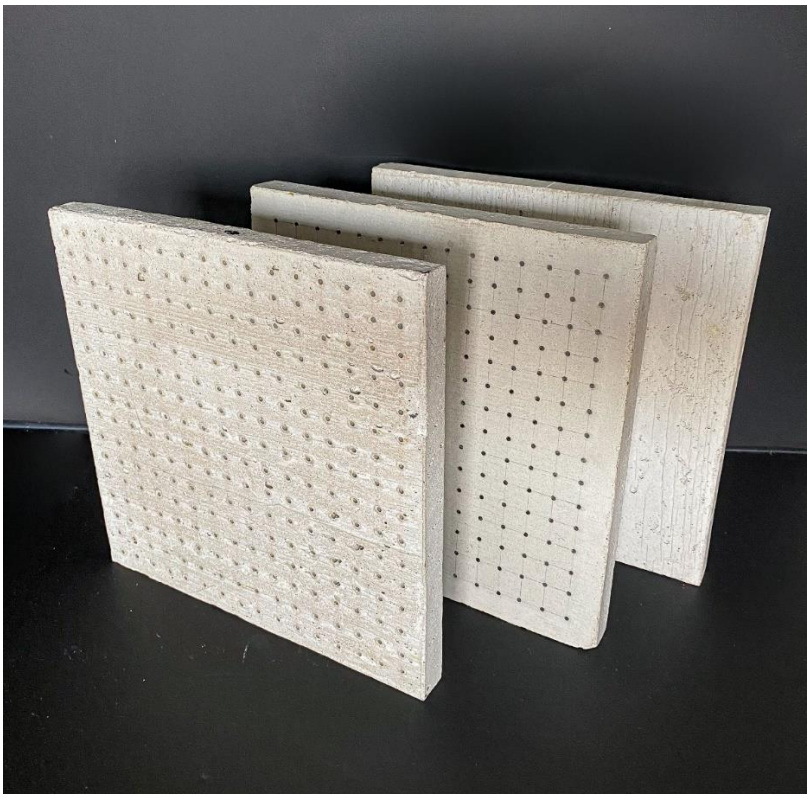

Figure 44: Samples of three types of used slabs

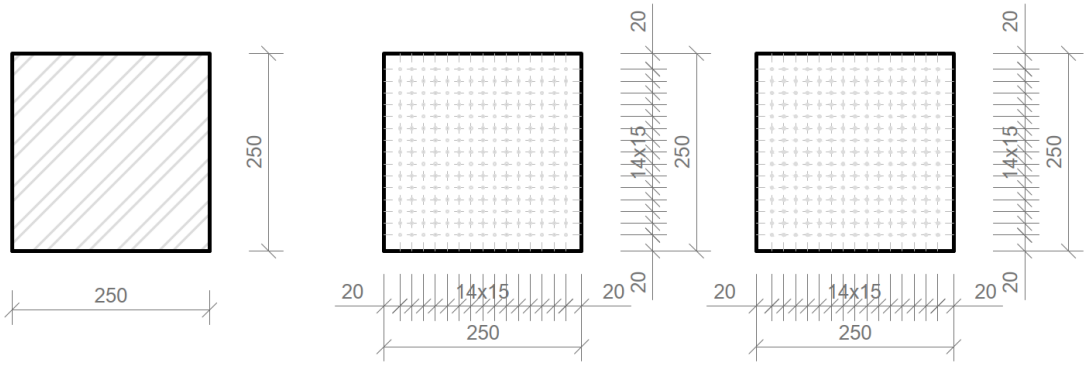

Figure 45: Drawings of concrete slabs used as a samples

Category A:

1) Concrete slab with optical fibers of thickness 3 mm and glass fibers Anti-Crak HP (62.4), dimensions of 250x250x20 mm, POF was placed perpendicular to the exact grid at distance of 15x15 mm, shown in the Figure 46.

2) Concrete slab with optical fibers of thickness 3 mm and glass fibers Anti-Crak HP (62.4), dimensions of 250x250x30 mm, POF was placed perpendicular to the exact grid at distance of 15x15 mm, shown in the Figure 46.

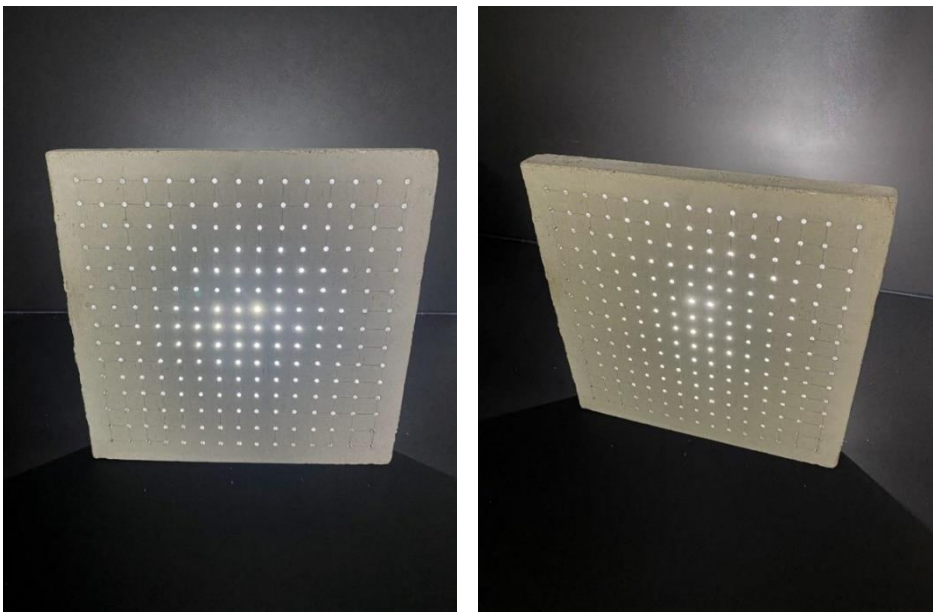

Figure 46: Slabs with POF and GF

Category B:

1) Concrete slab with air holes of thickness 3 mm and glass fibers Anti-Crak HP (62.4), dimensions of 250x250x20 mm, air holes were placed perpendicular to the exact grid at distance of 15x15 mm, shown in the Figure 47.

2) Concrete slab with air holes of thickness 3 mm and glass fibers Anti-Crak HP (62.4), dimensions of 250x250x30 mm, air holes were placed perpendicular to the exact grid at distance of 15x15 mm, shown in the Figure 47.

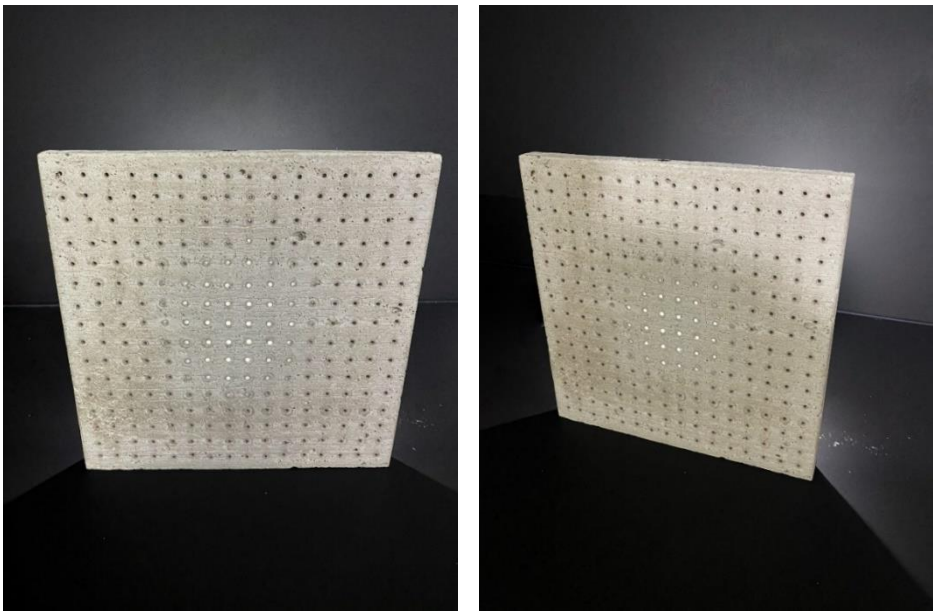

Figure 47: Slabs with air holes and GF

Category C:

1) Concrete slab with glass fibers Anti-Crak HP (62.4), dimensions 250x250x20 mm, shown in the Figure 48.

2) Concrete slab with glass fibers Anti-Crak HP (62.4), dimensions 250x250x30 mm, shown in the Figure 48.

Figure 48: Solid slabs with GF

5.4 Production of samples

A wooden form from medium density fiber board MDF with smooth surface and penetrations for optical fibers was constructed for the casting of translucent concrete, like in the Figure 50 and Figure 57. The form of plywood was designed for the production of unified slabs with dimensions of 250x250x20 mm and 250x250x30 mm, in which the optical fibers were laid in the transverse direction. Optical fibers were placed in a precise orthogonal grid and pulled through individual holes. The same procedure was repeated for the air holes slabs samples, where the fibers were replaced by plastic tubes with steel wires, which were then removed. The mold was sufficiently sealed to prevent cement milk from leaking out of the mold during subsequent compaction. Next, we carefully poured the concrete mixture with glass fibers into the prepared forms between the optical fibers and the rubber tubes, which were reinforced with wires for their stability. We repeated this procedure gradually after several were poured layers. It is very important to compact the concrete mixture carefully, and to remove any air bubbles, which would have a negative impact on compressive and tensile flexural strength. Compaction is complicated by glass fibers so great care must be taken to evenly distribute the mixture between the optical fibers and the rubber tubes with wires. To avoid this outcome, we used a vibrating table to compact the concrete mixture which prevented any air pores from developing as the concrete was poured layer by layer. In addition, we added superplasticizers to better process the mixture and to spread it evenly throughout the mold. After the samples were removed from the framework, any protruding optical fibers were cut, and the slabs were sanded smooth to achieve equality. Finally, the ends of the fibers were cleaned of dirt and any remnants of the concrete mixture and subsequently polished so that their permeability would be of the highest quality. One of the most important factors is also a properly impregnated formwork for a sample of light-transmitting concrete. So that in order to create a product of greater quality than ordinary concretes, it is important that the surface is uniform without air bubbles caused by poor vibration of the mixture in the formwork, so that the samples look according to the required surface quality shown in the Figure 49.

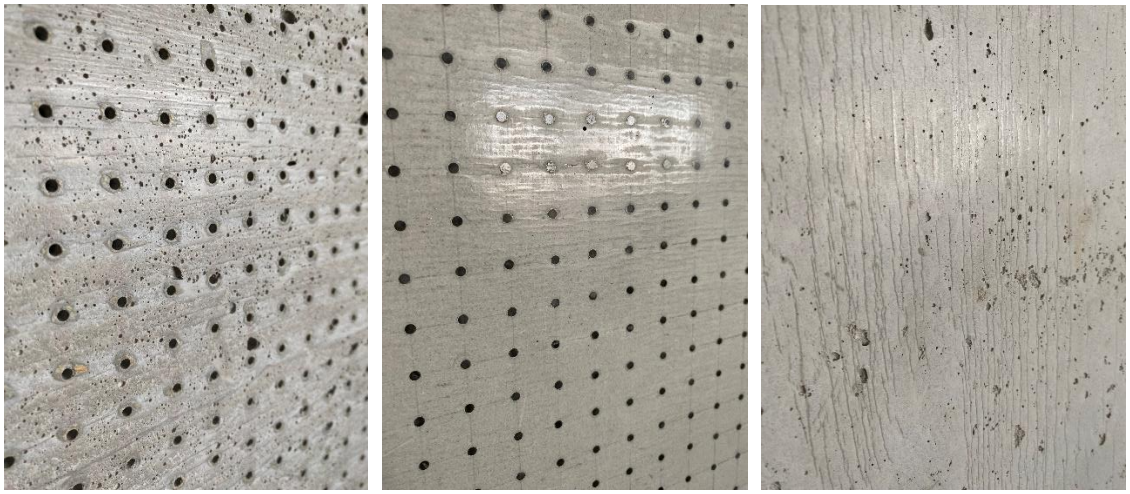

Figure 49: Examples of the surfaces of individual slabs from light-transmitting concrete

5.5 Description of production process

The method of manufacturing unified slabs is divided into several steps. The first step is to create a framework of the given dimensions, including prepared holes, like in the Figure 52, for optical fibers and air holes shown in the Figure 56. In the second step, the framework is precisely impregnated with release oil so that the sample can be removed from the framework without damage and with a visible structure. Light-transmitting concrete slabs could be reinforced with polymer or glass fibers, or 3D glass-textile reinforcement, which is used for textile reinforced concrete (TRC). In our case, unfortunately, we cannot use glass-textile reinforcement, because its placement due to the regular raster network of optical fibers is very difficult. That's why we choose between polymer or glass fibers, in our case, glass fibers seem better in terms of properties. In the third step, glass fibers are mixed into the concrete mixture. In the fourth step, the optical fibers are placed in the framework and regularly arranged in the transverse direction. In the fifth step, the framework is subjected to mechanical pressure or vibration, so that the individual poured layers of concrete mixture with glass fibers are evenly dispersed between the optical fibers and the mixture reaches all places of the framework. In the sixth step, it is necessary to ensure sufficient moisture to harden the sample. In the seventh step, the framework is removed, and the sample is removed. If the slabs are used for a facade system, in the eighth step, it is necessary to apply textile reinforcement to the slab from the non-visible side and coat it with epoxy resin and drill to create holes for masonry screws that are screwed to the anchors.

Figure 50: Formworks for making samples

1) Create a formwork for a LTC unified slabs with optical and glass fibers vias placed in a regular raster grid. The form must be sufficiently impregnated with removal oil for the visibility of the element and easier removal, like in the Figure 57.
2) We perform a complete impregnation of the formwork with removal oil to achieve the visual characteristics of the final product and to allow the block to be easily removed from the form.
3) Place the POF optical fibers, like in the Figure 55, rubber tubes with wires shown in the Figure 56 and Figure 54 and concrete mixture into the impregnated formwork.
4) Check the continuous arrangement of the optical fiber layers in the form. A plurality of optical fibers is placed in the form in parallel shape.
5) Pouring the POF and the GF reinforcement with high-performance concrete. We expose the mixture to mechanical pressure or vibration so that the mixture in the formwork spreads evenly, pours over the optical fibers and does not have air bubbles in it.
6) We provide the specimen with conditions for ideal hardening of the mixture for a minimum of 48 hours in a humid environment to acquire 50% of its strength. This shown in the Figure 51.
7) Carefully remove the samples by unforming. The sample should be easy to remove from the formwork when using a good quality impregnation or removal oil.
8) Shorten the optical fibers according to the surface of the slabs and polish for better light absorption. We also polish the cement surface of the sample to fulfil its aesthetic function.
9) Final sample of the LTC unified slabs, shown in the Figure 58 and Figure 59.

Figure 51: Formworks for making samples

Figure 52: Making penetrations for optical fibers

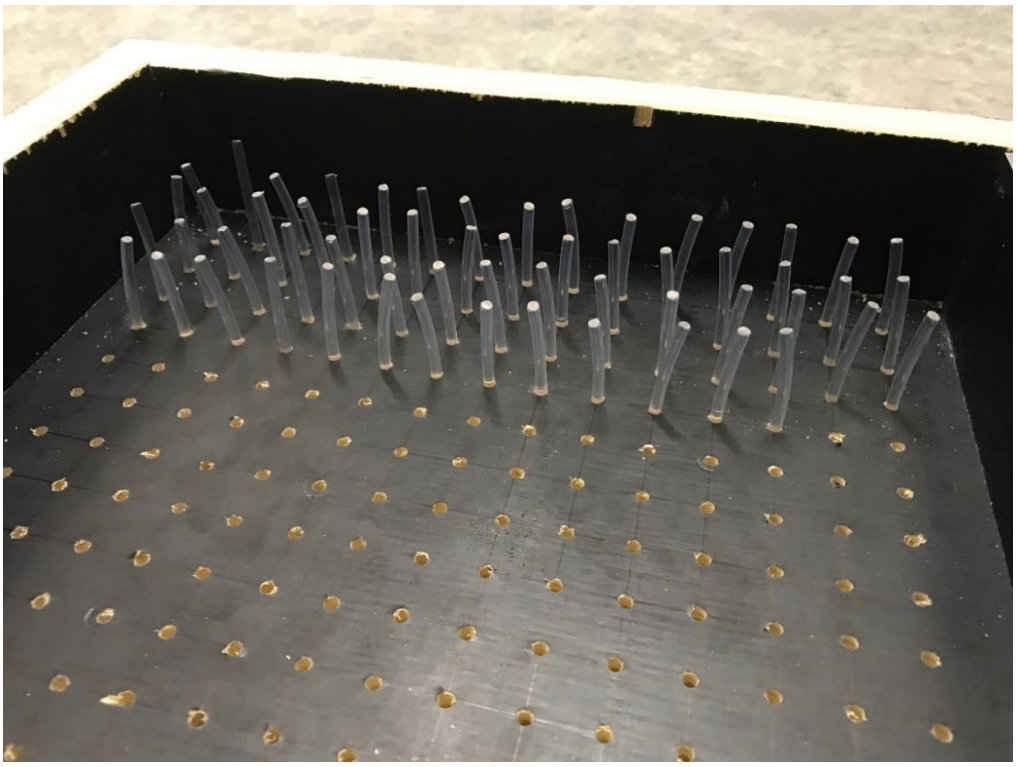

Figure 53: Framework prepared for slabs with plastic optical fibers

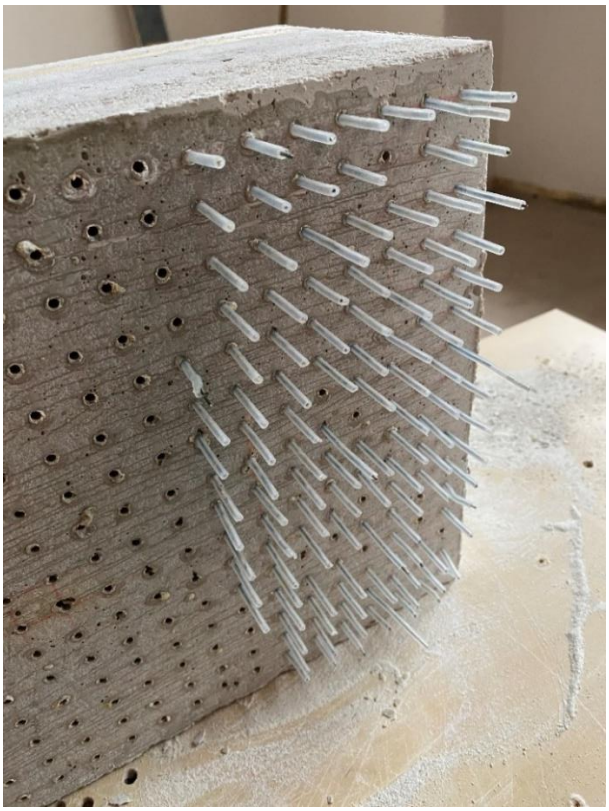

Figure 54: Sample with air holes, created by plastic tubes with wires

Figure 55: Sample with optical fibers POF

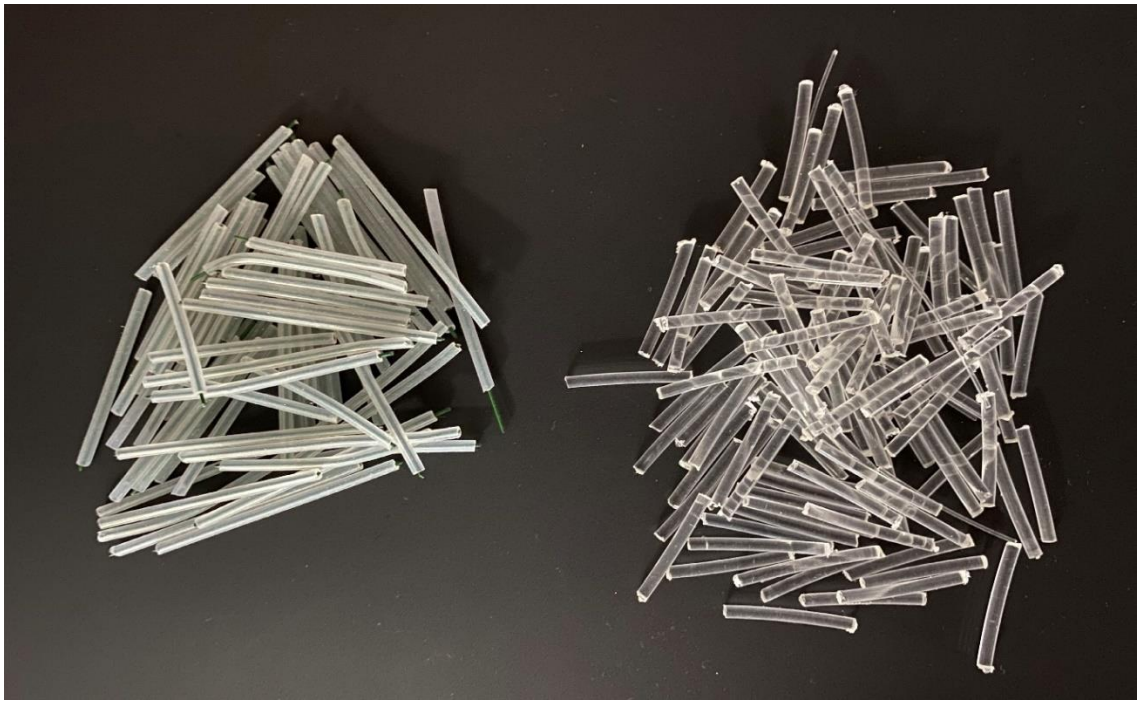

Figure 56: Plastic tubes with wires and optical fibers POF used for experiment

Figure 57: Formworks for making samples

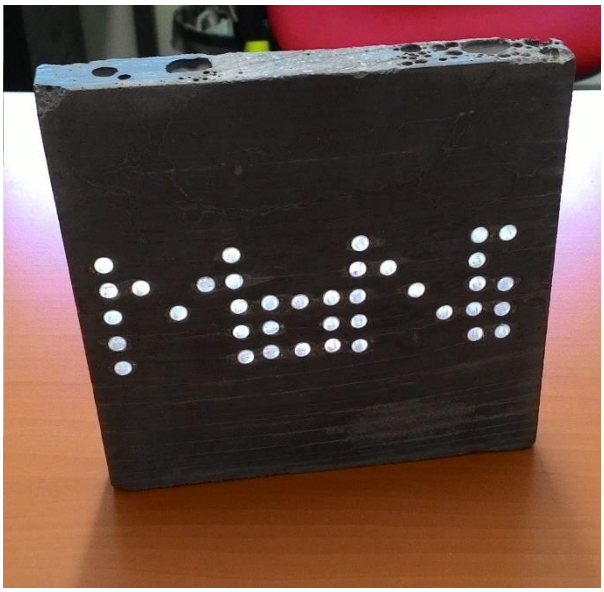

Figure 58: Example of light transmission through the sign on the LTC slab

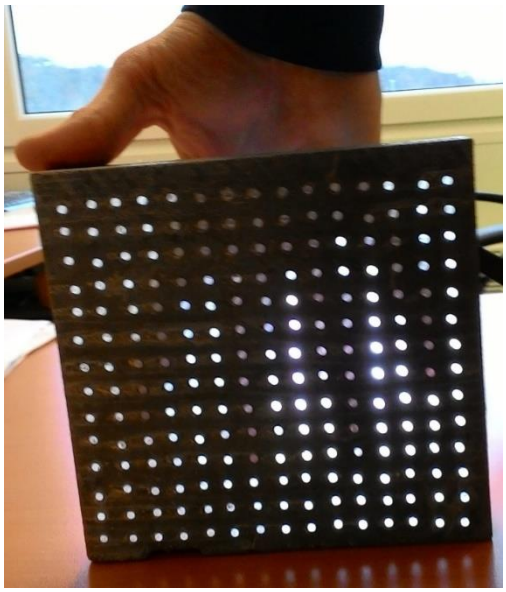

Figure 59: Example of light transmission of the LTC slab

6 Experimental Part – Lightning

6.1 Physical definition of solar radiation

The sun is a source of electromagnetic radiation in a wide range of wavelengths, from cosmic rays λ= 10-13 nm to radio waves λ= 10 nm and more meters. However, only part of this radiation penetrates the earth's surface. Most of the solar radiation is deflected by the Earth's magnetic field or absorbed by the atmosphere. As can be seen in Figure 1, only radiation with a range of 100 to 1400 mm (so-called optical radiation) falls on the earth's surface. Optical radiation is usually divided into three parts; ultraviolet radiation (UV); visible radiation (VR); and infrared radiation (IR). An Air mass (AM) is a coefficient, which we use to define light spectrum at mid-latitudes through the Earth's atmosphere. AM1.5, 1.5 atmosphere thickness, corresponds to a solar zenith angle of z= 48.2°. The AM number is necessary for the overall yearly average for mid-latitudes [55]. It is determined that AM1.5 global irradiation mainly consists of visible light (53.5%), followed by IR (43.2%), and by UV radiation (3.3%) [56]. Ultraviolet radiation has positive effect on human health, as it is necessary for to produce vitamin D, but excessive exposure to UV light can cause degenerative changes in the skin or cause the formation of malignant tumors. Within optical radiation, radiation visible to the human eye with wavelengths of 380 to 760 nm is perceived as a spectrum of colors from violet to blue, to green, to yellow, and red [57]. The electromagnetic spectrum is explained in the Figure 60. Visible light is essential for stimulating sensation in the optical nerves allowing us to perceive the world around us. The last component of optical radiation is infrared radiation. We perceive this radiation on the surface of the body in the form of heat. Regarding building interiors, in the summer, radiation produces unpleasant overheating, but in the winter, it contributes to the heating of buildings. Thermal losses and gains are one of the positive properties of this light-transmitting slabs [58]. This has been proven by a study of translucent concrete panels (TC), which shows us, that the TC panels can reduce energy expenditure by 18% for a fiber volumetric ratio of 5.6%. This demonstrates the practicality of the fabricating TC panels [59]. Due to the high demand for energy in the construction industry, along with its increasing price and market instability, it is crucial to solve the problem of how to reduce these costs. Energy consumption in the industry is estimated at 30-40 % of total world consumption [60]. Even after its completion, continued operation of the building is an energy drain with artificial lighting consuming 19% of the total electricity supplied worldwide [61] [62]. Studies claim that buildings covered with translucent concrete panels consume less energy thus lowering costs and speeding up payback time [63].

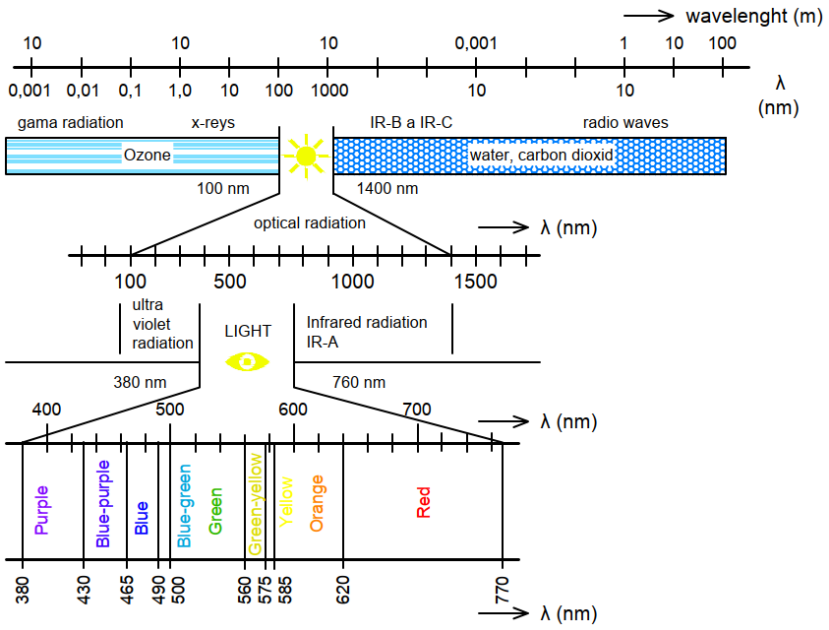

Figure 60: Diagram of electromagnetic Spectrum

6.2 Daylight assessment

To assess the amount or quality of daylight, we worked with a calculation model. Our calculations considered the light scattered in the atmosphere not the influence of direct sunlight on the assessed spaces. Thus, we sought the least favorable sky condition, a uniformly cloudy sky in the winter with dark terrain. Because the sky is brighter forward the Zenith, we considered the graded brightness of the sky. There are two graded brightness models which can be used. For dark terrain CIE 1:3 is used, meaning that the zenith brightness is three times greater than the horizon brightness, while for the snowy terrain model CIE 1:2 is used, which tells us that the zenith brightness is two times greater than horizon brightness. The assessment of daylight is extremely difficult precisely because of these requirements, as the condition of uniformly overcast skies, according to the CIE, occurs only a few days a year. In order to determine a suitable lighting environment, quantitative and qualitative requirements must be fulfilled [64] [65]. The daylighting of indoor spaces in buildings is designed and assessed according to several basic criteria, including: the level of daylight (expressed in terms of daylight factor values); the uniformity of illumination; glare; the distribution of luminous flux and the predominant direction of light; the occurrence of other phenomena affecting visual comfort (e.g., the color of light and its reflection). In our experimental measurements, we assess the side illumination of a room through the perimeter wall of the building. In rooms with permanent residence of people, which are illuminated by side light, at two control points at half the depth of the room, 1 m away from the inner surfaces of the side walls, the value of the daylight factor must be at least 0.7 % at the furthest 3 m away from the window and the average value of these two points must be at least 0.9 %. If the windows are in two adjacent walls, this requirement is sufficient for at least one of the two pairs of these control points. [66]

6.3 Daylight factor assessment

To obtain the values of the daylight factor at the control points, the measurement of the daylight factor under the real sky was used. The daylight factor is not directly measured but is defined as a percentage expression of the illuminance at the control point *E (lx)* to the current horizontal exterior illuminance on an unshaded plane E_h *(lx)*. The instruments used for the measurements were a luxmeter and an illuminance meter. These devices will be discussed in the upcoming chapter 6.7. In order for the measurement to have a meaningful value, we performed a measurement close to the desired condition, that is, in a uniformly cloudy sky in winter [64] [65]. We measured under the real sky close to the conditions CIE 1:3. Due to the above-mentioned conditions of the cloudiness of the sky, the measurement is quite complicated. A scaled-down model of a reasonably sized room was used for the measurement, and a luxmeter sensor was subsequently placed in the model. It is important that all the materials used in the model correspond to a real setting with their type of color and light reflection factors. To verify the measurement performed to obtain these factors, a control calculation method was used. There are some important factors to consider when evaluating light-transmitting structures. The light falling on the structure must therefore be divided into several parts: transmitted light, reflected light and absorbed light [67] [68].

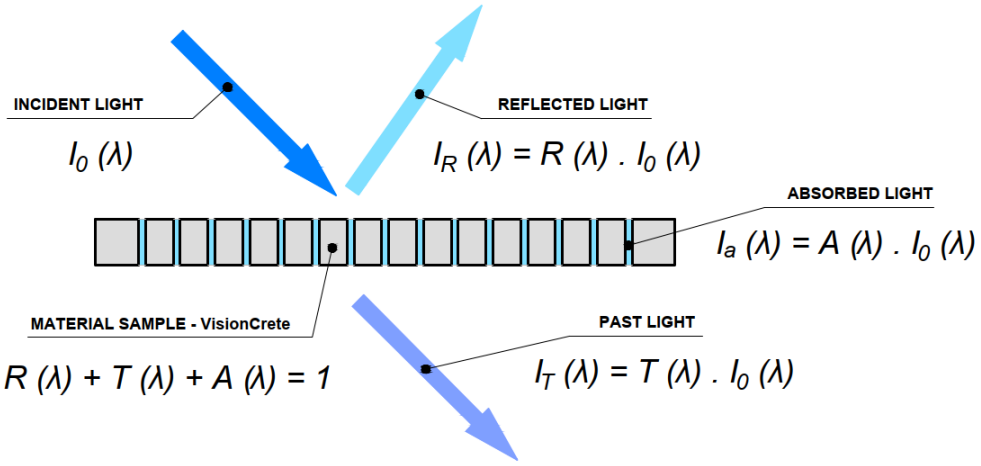

Figure 61: Diagram of the impact of the sun's rays

The spectral transmittance of the material T (λ) is defined as the ratio of the radiation I_T (λ) passed through the sample to the intensity of radiation I_0 (λ) incident on the sample, as shown in the Figure 61. The light transmission performance of translucent concrete decreases as the angle of incidence of light increases, 30° is the limit of the acceptance angle of an optical fiber, and at this point most of the light is outside the acceptance cone, meaning that it contains the entire area of internal reflection [69].

6.4 Quantitative and qualitative level of daylight

The daylight factor *D (%)* is used to express the quantitative level of daylight. This factor is defined as a percentage expression of the illuminance at the control point *E (lx)* to the current horizontal exterior illuminance on an unshaded plane E_h *(lx)*. The measurement of the individual parameters must take place at the same time. The relationship from which I am able to calculate the daylight factor is given in the Equation 2 below:

$$D = \frac{E}{E_h} . 100 \ (\%) \tag{2}$$

The horizontal exterior illuminance E_H *(lx)* is dependent on the average brightness of the sky L_m *(cd.m²)*, it represents the sky illuminance incident on a horizontal plane that is not shaded and is determined from the relationship in the Equation 3 below:

$$E_h = \pi . L_m \ (lx) \tag{3}$$

The quality criteria of daylighting include, distribution of light flux, distribution of brightness of surfaces in the field of vision, prevention of glare, color design of the interior and uniformity of daylight.

The uniformity of daylight can be influenced by certain factors. Such as the height of the room and even, the height of the room. Even bright painting, or the use of light-scattering materials like curtains and glass. Evenness of daylight is also influenced by the position of the windows (a higher location is preferable) and the color of the shading objects (the lighter the better) [59].

For our case, illuminance is one of the most important physical quantities to be detected. In practice, it is one of the most used criteria in the evaluation of light.
The illuminance E is defined by the value of the luminous flux dΦ falling on an area of 1 m^2. Illuminance is given in lux *(lx)*, which represents a luminous flux of 1 lumen *(lm)* spread over an area of 1 m^2. It was calculated from the relationship in the Equation 4 below, but in our case, it will be measured with the appropriate instruments.

$$E = \frac{d\Phi}{dS} \ (lx) \tag{4}$$

6.5 Light reflection factor assessment

One of the key parts of this article is the measurement of the light reflection factor ρ (-) on the individual surfaces of the unified plates. This factor is based on the relationship in the Equation 5 below:

$$\rho = \frac{\pi .L}{E} \text{ (-)} \quad (5)$$

Partial values for obtaining the light reflection factor were measured using an illuminance meter and a luxmeter. The measurements took place in such a way that the illuminance meter was aimed and focused in a direction perpendicular to the measured surface and the surface brightness *L (cd/m²)* was taken. At the same time, the illuminance *E (lx)* of the given surface was measured using a luxmeter. During measurement, the sensor of the luxmeter could not interfere with the viewing angle of the illuminant, and at the same time the illuminant and the person operating the device must not shade the sensor of the luxmeter. Because the measurement of brightness and illuminance must be carried out simultaneously, it is necessary to engage the cooperation of two experimental workers. The values of the light reflection factor were normally proposed for main surfaces of the interior spaces in average values, where we use the reflection factor value of 0.7 for ceilings, 0.5 for walls and 0.3 for floors or floor coverings.

6.6 Measurement of the light transmission factor

The values of the light transmission factor for clear plate glass from 3mm to 4mm has a value of $\tau_{S,nor}$= 0.92, row glass $\tau_{S,nor}$= 0.88, laminate with fiberglass $\tau_{S,nor}$= 0.35-0.85, clear acrylic (commonly known as Plexiglas) then has values of $\tau_{S,nor}$= 0.85-0.92.

Another investigated parameter is the light transmission factor of filling the lighting holes, which was determined from the relationship mentioned in the Equation 6 below:

$$\tau_{s,nor} = \frac{L_S}{L_0} \text{ (-)} \quad (6)$$

First, the brightness of the sky or other background is measured through the illumination hole, in a perpendicular direction, using an illuminance meter. This gives the brightness value L_s *(cd/m²)* during the measurement. After that, the aperture is opened as quickly as possible and the brightness of the sky or other background is measured without the influence of the aperture, which gives us the brightness value L_0 *(cd/m²)*. Than the measured brightness values are inserted into relation $\tau_{S,nor} = L_S/L_0$ and thereby obtain the light transmission factor of the filling of the lighting opening $\tau_{s,nor}$. Measured values are shown in the Table 5.

Table 5: Light transmission factor $\tau_{s,nor}$ (-)

Light transmission factor $\tau_{s,nor}$ (-):		
values of the light transmission factor when measured against a sunny facade		
Slab 250x250mm, with optical fibers d= 3mm, thickness 20mm		
L_S (cd/m²)	***L_O (cd/m²)***	***$\tau_{s,nor}$ (-)***
158.1	4733	0.033
181.7	1779	0.102
220.5	1398	0.158
values of the light transmission factor when measured against a non-sunlit facade		
Slab 250x250mm, with optical fibers d= 3mm, thickness 20mm		
L_S (cd/m²)	***L_O (cd/m²)***	***$\tau_{s,nor}$ (-)***
151.7	1166	0.130
387.5	1117	0.347
307.0	1075	0.286
values of the light transmission factor when measured against a white wall in the room		
Slab 250x250mm, with optical fibers d= 3mm, thickness 20mm		
L_S (cd/m²)	***L_O (cd/m²)***	***$\tau_{s,nor}$ (-)***
36.18	170.7	0.212
37.94	170.8	0.222
39.18	171.8	0.228

6.7 Measuring devices and aids

In order to obtain the input values of the light reflection factor of individual surfaces and the input data for determining the light transmission factor through the unified slabs using optical fibers, two measuring devices were used, namely an illuminance meter and a luxmeter. These measuring devices are the property of the Department of Building Structures of the Faculty of Civil Engineering of the Czech Technical University in Prague. Per the accuracy requirements, instruments were calibrated (corresponded to the accuracy) ČSN 36 0011-1 [67].

Konica Minolta Luminance Meter LS - 110, which has the following parameters in the Table 6, was used to measure illuminances *L (cd.m²)*:

Table 6: Device for measuring illuminance - Konica Minolta Luminance Meter LS-110

Konica Minolta Luminance Meter LS - 110	
Measuring angle	1/3°
Viewing angle	9°
Range from 0.001 cd.m² to 299.99 cd.m²	
Focusing distance from 1014 mm to infinity	
The relative spectral response is 8 % of the CIE spectral luminous efficiency V (λ)	

Konica Minolta Illuminance Meter T – 10AM was used as another device to measure illuminance. It is a luxmeter with a removable receptor head and has the following parameters, which are in the Table 7 below:

Table 7: Device for measuring illuminance - Konica Minolta Illuminance Meter T-10AM

Konica Minolta Illuminance Meter T - 10AM
Accuracy ±2 % ± 1 digital displayed value
Equipped with a cosine deviation filter
Range from 0.001 lx to 299.99 lx
Relative spectral response is 6 % of CIE spectral luminous efficiency

6.8 Daylight transmission test of a simulated horizontal structure made of light-transmitting concrete on a down-scaled model of the room

Climatic conditions, which significantly affect the measurement itself, we were documented prior at beginning. When we measured the daylight factor values, we chose a day with uniformly cloudy sky, which form a kind of diffuser that evenly scatters the light. At the same time, we tried to approximate the 5000 lx illuminance values on an outdoor unshaded horizontal plane when assessing illuminance. In addition, to 20 000 lx of illuminance on an outdoor unshaded horizontal plane when assessing lighting quality, such as daylight uniformity. Measured values are shown in the Table 8. Daily temperatures were 18 to 22°C. North-easterly wind was at a speed of 2 to 6 m/s. Relative air humidity was 83%. Each time, we first measured the brightness of the sky and then the illuminance at the control points. To simulate the passage of daylight through the light-transmitting concrete structure, we created a modified room model. The scaled-down model of a room of dimensions 250x250x250 mm has been created at a scale of 1:20 and is therefore intended to symbolize a room of dimensions 5x5x5 m, with one of its perimeter walls made of light-permeable concrete, it is shown in the Figure 62. In our case, the ceiling structure was replaced by a concrete slab made of translucent concrete, through which light can pass into the interior. The scaled-down model was made of dark-colored wooden medium density fiber boards to avoid light reflection as much as possible. Whole design of the model is shown in the Figure 63. During the measurement, the entire space is closed in order to limit the leakage of light or its penetration into the model. The ends of the optical fibers are carefully cleaned and polished so that the measurement cannot be affected by the contamination factor. Shading obstacles that could affect the measurement are eliminated in our case as we focus on the light values of the material itself.

For the horizontal construction, we used several types of slabs, as shown in the Figure 65, which we then measured separately through control points in a scaled-down model of the room. Subsequently, we placed the control points on the comparison

plane of the room, or on the bottom plate of the reduced model of the room. Measurements were made using two luminometers, which simultaneously measured the illuminance at the point under consideration inside the room E (lx) and the exterior illuminance on the unshaded horizontal plane Eh (lx). The layout of the measurement points is defined in the Figure 64. There are 7 control points. We used several types of slabs: 1) 20 and 30 mm thick concrete mix slabs with 3 mm diameter plastic optical fibers (POF) 2) 20 and 30 mm thick concrete mix slabs with 3 mm diameter air holes 3) Solid 20 and 30 mm thick concrete mix slabs. Measured values of illumination are shown in the Table 9 and values of reflection factor are shown in the Table 10.

The results of the daylight factor measurements are then plotted and compared in the Figure 66. The results of the reflection factor measurements are then plotted and compared in the Figure 67.

Table 8: Distribution of the Sky Brightness

Distribution of the Sky Brightness				
Zenith:	**19390**	**cd/m²**	**18740**	**cd/m²**
Horizon:	5203	cd/m²	5180	cd/m²
	4892	cd/m²	4998	cd/m²
	5357	cd/m²	5287	cd/m²
	4592	cd/m²	4624	cd/m²

Figure 62: Down-scaled model for measurements

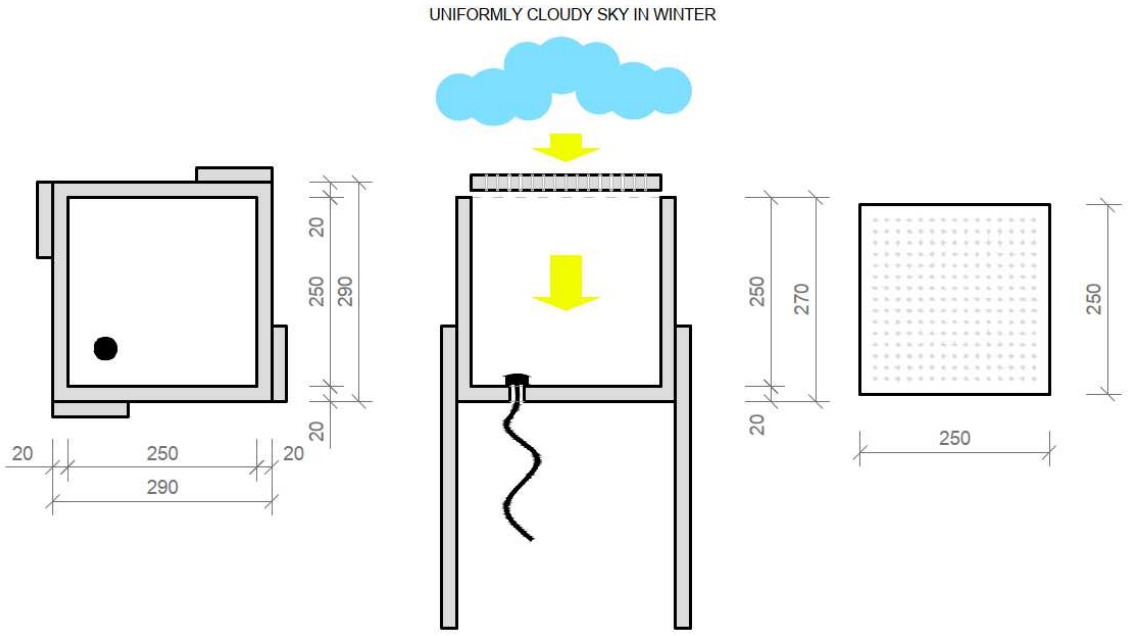

Figure 63: Plans and sections of the scaled-down model used for measuring

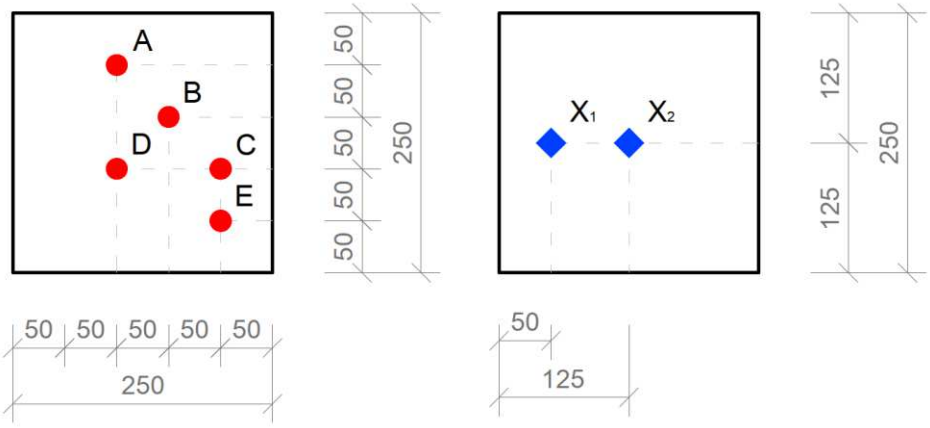

Figure 64: Drawings of measurement points on horizontal plane

Figure 65: LTC slab on top of the Down-scaled model ready for measuring

Table 9: Illumination E (lx) and Daylight factor D (%)

Illumination E (lx) and Daylight factor D (%):			
Slab 250x250 mm, with optical fibers d= 3 mm, thickness 20 mm			
Bod	***E (lx)***	***E_H(lx)***	***D (%)***
A	18.30	5250	0.348
B	23.70	4860	0.488
C	22.00	5180	0.425
D	23.90	5190	0.460
E	21.60	5940	0.363
1	10.70	4800	0.223
2	15.10	4800	0.314
Slab 250x250 mm, with air holes d= 3 mm, thickness 20 mm			
Bod	***E (lx)***	***E_H(lx)***	***D (%)***
A	1.80	5760	0.031
B	2.49	5500	0.045
C	2.40	5910	0.041
D	2.18	4920	0.044
E	3.78	5835	0.065
1	0.90	4600	0.020
2	1.14	4780	0.024
Slab 250x250mm, with optical fibers d= 3mm, thickness 30mm			
Bod	***E (lx)***	***E_H(lx)***	***D (%)***
A	18.70	4900	0.382
B	23.10	5250	0.440
C	23.10	5680	0.406
D	20.60	4760	0.432
E	22.20	5260	0.421
1	14.00	4640	0.301
2	16.00	4760	0.336
Slab 250x250mm, with air holes d= 3mm, thickness 30mm			
Bod	***E (lx)***	***E_H(lx)***	***D (%)***
A	1.30	4880	0.027
B	1.14	5225	0.022
C	0.82	5710	0.014
D	0.96	4490	0.021
E	0.78	5110	0.015
1	0.54	4720	0.011
2	0.50	4740	0.011
Solid slab 250x250mm, thickness 20mm and 30mm			
Bod	***E (lx)***	***E_H(lx)***	***D (%)***
A	0.00	4790	0.000
B	0.00	5180	0.000
C	0.00	5670	0.000
D	0.00	4390	0.000
E	0.00	5080	0.000
1	0.00	4670	0.000
2	0.00	4690	0.000

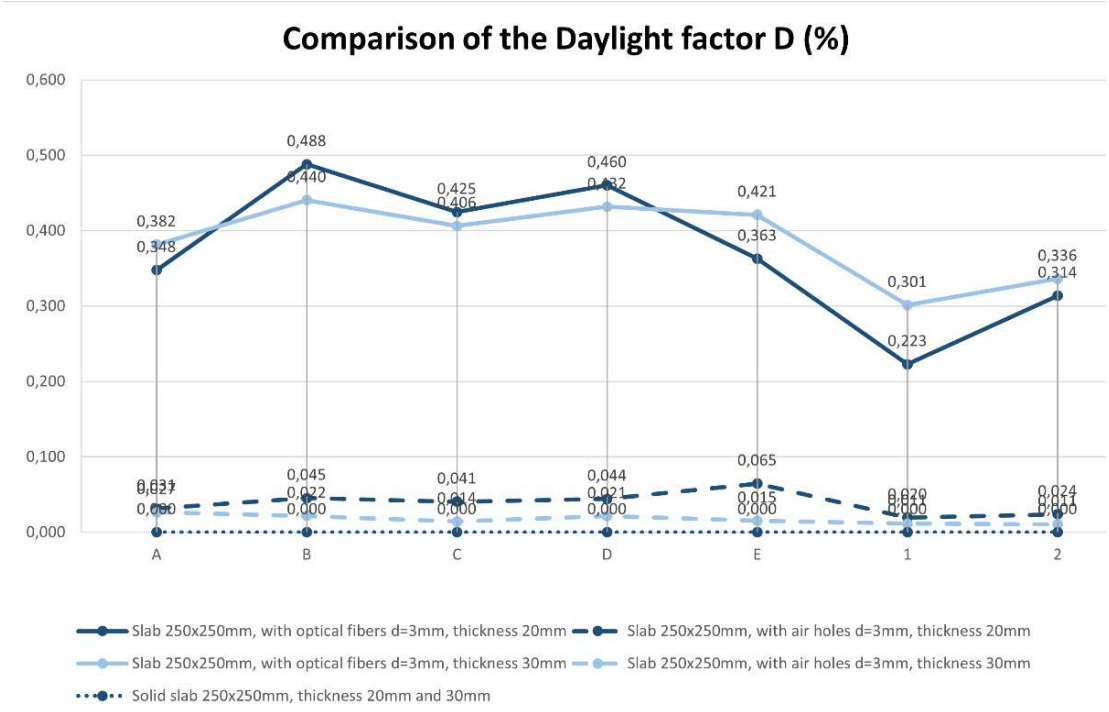

Figure 66: Comparison of the Daylight factor D (%)

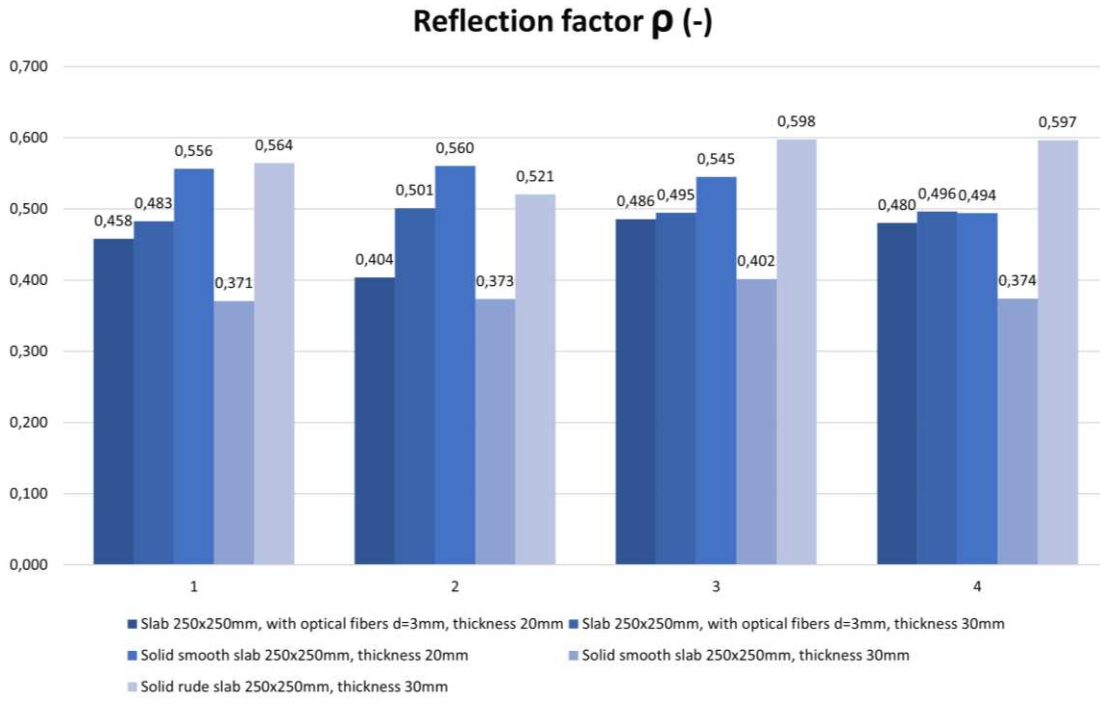

Figure 67: Reflection factor ρ (-)

Table 10: Reflection factor ρ (-)

Reflection factor ρ (-):		
Slab 250x250mm, with optical fibers d= 3mm, thickness 20mm		
E (lx)	***L (cd/m2)***	***ρ (-)***
5010	730.6	0.458
5080	652.9	0.404
4960	767.0	0.486
4980	761.5	0.480
Slab 250x250mm, with optical fibers d= 3mm, thickness 30mm		
E (lx)	***L (cd/m2)***	***ρ (-)***
4910	754.6	0.483
4930	786.6	0.501
4770	750.9	0.495
4690	740.7	0.496
Solid smooth slab 250x250mm, thickness 20mm		
E (lx)	***L (cd/m2)***	***ρ (-)***
4540	804.0	0.556
4450	793.6	0.560
4450	771.9	0.545
4400	691.7	0.494
Solid smooth slab 250x250mm, thickness 30mm		
E (lx)	***L (cd/m2)***	***ρ (-)***
4070	480.4	0.371
4030	478.9	0.373
3990	510.3	0.402
3920	467.0	0.374
Solid rude slab 250x250mm, thickness 30mm		
E (lx)	***L (cd/m2)***	***ρ (-)***
4410	792.1	0.564
4150	687.6	0.521
4110	782.0	0.598
4100	778.7	0.597

6.9 Measurement of light transmission from an artificial light source through a simulated vertical structure from light-transmitting concrete between two rooms on their down-scaled model

Climatic conditions, which significantly affect the measurement itself, were documented before the measurement. On the day of the measurement, it was uniformly cloudy sky. Daily temperatures were 22 to 26°C. South-east wind was at a speed of 2 to 6 m/s. Relative air humidity was 91%.

Used light source: RYET LED 400lm; 4.4W; 2700K; 15,000 hours; E14; 220-240V~50/60Hz; CRI>80; 91lm/W; LED1717G5

For our measurement of light transmission from an artificial source, we used a similar scaled-down room model to measure the illumination, like in the Figure 68 and Figure 69. We research light transmission through the dividing wall between two rooms without access to daylight, where the only light was from an artificial light source. Shading obstacles that could affect the measurement are eliminated in our case as we focus on the light values of the material itself. A scaled-down model of two adjacent rooms with dimensions of 250x250x250 mm at a scale of 1:20 was chosen and shown in the Figure 72. We made the walls, floor and ceiling of the model from black boards. The rooms were 100% sealed against the access of any other light that could negatively affect the measurement. In general, for measurement dark color is better to used, so that there is no light reflection, or the values of reflection factor were close to zero. At the same time the surface is not shiny, so that the measurement is as accurate as possible. During the measurement, the entire space is closed in order to limit the leakage of light or its penetration into the model. It assesses the amount of light that the source emits and that passes through the construction simulating the wall. The ends of the optical fibers are carefully cleaned and polished so that the measurement cannot be affected by the contamination factor. We gradually move the vertical structure away from the source by enlarging one room and changing the other. We gradually measure the values of light penetration into the other room and the light emitted in the room with the source for both cases at individual control points. Thanks to the light-transmitting concrete construction, we are able to multiply the effectiveness of the artificial light source. When the rays from this source will illuminate the room not only the one with the light source, but also the adjacent room when passing through the light-transmitting concrete structure. We placed the control points on the comparison plane of the room, or on the bottom plate of the reduced model of the room. The layout of the measurement points is defined in Figure 73. There are 7 control points. Due to the optical fibers, both natural and artificial light can transmit through the translucent concrete. The main goal is to reduce the lighting power consumption by using sunlight as a light source or use an artificial light source for more spaces or multiply its potential [70]. We use several types of slabs: 1) 20 and 30 mm thick concrete mix slabs with 3 mm diameter plastic optical fibers (POF) 2) 20 and 30 mm thick concrete mix slabs with 3 mm diameter air holes 3) Solid 20 and 30 mm thick concrete mixture slabs. The measurement process is shown in the Figure 70 and Figure 71. Measured

values of illumination are shown in the Table 11 and Table 12. On the contrary, values of reflection factor are shown in the Table 13. The results of the illumination measurements are then plotted and compared in the Figure 74. Measurements of the reflection factor are then plotted and compared in the Figure 75.

Figure 68: Down-scaled model for measurement

Figure 69: Down-scaled model for measurement

Figure 70: Down-scaled model, points of measurement, artificial light source

Figure 71: Down-scaled model, points of measurement, artificial light source, sensor

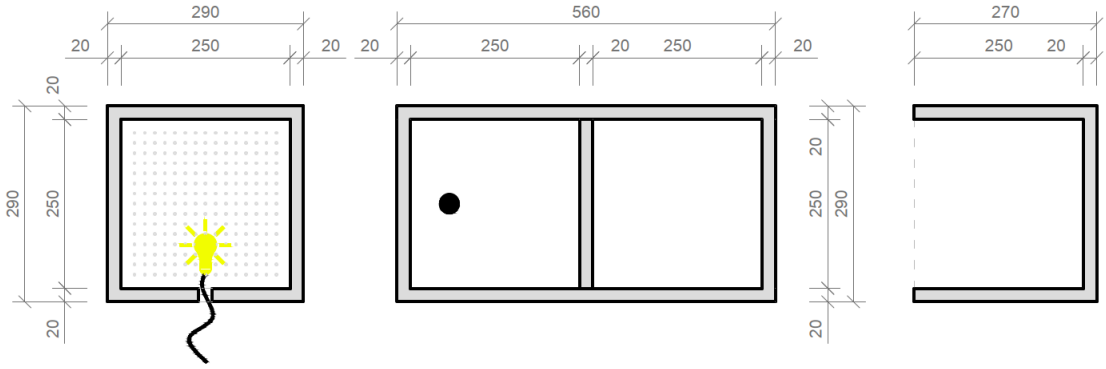

Figure 72: Plans and sections of the scaled-down model

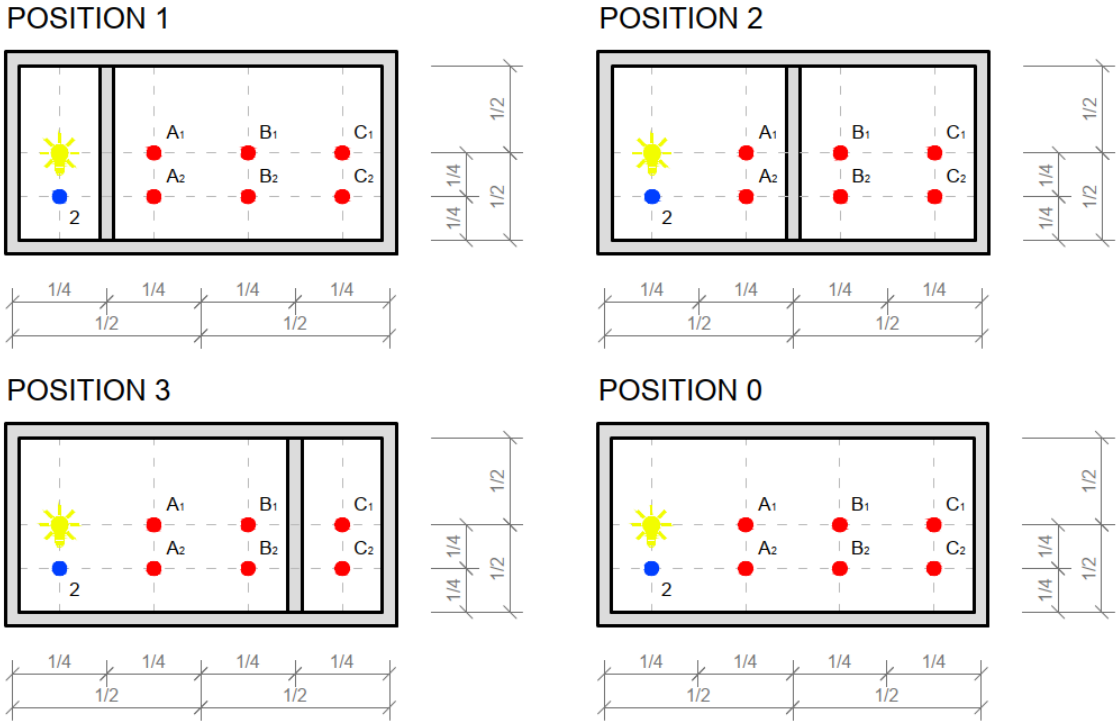

Figure 73: Drawing of measurement points

Table 11: Illumination E (lx) – Part 1

Illumination E (lx):			
Slab 250x250mm, with optical fibers d= 3mm, thickness 20mm			
Point	***Position 1***	***Position 2***	***Position 3***
	E (lx)	***E (lx)***	***E (lx)***
A1	5.40	x	x
A2	3.29	x	x
B1	4.28	2.23	x
B2	3.77	1.49	x
C1	1.60	1.83	1.06
C2	1.72	1.19	0.72
Slab 250x250mm, with air holes d= 3mm, thickness 20mm			
Point	***Position 1***	***Position 2***	***Position 3***
	E (lx)	***E (lx)***	***E (lx)***
A1	0.05	x	x
A2	0.02	x	x
B1	0.06	0.05	x
B2	0.04	0.03	x
C1	0.06	0.04	0.04
C2	0.05	0.04	0.04
Slab 250x250mm, with optical fibers d= 3mm, thickness 30mm			
Point	***Position 1***	***Position 2***	***Position 3***
	E (lx)	***E (lx)***	***E (lx)***
A1	5.17	x	x
A2	3.37	x	x
B1	5.56	2.10	x
B2	4.18	2.07	x
C1	2.11	1.85	1.26
C2	2.38	1.66	1.05
Slab 250x250mm, with air holes d= 3mm, thickness 30mm			
Point	***Position 1***	***Position 2***	***Position 3***
	E (lx)	***E (lx)***	***E (lx)***
A1	0.02	x	x
A2	0.00	x	x
B1	0.01	0.02	x
B2	0.00	0.00	x
C1	0.01	0.02	0.02
C2	0.00	0.01	0.02

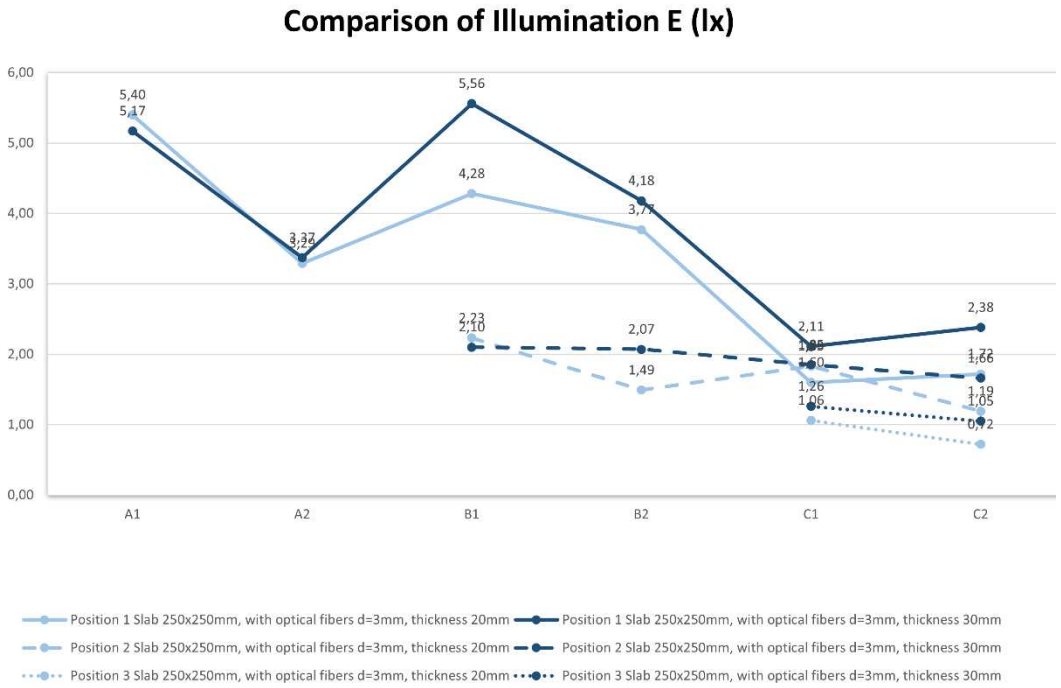

Figure 74: Comparison of Illumination E (lx)

Table 12: Illumination E (lx) – Part 2

Illumination E (lx):			
Empty test model/sample 500x250x250mm		**Empty test model/sample 250x250x250mm**	
Point	***E (lx)***	***Point***	***E (lx)***
A1	402.00	A1	442.00
A2	338.00	A2	368.00
B1	109.10	B1	x
B2	101.90	B2	x
C1	48.70	C1	x
C2	45.80	C2	x
1	position of light source	1	position of light source
2	698.00	2	730.00
Empty test model/sample 375x250x250mm		**Empty test model/sample 125x250x250mm**	
Point	***E (lx)***	***Point***	***E (lx)***
A1	394.00	A1	x
A2	342.00	A2	x
B1	107.10	B1	x
B2	103.30	B2	x
C1	X	C1	x
C2	X	C2	x
1	position of light source	1	position of light source
2	711.00	2	762.00

Table 13: Reflection factor ρ (-)

Reflection factor ρ (-):					
Slab 250x250mm, with optical fibers d= 3mm, thickness 20mm			**Slab 250x250mm, with optical fibers d= 3mm, thickness 30mm**		
E (lx)	***L (cd/m2)***	***ρ***	***E (lx)***	***L (cd/m2)***	***ρ***
369	71.20	0.606	551	85.26	0.486
377	73.59	0.613	547	88.46	0.508
471	77.42	0.516	542	90.65	0.525
527	76.66	0.457	535	88.03	0.517
525	74.30	0.445	564	87.17	0.486
533	74.40	0.439	565	88.35	0.491
Solid smooth slab 250x250mm, thickness 20mm			**Solid smooth slab 250x250mm, thickness 30mm**		
E (lx)	***L (cd/m2)***	***ρ (-)***	***E (lx)***	***L (cd/m2)***	***ρ (-)***
454	90.90	0.629	444	43.79	0.310
477	83.09	0.547	406	52.13	0.403
450	88.38	0.617	425	58.32	0.431
456	79.39	0.547	418	56.45	0.424
Solid rude slab 250x250mm, thicknes 30mm			**Black smooth slab 250x250mm, thickness 30mm**		
E (lx)	***L (cd/m2)***	***ρ (-)***	***E (lx)***	***L (cd/m2)***	***ρ (-)***
440	86.69	0.619	473	1.74	0.012
472	89.44	0.595	479	1.89	0.012
457	99.69	0.685	429	1.35	0.010
452	92.43	0.642	435	1.43	0.010

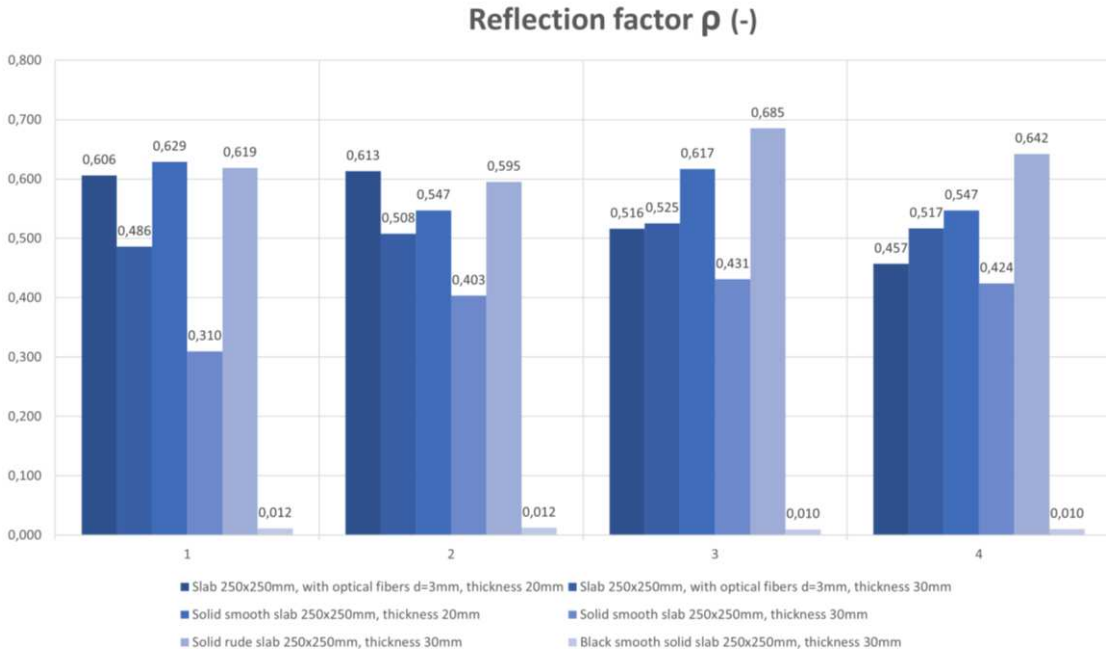

Figure 75: Reflection factor ρ (-)

7 Experimental Part – Compressive and tensile flexural strength

7.1 Characteristics of the strength of translucent concrete slabs

It will be necessary to experimentally prove the sufficient resistance of unified slabs made of light-transmitting concrete to the applied load. The samples used for our study were subjected to compressive and tensile flexural strength tests [71] [72] [73]. The results of these tests showed that the strength of the slabs made from the mixture containing the 3 mm thick optical fibers, does not particularly reduce the strength of the samples themselves. The strengths of the created samples, both compressive strength and tensile flexural strength, can be compared with, for example, the strength of travertine stone, which is 76.1 MPa in compression strength, and 12.5 MPa in tensile flexural strength. This claim is also supported by studies, which confirmed that translucent concrete does not lose its strength by adding optical fibers. The maximum 28 days compressive strength obtained was 48 MPa for TSC cubic specimens incorporating 4% volume of 3 mm diameter of POF [74]. It was stated that translucent concrete samples (TCS) can provide a high light transmittance and good mechanical properties. TCS with a 4% POF volume ratio performs up to 21.4% of natural light transmittance and 24.7% of artificial light transmittance near-cube face, which is enough lighting for commercial and residential buildings [75]. It has also been confirmed in another study of TC slabs that compressive strength has not been affected by adding optical or any other fibers. Mechanical properties decrease with increasing POF volume ratios and diameters, which in turn significantly increase light transmittance. It has been demonstrated that concrete mixtures can up light transmittance to 21.4% with a volume ratio of 4% POF and 3 mm POF diameter. Good mechanical properties such as compressive strength are minimally affected [76]. To increase strength, it is also possible to mix fibers reinforcement into the concrete mixture, ideally plastic or glass fibers that are added to fiber concrete. Is it possible to use glass-textile reinforcement (TRC) used for thin-walled concrete structures, but in this study I used GF. The use of TRC is complicated due to the optical fiber network. The different types of stone are shown in the Figure 76 and its parameters in the Table 14 .

Figure 76: Travertino Romano Classico, Bianco Carrara C, Giallo Veneziano, Light-transmitting Concrete [77]

Table 14: Comparison of stone properties (travertine, marble, granite), https://www.brachot.com/

Travertino Romano Classico - sedimentary rock - Italy					
Hardness (Mohs)	Volume Density (kg/m^3)	Water absorption (%)	Porosity (%)	Compressive strength (MPa)	Tensile flexural strength (MPa)
3	2516	0.5	1.25	**76.1**	**12.5**
Bianco Carrara C - metamorphic rock - Italy					
Hardness (Mohs)	Volume Density (kg/m^3)	Water absorption (%)	Porosity (%)	Compressive strength (MPa)	Tensile flexural strength (MPa)
3	2694	0.1	0.31	**107.0**	**17.0**
Giallo Veneziano - volcanic rock - Brazil					
Hardness (Mohs)	Volume Density (kg/m^3)	Water absorption (%)	Porosity (%)	Compressive strength (MPa)	Tensile flexural strength (MPa)
6-7	2630	0.3	-	**112.1**	**9.3**

7.2 Measurement of compressive strength of light transmitting concrete slabs

The compressive strength of concrete is one of the initial material characteristics that is used in the classification of concrete class and the calculation of other specific concrete properties. Compressive strength test diagram of light transmitting slabs, is shown in the Figure 77. It is one of the basic mechanical properties that is determined by destructive tests as standard on cubes 150×150×150 mm or cylinders with a diameter of 150 mm and a height of 300 mm. In our case, we assessed light-transmitting concrete slabs with dimensions of 250x250x20(30) mm. Before the actual test, the geometry of the test sample must be verified. For a series of tests to determine the compressive strength of concrete slabs, 7 slabs with a thickness of 30 mm and 7 slabs with a thickness of 20 mm were produced. My samples for compressive strength test are shown in the Figure 81. The slabs come in three types of design: slabs with glass and optical fibers, slabs with glass fibers and air holes, solid slabs with glass fibers. The compressive strength at fast $f_{c,k}$ is determined from the relationship in the Equation 7 below:

$$f_{ck} = \frac{F}{A_c} = \frac{F}{b \,.\, h} \; (MPa) \tag{7}$$

where *F* is the maximum load at specimen failure and *b, h* are the dimensions of the cross-sectional area of the test body to which the compressive load is applied.

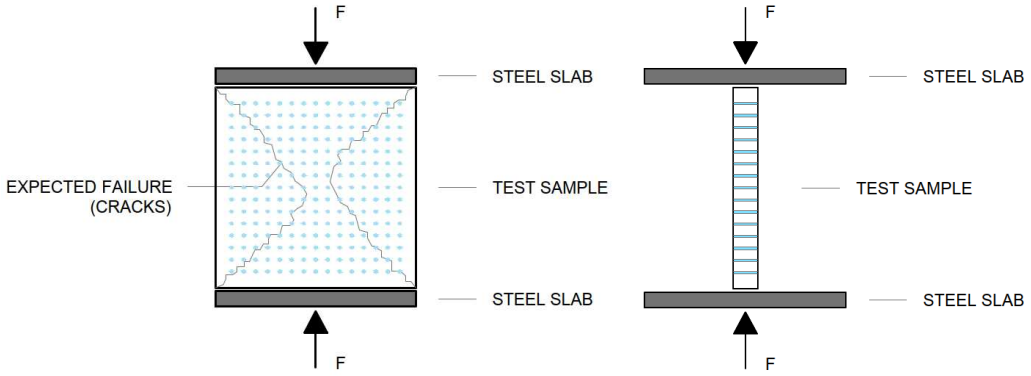

Figure 77: Compressive strength test diagrams

The compressive strength of the LTC slabs was tested on specimens using a Controls C68Z00 test press, which is shown in the Figure 78 and its properties in the Table 15. The test specimens were loaded sequentially until the specimen failed in the compressive test. We removed all residual loose material and concrete pours from the surface of the sample, especially on the areas to be loaded and in contact with the press plates. The slabs were placed in the press at the center of the bottom pushed slab so that they were loaded in a direction perpendicular to the direction of concrete mixture placement. Next, we set a constant loading rate. We loaded continuously without any surges. Based on the measured values, we recorded the maximum load achieved. For light-transmitting concrete slabs, the stress increases uniformly up to the ultimate strength. Beyond the ultimate strength, destruction occurs by crushing or outright shattering of the material. Surface cracks usually appear but may not indicate major deformation or a breakdown in overall cohesion. The process of my compressive strength testing of individual slabs is documented from the Figure 82 to Figure 96. The method of fracture is influenced by the structure of the material. The results of the compressive strength measurements are recorded in the Table 16 and Table 17, and evaluated in the Figure 79 and Figure 80.

Table 15: Properties of compressive strength measuring machine – Controls C68Z00

Controls C68Z00		
Capacity force max		4000 kN
Ram area		77931.1 mm2
Ram stroke		50 mm
Machine weight		1950 kg
Platens diameter		305x350 mm
Surfaces hardness		53 HRC
Flatness tolerance		0.03 mm
Max. vertical deylight		520 mm
Horizontal daylight		425 mm
For specimen size		
	Cubes	15; 20; 30
	Cylinders	15x30; 16x32; 25x50
Overall dimensions (l x d x h)		600x370x1500 mm
Weight approximately		740 kg

Figure 78: Compressive strength measuring machine – Controls C68Z00

Table 16: Properties of slabs 20 mm thick for measuring Compressive strength

Slabs 20mm	Type of slab	Length (mm)	Width (mm)	Thickness (mm)	Weight (kg)	Area (m2)	Load (kN)	**Compressive strength (MPa)**
A	Solid	250	252	24.12	2.85	0.06	423.70	67.25
B	Solid	249	250	21.97	2.72	0.06	389.60	62.59
C	Solid	250	248	22.00	2.74	0.06	354.80	57.23
D	POF	254	250	19.30	2.29	0.06	319.30	50.28
E	POF	252	250	20.70	2.45	0.06	356.40	56.57
F	Air	249	250	20.62	2.51	0.06	342.80	55.07
G	Air	251	251	21.09	2.53	0.06	321.70	51.06

Table 17: Properties of slabs 30 mm thick for measuring Compressive strength

Slabs 30 mm	Type of slab	Length (mm)	Width (mm)	Thickness (mm)	Weight (kg)	Area (m^2)	Load (kN)	**Compressive strength (MPa)**
1	Solid	251	252	28.90	3.49	0.06	418.50	66.16
2	Solid	251	251	36.35	4.13	0.06	471.40	74.82
3	Solid	252	249	33.80	4.09	0.06	425.50	67.81
4	POF	250	253	29.79	3.67	0.06	407.60	64.44
5	POF	250	253	29.51	3.69	0.06	411.80	65.11
6	Air	250	253	29.95	3.69	0.06	371.20	58.69
7	Air	250	252	29.71	3.65	0.06	403.40	64.03

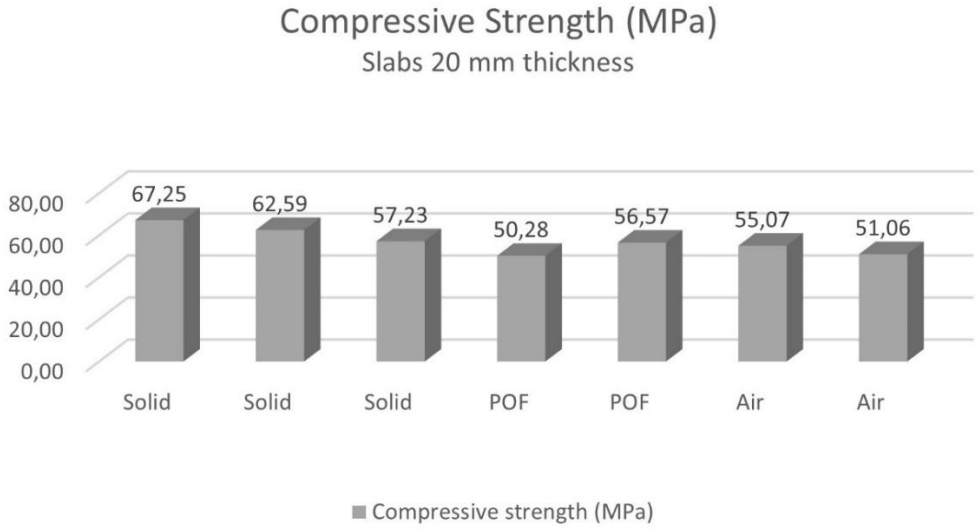

Figure 79: Compressive strength of a slab thickness 20mm

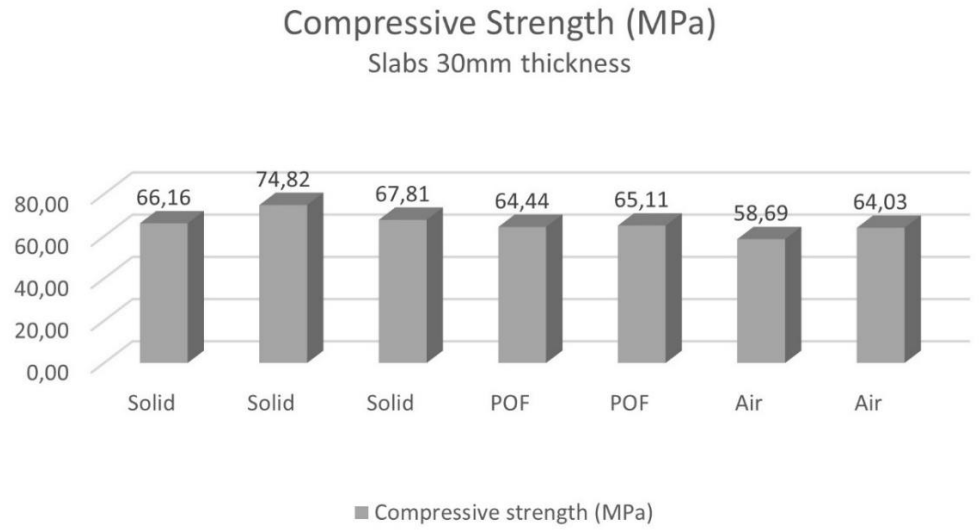

Figure 80: Compressive strength of a slab thickness 30mm

Figure 81: Samples for compressive strength test

Figure 82: Compressive Strength Test – Solid slab with GF

Figure 83: Compressive Strength Test – Solid slab with GF

Figure 84: Compressive Strength Test – Solid slab with GF

Figure 85: Compressive Strength Test – Solid slab with GF

Figure 86: Compressive Strength Test – Solid slab with GF

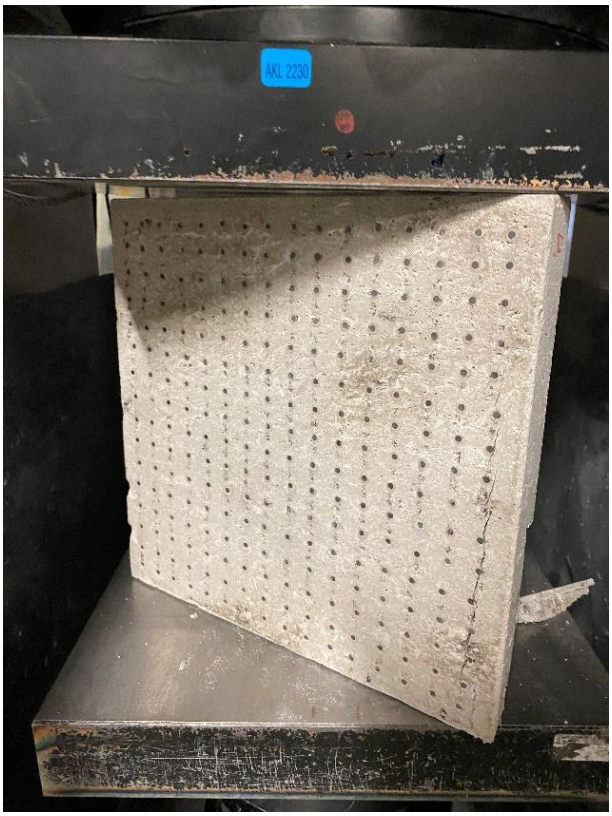

Figure 87: Compressive Strength Test – Slab with POF and GF

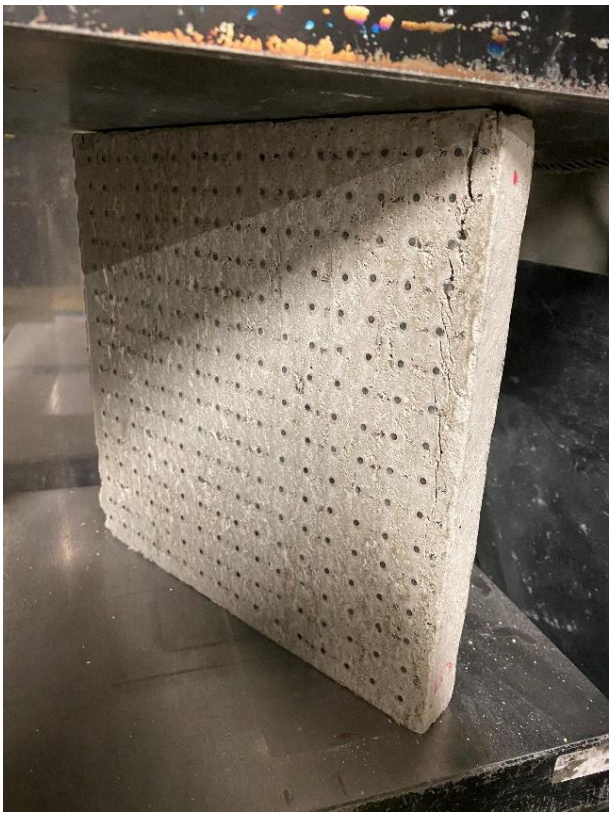

Figure 88: Compressive Strength Test – Slab with POF and GF

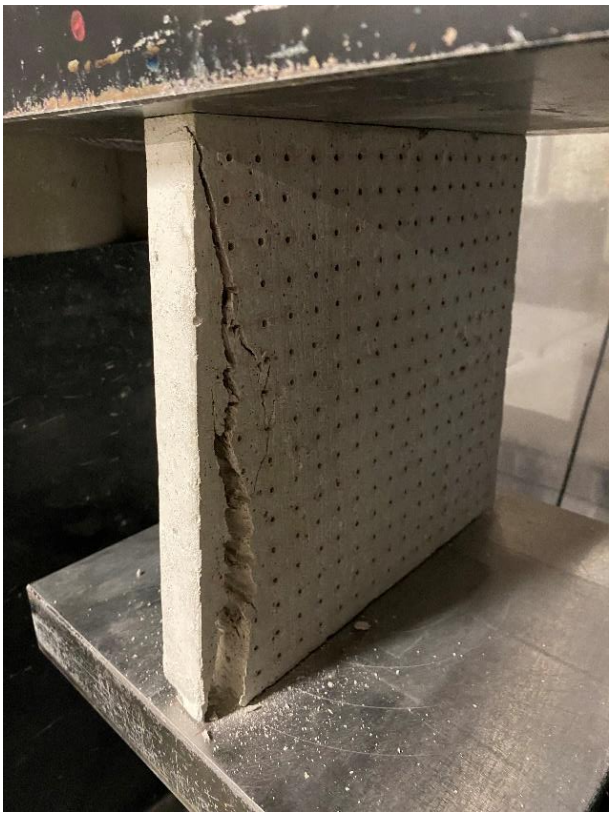

Figure 89: Compressive Strength Test – Slab with Air holes and GF

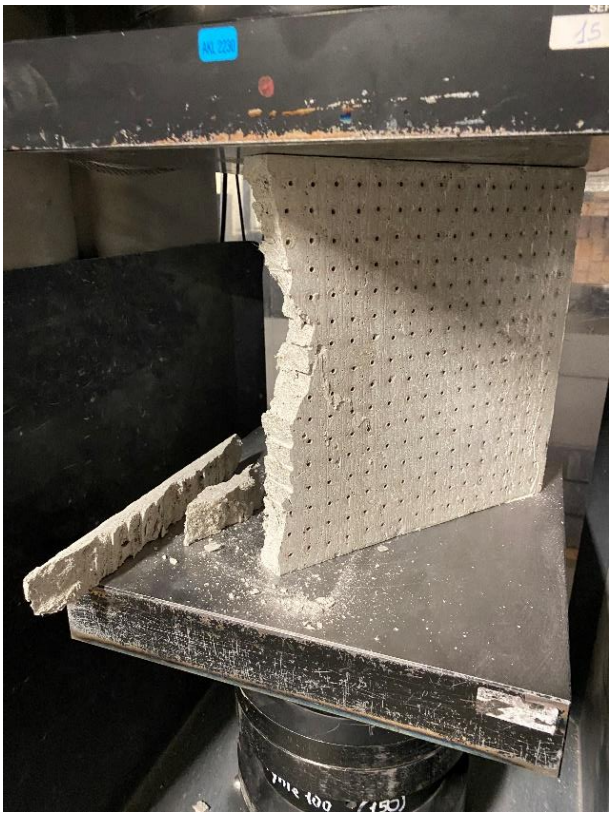

Figure 90: Compressive Strength Test – Slab with Air holes and GF

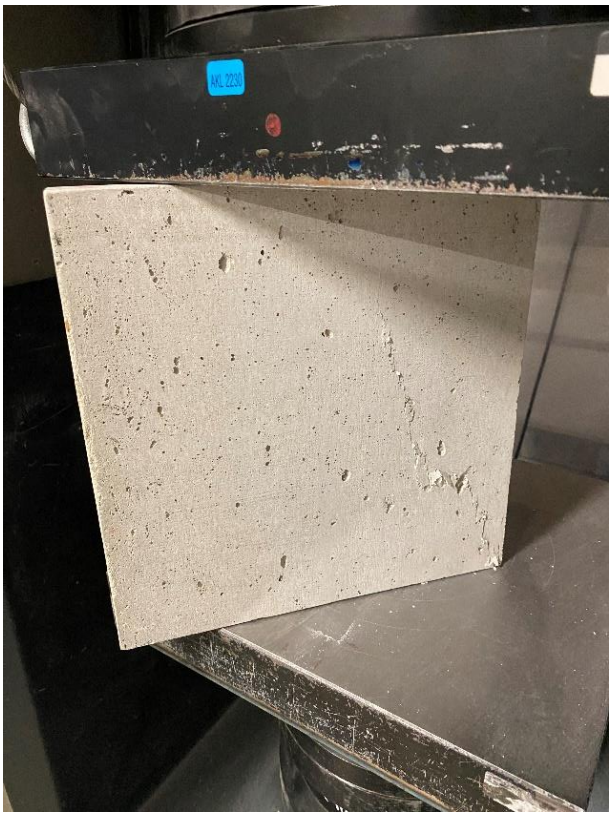

Figure 91: Compressive Strength Test – Solid slab with GF

Figure 92: Compressive Strength Test – Slab with POF and GF

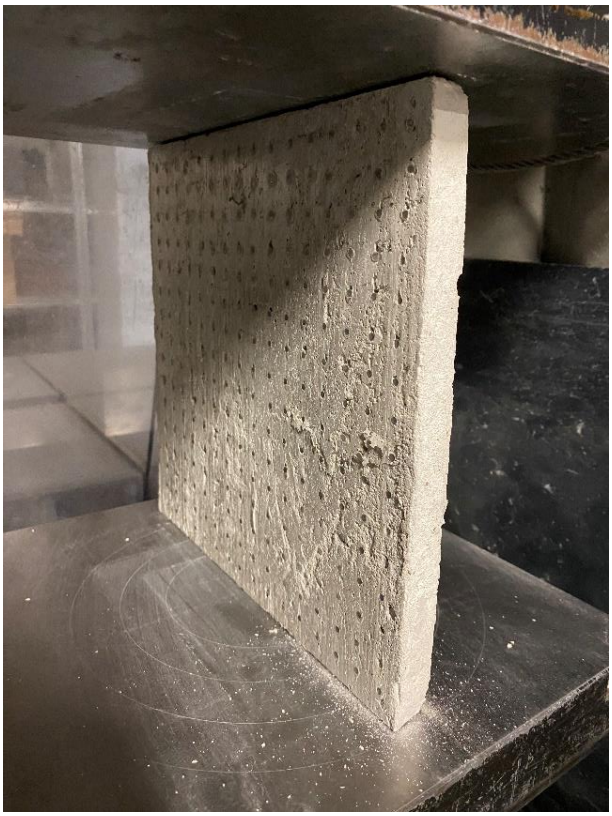

Figure 93: Compressive Strength Test – Slab with POF and GF

Figure 94: Compressive Strength Test – Slab with POF and GF

Figure 95: Compressive Strength Test – Slab with POF and GF

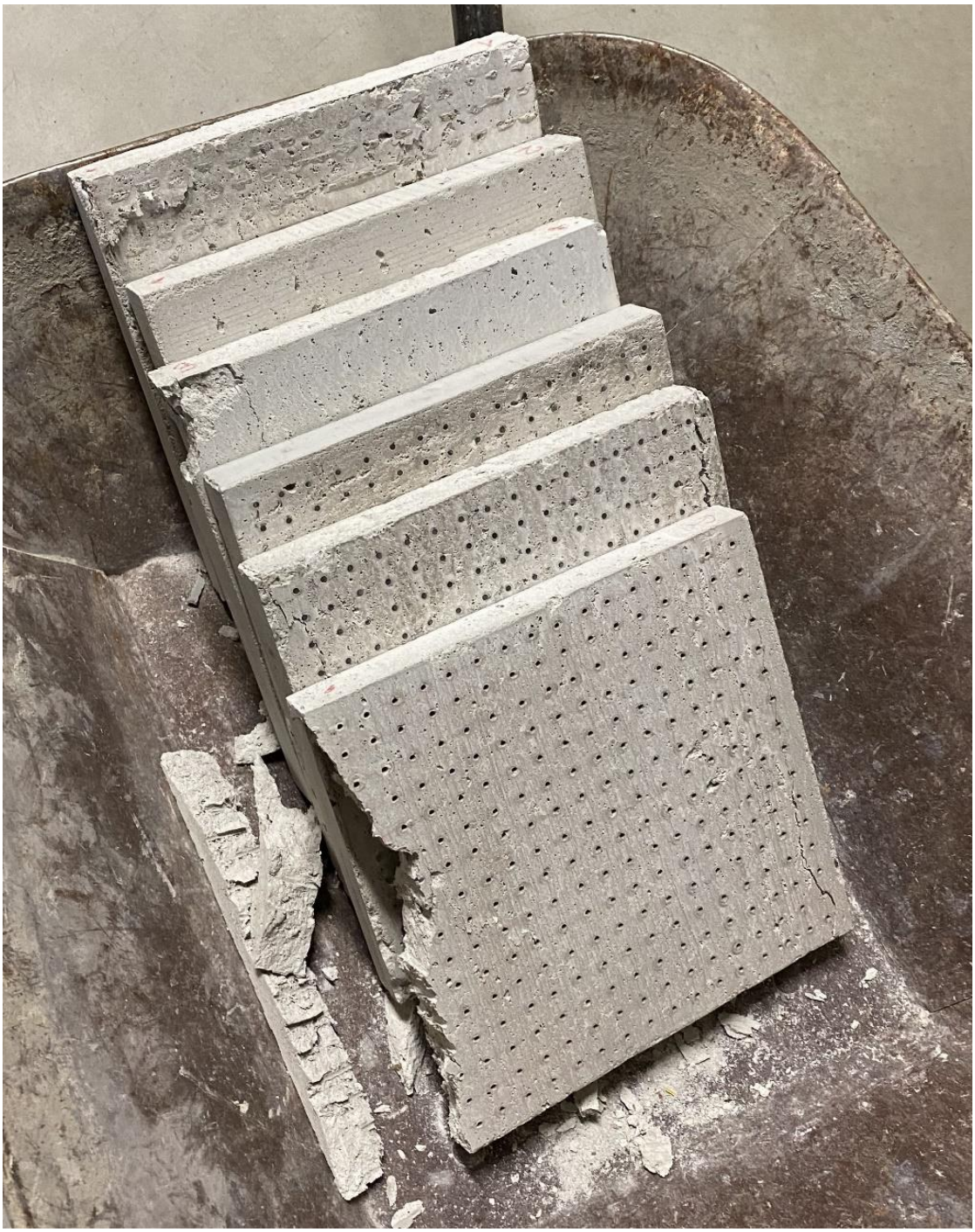

Figure 96: Destroyed samples from compressive strength test

7.3 Measurement of tensile flexural strength of light transmitting concrete slabs

The tensile flexural strength is determined by a three-point bending test on samples. The three-point test arrangement is always a combination of bending and shear. The calculation of the tensile flexural strength is influenced by the assumption of stress distribution along the cross-section and the non-linear behavior of concrete. The tensile flexural strength of concrete is one of the basic mechanical properties that is determined on the samples. A principle of the test itself and the sample placement is shown in the Figure 97. In our case, we assessed light-transmitting concrete slabs with dimensions of 250x250x20(30) mm. Before the actual test, the geometry of the test fixture must be verified. For a series of three-point bending tests to determine the tensile flexural strength of concrete slabs, 5 slabs with a thickness of 30 mm and 8 slabs with a thickness of 20 mm were produced. The slabs come in three types of design: slabs with glass and optical fibers, slabs with glass fibers and air holes, solid slabs with glass fibers. Plasticization of concrete and formation of microcracks occurs here. The tensile flexural strength of concrete for the three-point bending test is calculated from the relationship in the Equation 8 below:

$$f_{cf} = \frac{3F.l}{2b.(h)^2}\ (Mpa) \tag{8}$$

where *F* is the maximum load; *l, b* and *h* are the dimensions: span, width, and height of the section.

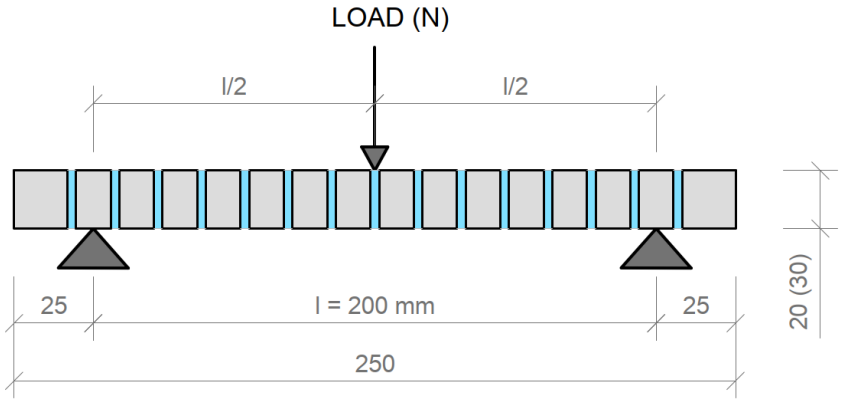

Figure 97: Tensile flexural strength test diagram

The tensile flexural strength of the translucent slabs was tested on samples using measuring machine Galdabini Quasar 100, which is shown in the Figure 98 and its properties is describe in the Table 18. The test samples were loaded sequentially until their failure in the tensile flexural test. We removed all residual loose and concrete pours from the surface of the slabs, especially on the areas to be loaded by 3-point bending test cylinders. The slabs were placed on the lower cylinders so that they were loaded in a direction perpendicular by the upper cylinder, like it shows on the 3-ponit bending test diagram. Next, we set a constant loading and rate *0.5 mm/min*.

We loaded continuously without any surges. Based on the measured values, we recorded the maximum load achieved.

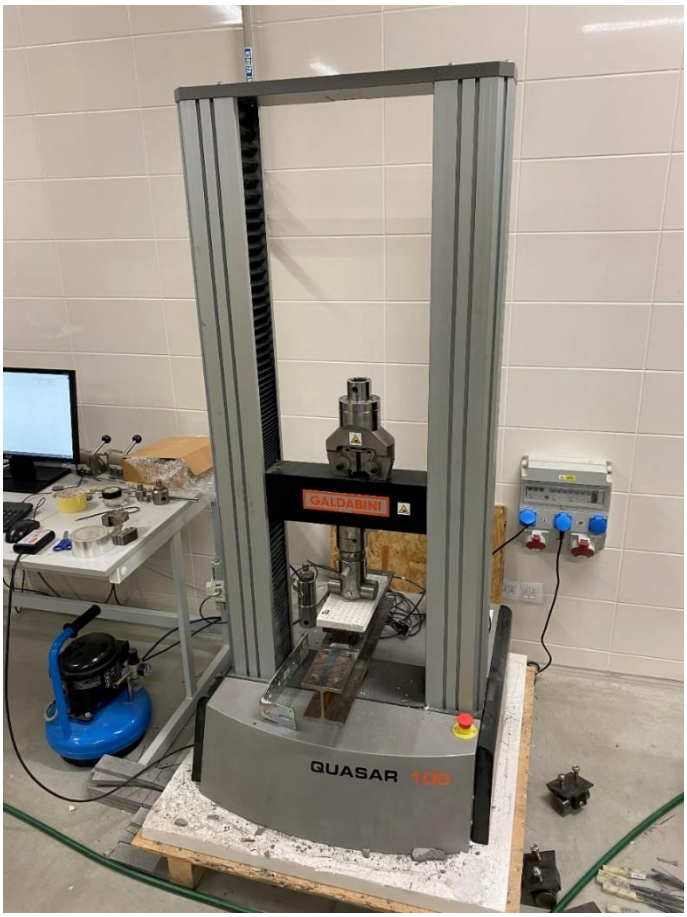

Figure 98: Tensile Flexural Strength Measuring Machine - Galdabini Quasar 100

Table 18: Properties of machine for measuring Tensile Flexural Strength - Galdabini Quasar 100

Galdabini Quasar 100	
Capacity of frame and max allowed load	100 KN (22.481 lbf)
Load cell nominal size (tensile and compression)	100 KN
Stadards met or exceeded	ISO 7500-1, ASTM E4, EN 10002-2, JIS B7721, GB/T 16825.1, DIN 51221, BS 1610 and other equivalent
Testing area depth	Unlimited
Power Rating	1 400 W
Machine weight (without accessories)	260 kg (794 lb)
Finishing	Silver RAL 9006/Black RAL 9011
PC interface	Ethercat (A dedicated Ethernet port on PC is required)
Noise level	< 72 dB
Height	1 682 mm
Width	783 mm
Depth	820 mm

The measured resultant tensile flexural strengths from the three-point bending test of individual light transmitting concrete slab are given in the in the Table 19 and Table 20, where are also its properties and dimensions. The resulting strength is sufficient for use as a cladding material in the interior or as a cladding material on the façade. The strength is comparable to stone slabs commonly used in the construction industry.

Table 19: Properties of slabs 20 mm thick for measuring Tensile Flexural Strength

Slabs 20 mm	Type of slab	Length (mm)	Width (mm)	Thickness (mm)	Weight (kg)	Area (m^2)	Load (kN)	**Tensile flexural strength (MPa)**
16	POF	252	121	20.38	1.20	0.03	1467.30	8.76
17	Solid	252	124	23.41	1.47	0.03	362.20	1.60
18	Solid	250	125	21.90	1.36	0.03	1865.03	9.33
19	Solid	257	123	21.86	1.32	0.03	1780.27	9.09
20	Air	250	125	21.43	1.27	0.03	1558.75	8.15
21	Air	251	122	20.73	1.21	0.03	1442.51	8.25
22	Air	251	124	20.93	1.24	0.03	1393.22	7.69
23	Air	250	124	20.97	1.26	0.03	1494.15	8.22

Table 20: Properties of slabs 30 mm thick for measuring Tensile Flexural Strength

Slabs 30 mm	Type of slab	Length (mm)	Width (mm)	Thickness (mm)	Weight (kg)	Area (m^2)	Load (kN)	**Tensile flexural strength (MPa)**
11	Solid	250	122	31.89	2.10	0.03	2944.63	7.12
12	Solid	249	126	26.81	1.71	0.03	2842.74	9.42
13	POF	251	126	30.72	1.89	0.03	2685.12	6.77
14	Air	251	125	28.97	1.81	0.03	2784.94	7.96
15	Air	251	122	30.34	1.79	0.03	2856.64	7.63

Comparison of tensile flexural strengths of solid slabs with GF, slabs with POF and GF and slabs with air holes and GF is shown on Figure 105 and Figure 106. As we can see in the Figure 99 and Figure 100, that the tensile flexural strength of all slabs averages around 7.8 MPa for 30mm and 7.6 MPa 20mm slabs. Tensile flexural strength of solid slabs is on average 9.2 MPa for 20mm thickness and 8.3 MPa for 30mm thickness. On the contrary, the measured strength of slabs with optical fibers and glass fibers is around the value 6.8 MPa for 30 mm thickness and 8.8 MPa for 20 mm thickness. Finally, the strength of slabs with air holes and GF is in the range of 8.1 MPa for 20 mm thickness and 7.8 for 30mm thickness. Individual comparisons of tensile flexural strength of various slabs are then shown from the Figure 101 to Figure 104. The individual specimens tested for tensile flexural strength are shown in the Figure 107 and the entire test procedure including individual photographs of the specimens and their loading charts are from the Figure 108 to Figure 134.

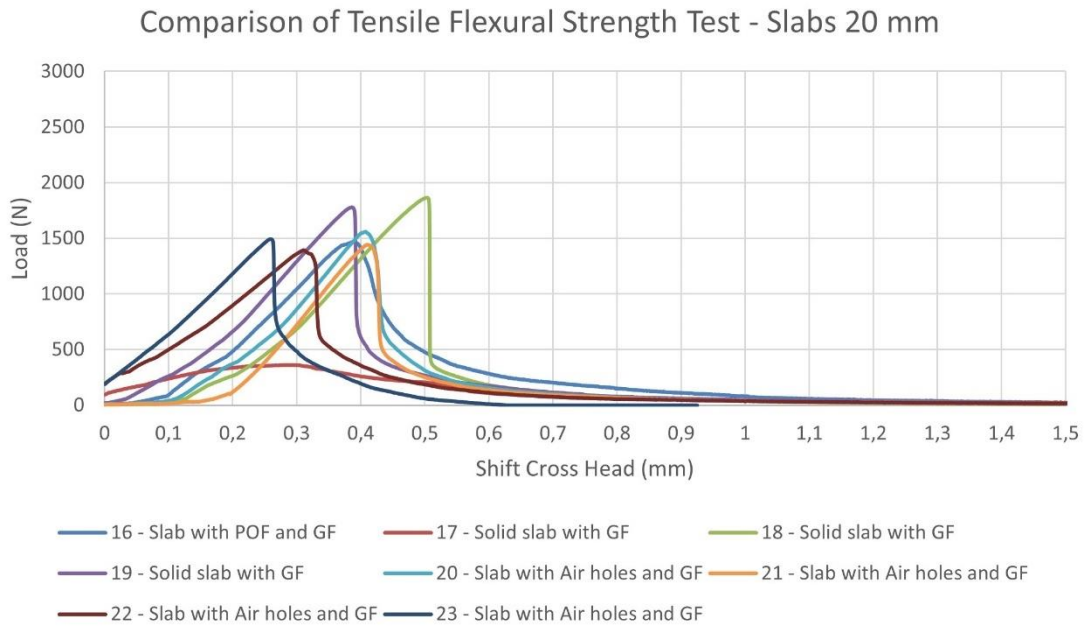

Figure 99: Comparison of Tensile Flexural Strength Test of slabs thick 20 mm

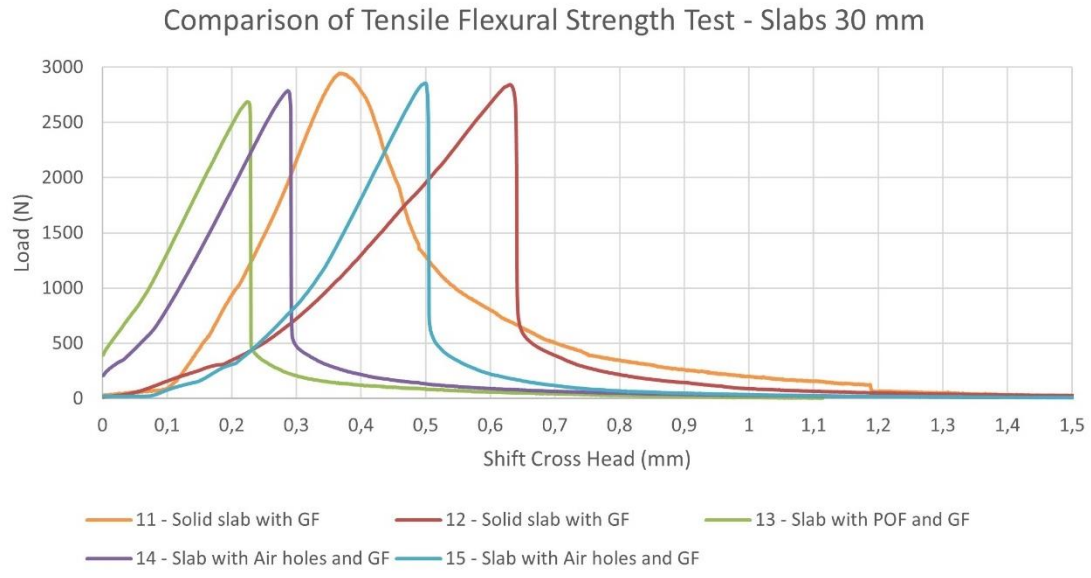

Figure 100: Comparison of Tensile Flexural Strength Test of slabs thick 30 mm

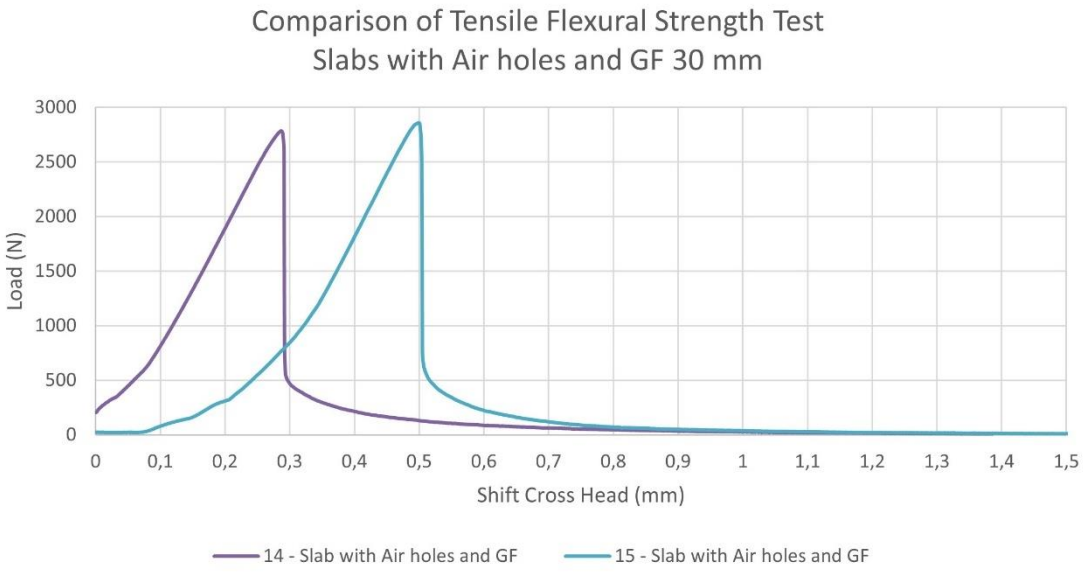

Figure 101: Comparison of Tensile Flexural Strength Test of Slabs with Air holes and GF thick 30 mm

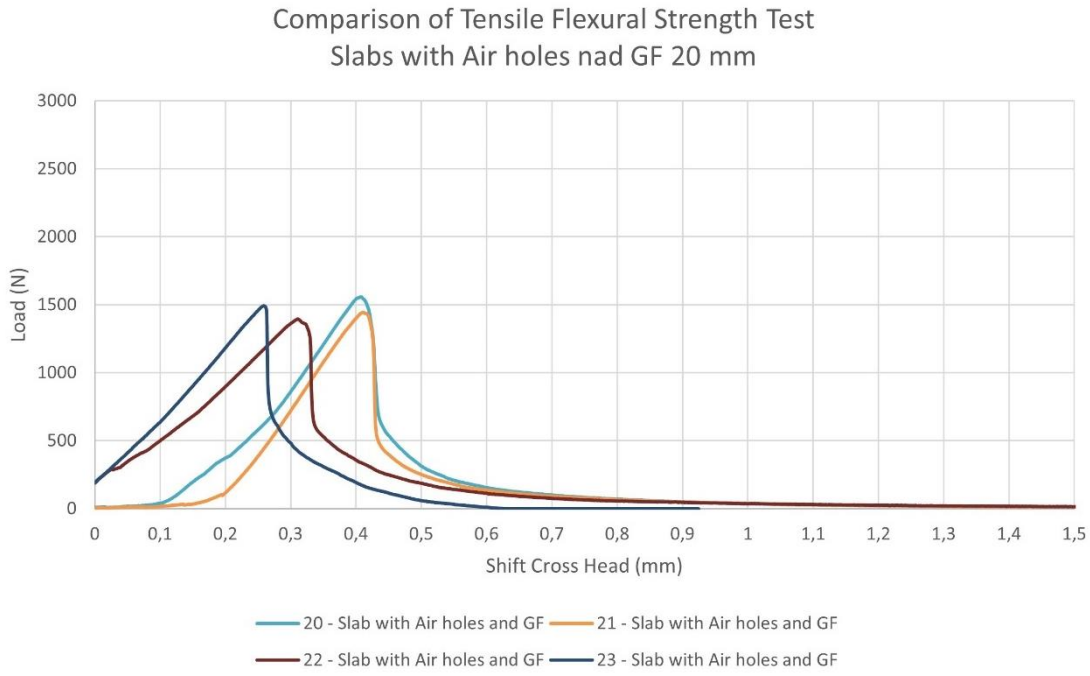

Figure 102: Comparison of Tensile Flexural Strength Test of Slabs with Air holes and GF thick 20 mm

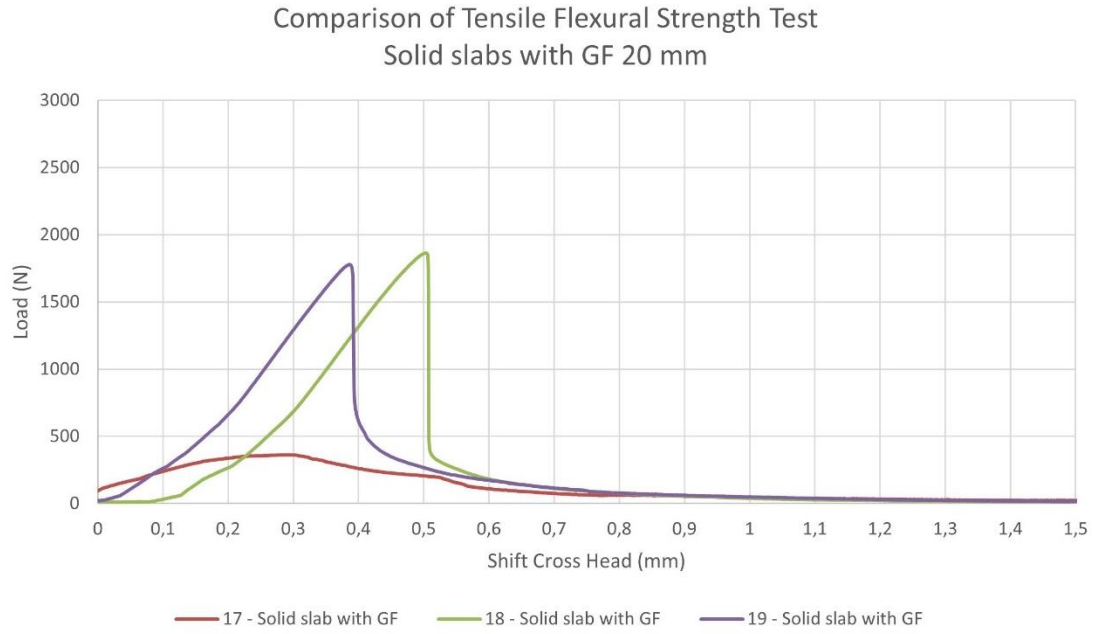

Figure 103: Comparison of Tensile Flexural Strength Test of Solid slabs with GF thick 20 mm

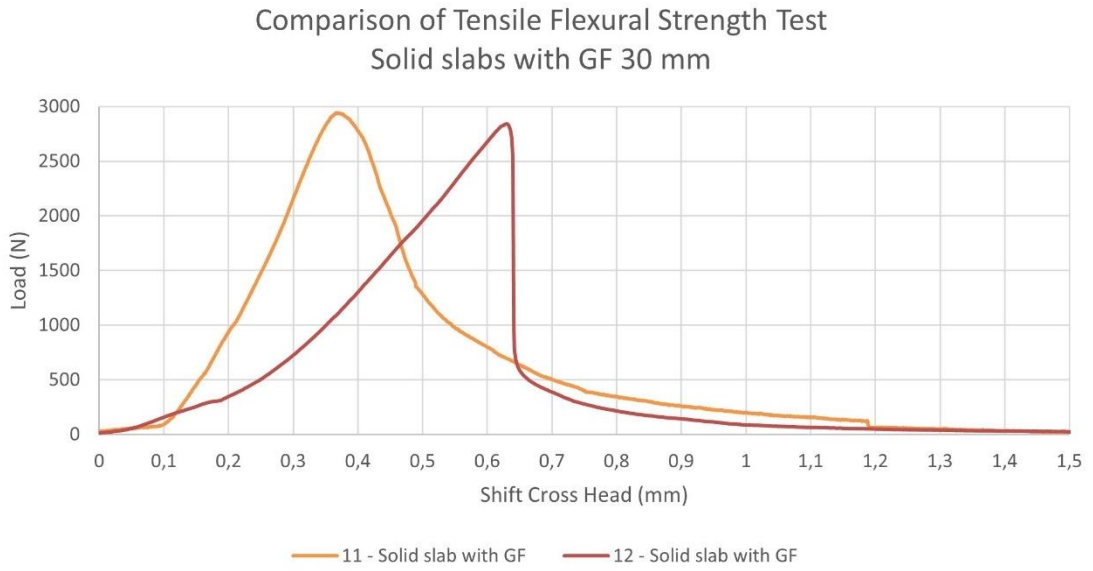

Figure 104: Comparison of Tensile Flexural Strength Test of Solid slabs with GF thick 30 mm

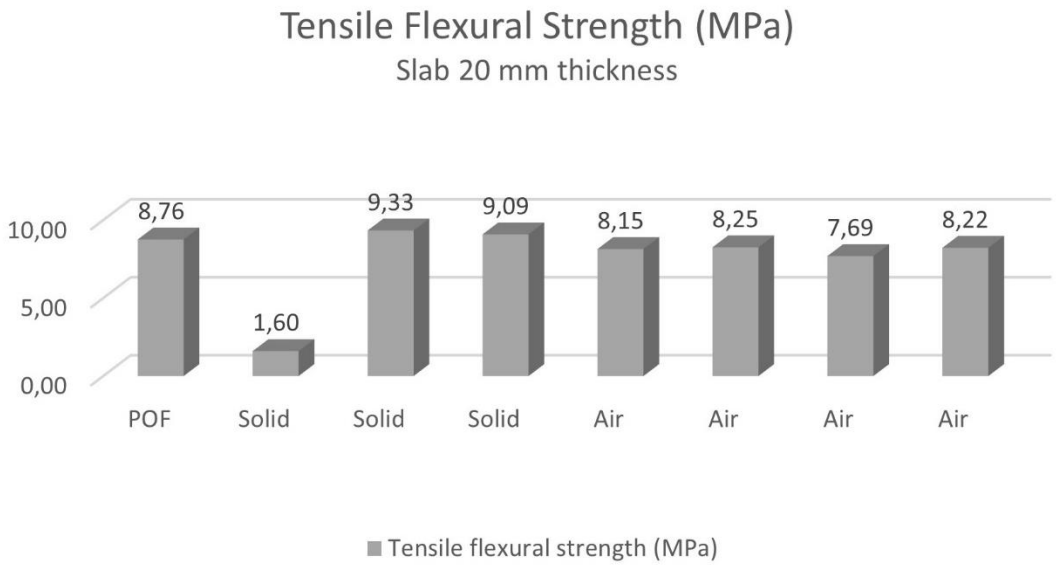

Figure 105: Tensile flexural strength of a slab thickness 20mm

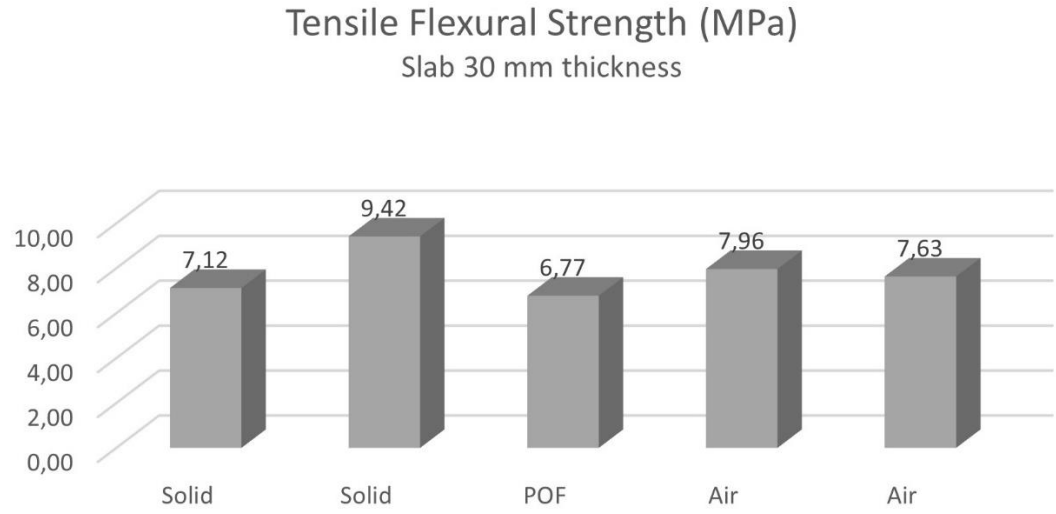

Figure 106: Tensile flexural strength of a slab thickness 30mm

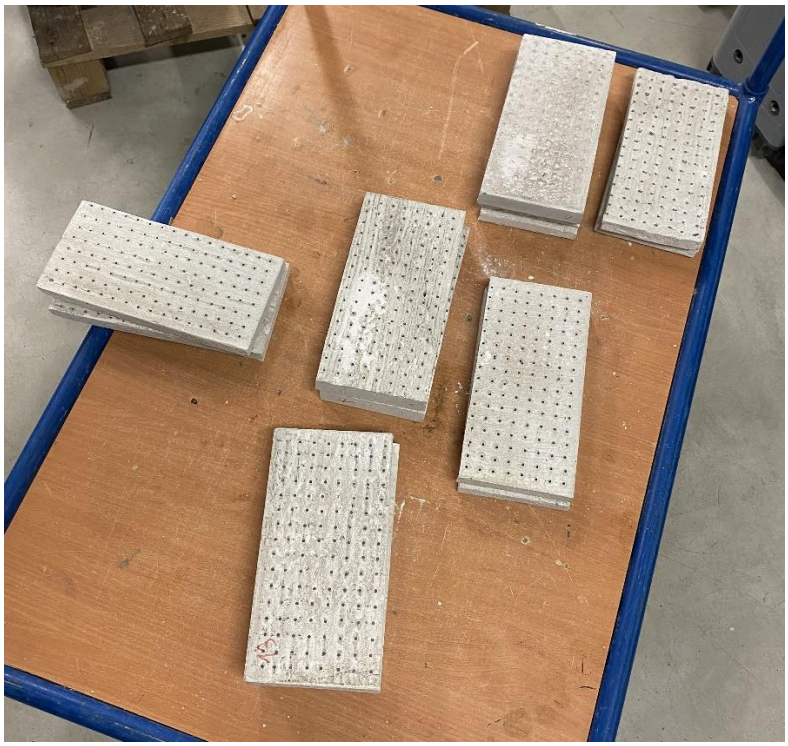

Figure 107: Samples for tensile flexural strength test

Figure 108: Tensile Flexural Strength 3-Point Test

Figure 109: Tensile Flexural Strength Test - Solid slab with GF – Sample 11

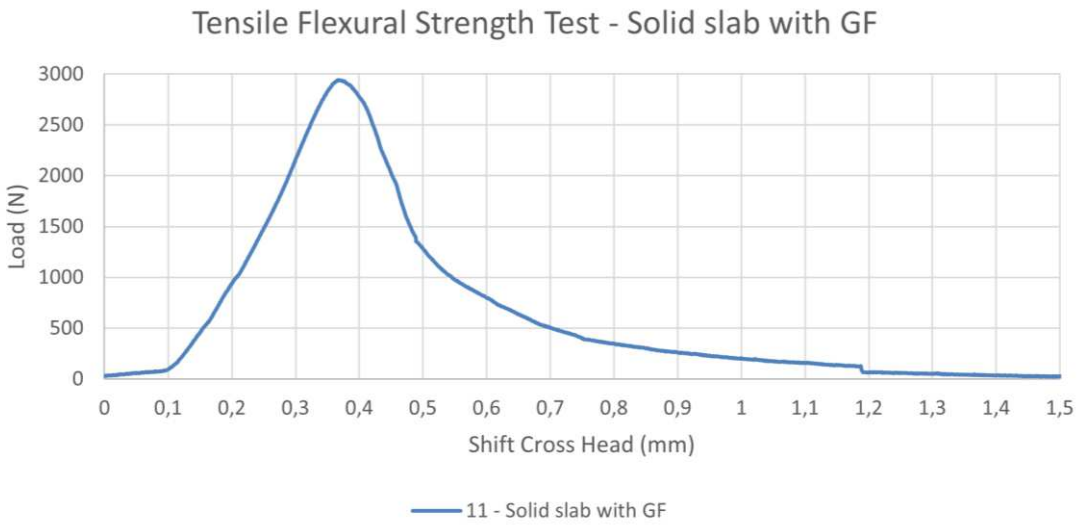

Figure 110: Tensile Flexural Strength Test - Solid slab with GF - Sample 11

Figure 111: Tensile Flexural Strength Test - Solid slab with GF – Sample 12

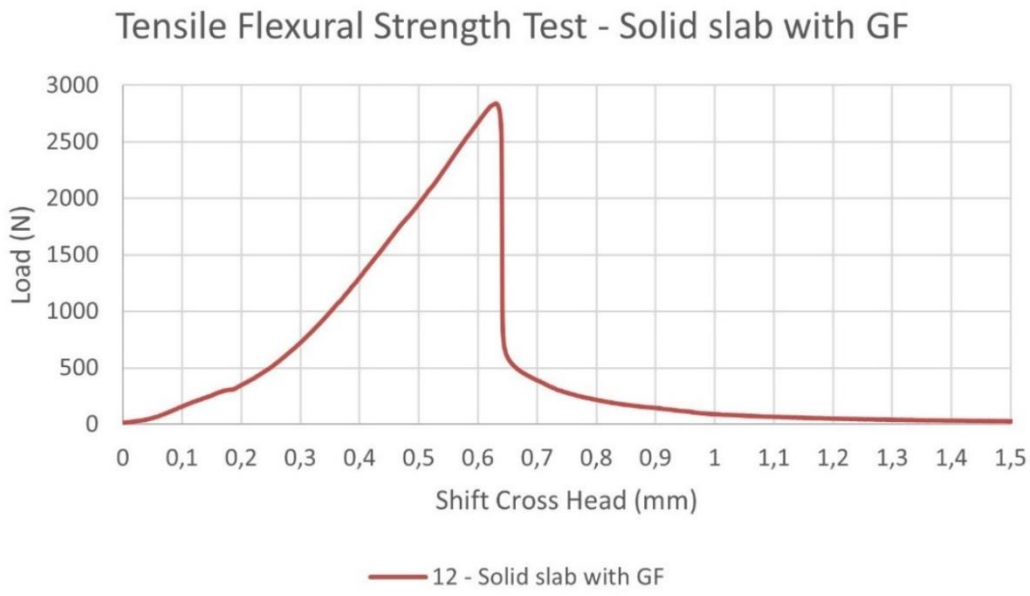

Figure 112: Tensile Flexural Strength Test - Solid slab with GF - Sample 12

Figure 113: Tensile Flexural Strength Test - Slab with POF and GF – Sample 13

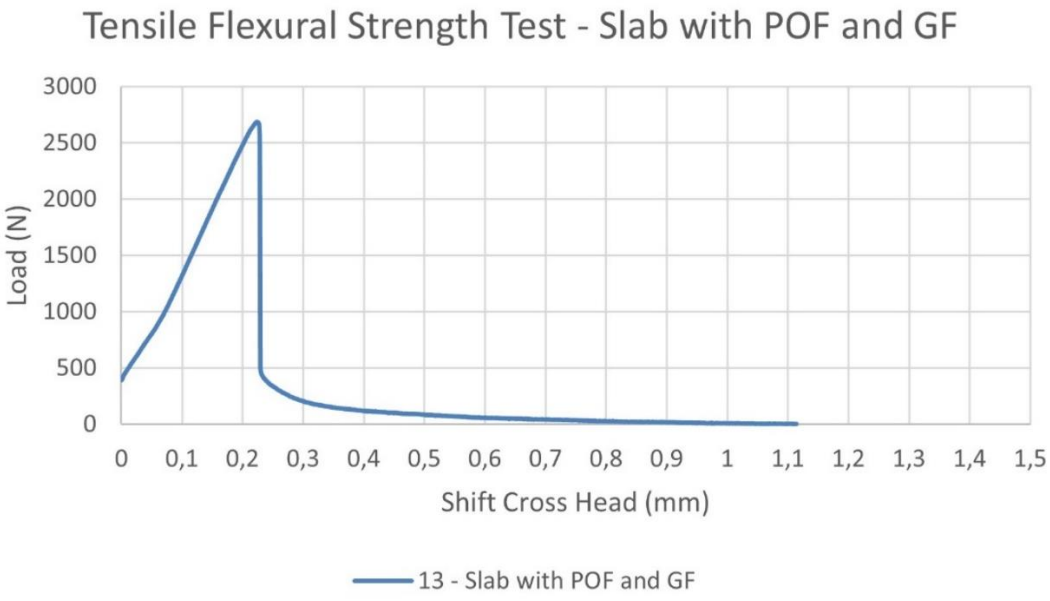

Figure 114: Tensile Flexural Strength Test - Slab with POF and GF - Sample 13

Figure 115: Tensile Flexural Strength Test - Slab with Air holes and GF – Sample 14

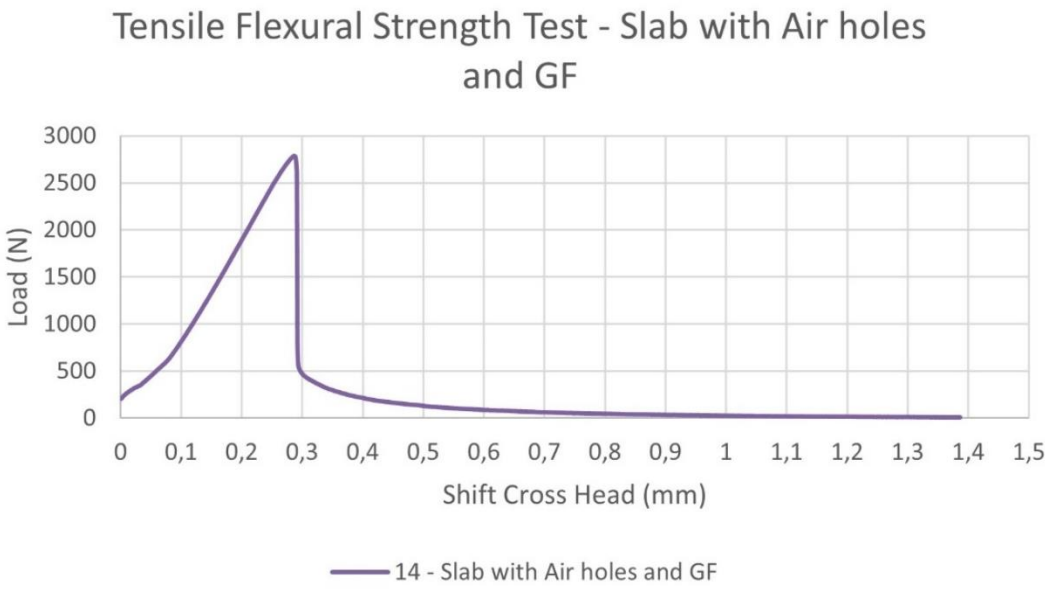

Figure 116: Tensile Flexural Strength Test - Slab with Air holes and GF - Sample 14

Figure 117: Tensile Flexural Strength Test - Slab with Air holes and GF – Sample 15

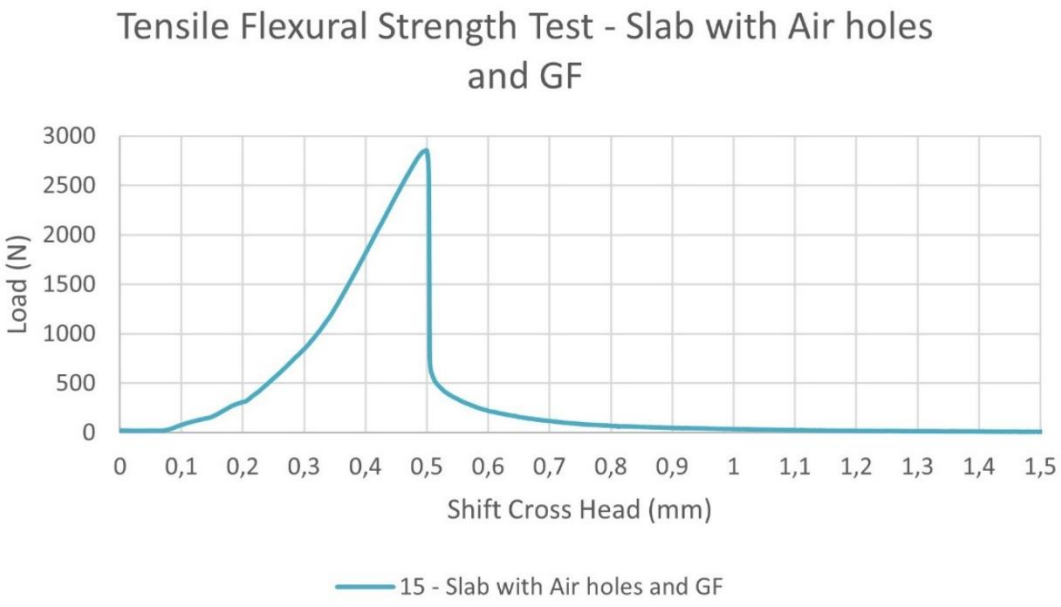

Figure 118: Tensile Flexural Strength Test - Slab with Air holes and GF - Sample 15

Figure 119: Tensile Flexural Strength Test - Slab with POF and GF – Sample 16

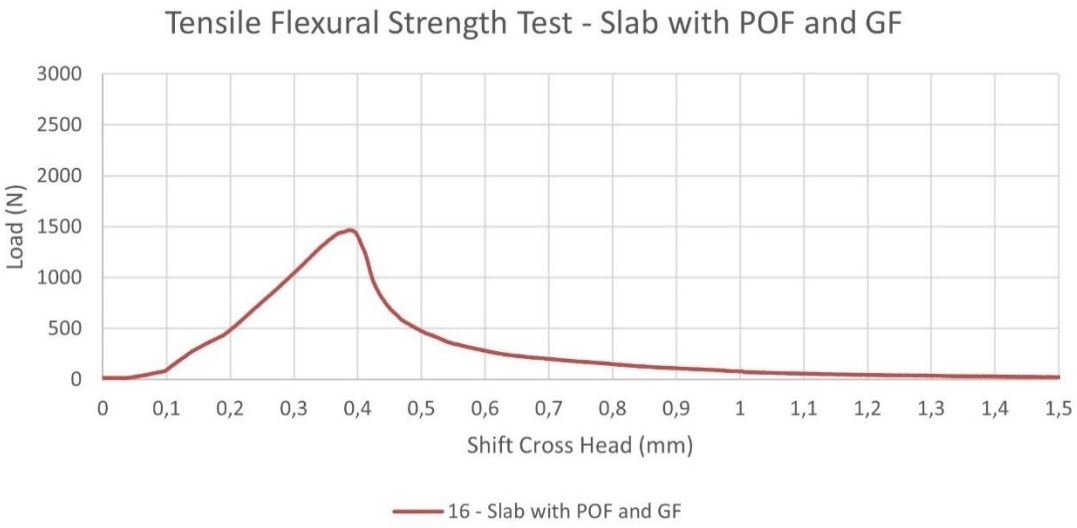

Figure 120: Tensile Flexural Strength Test - Slab with POF and GF - Sample 16

Figure 121: Tensile Flexural Strength Test - Solid slab with GF – Sample 17

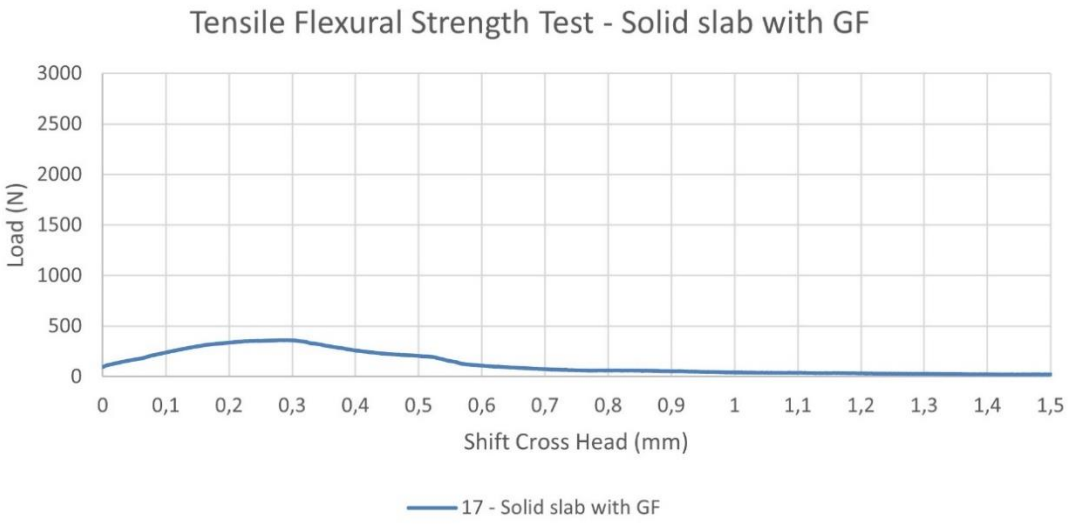

Figure 122: Tensile Flexural Strength Test - Solid slab with GF - Sample 17

Figure 123: Tensile Flexural Strength Test - Solid slab with GF – Sample 18

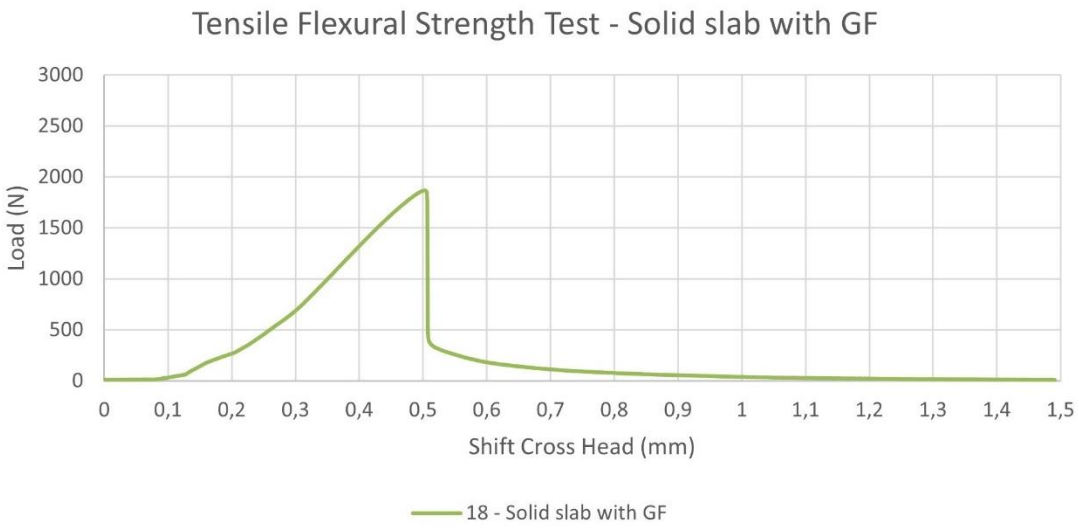

Figure 124: Tensile Flexural Strength Test - Solid slab with GF - Sample 18

Figure 125: Tensile Flexural Strength Test - Solid slab with GF – Sample 19

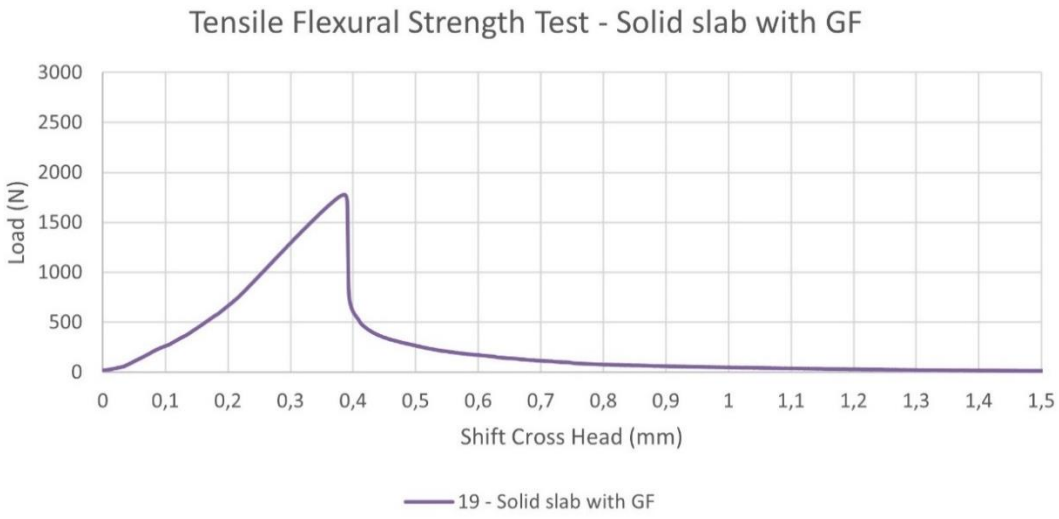

Figure 126: Tensile Flexural Strength Test - Solid slab with GF - Sample 19

Figure 127: Tensile Flexural Strength Test - Slab with Air holes and GF – Sample 20

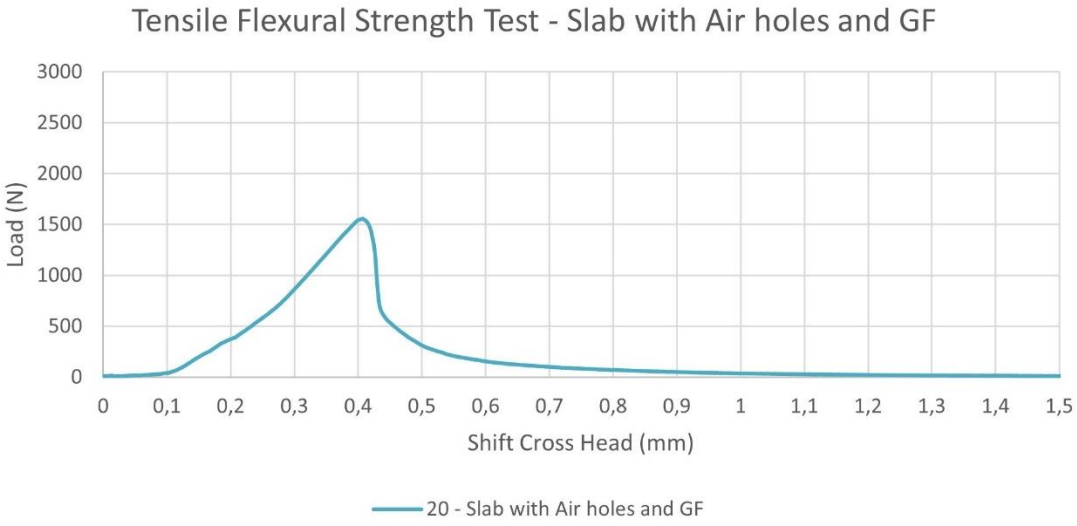

Figure 128: Tensile Flexural Strength Test - Slab with Air holes and GF - Sample 20

Figure 129: Tensile Flexural Strength Test - Slab with Air holes and GF – Sample 21

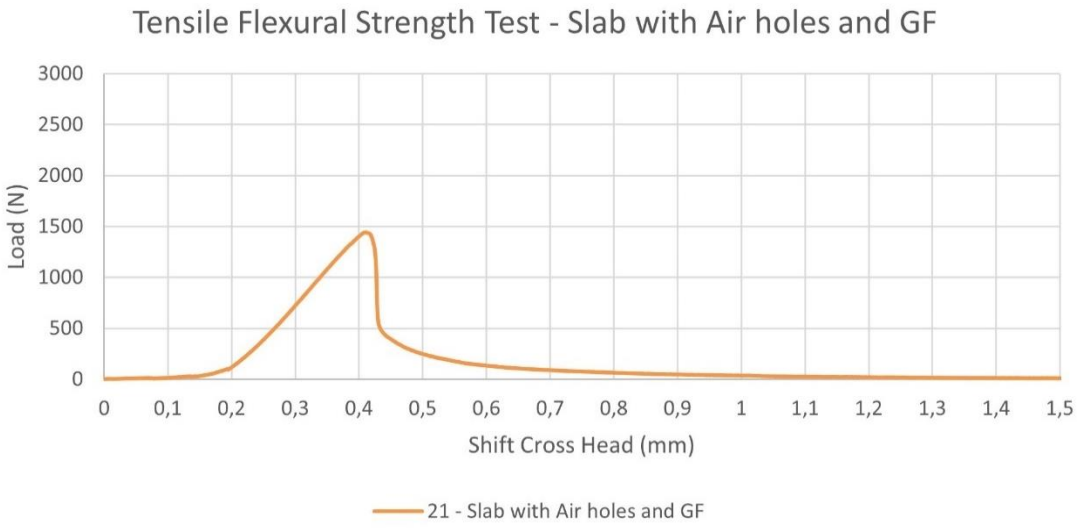

Figure 130: Tensile Flexural Strength Test - Slab with Air holes and GF - Sample 21

Figure 131: Tensile Flexural Strength Test - Slab with Air holes and GF – Sample 22

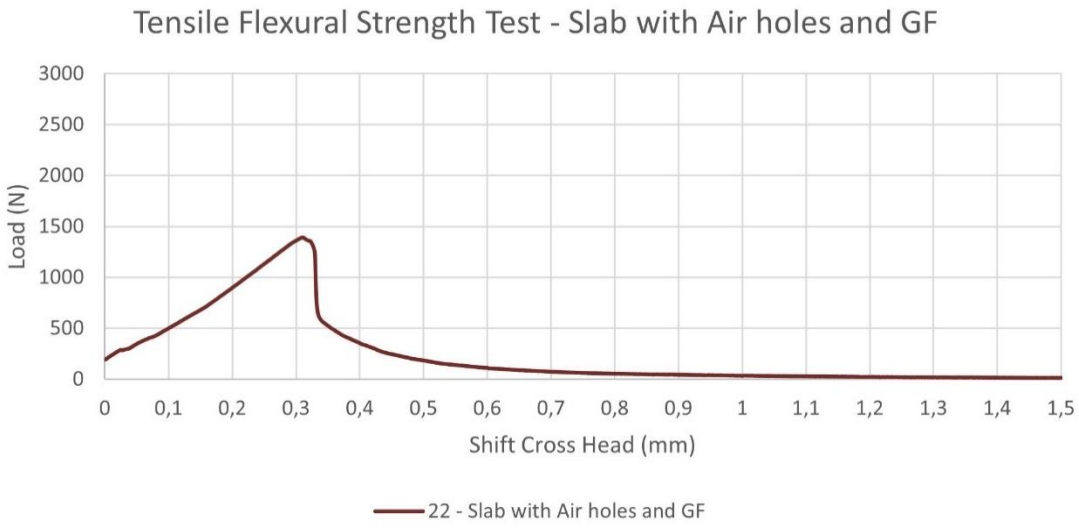

Figure 132: Tensile Flexural Strength Test - Slab with Air holes and GF - Sample 22

Figure 133: Tensile Flexural Strength Test - Slab with Air holes and GF – Sample 23

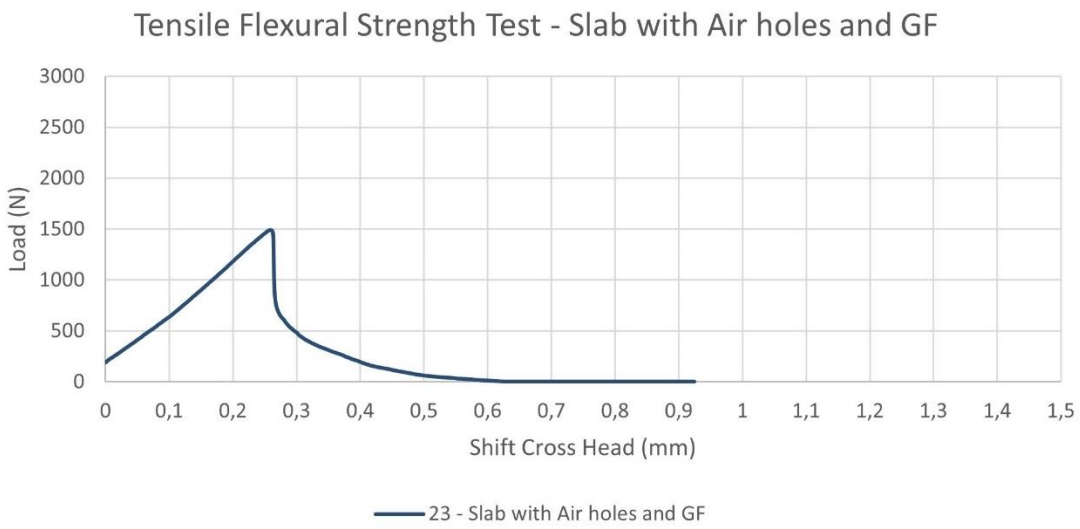

Figure 134: Tensile Flexural Strength Test - Slab with Air holes and GF – Sample 23

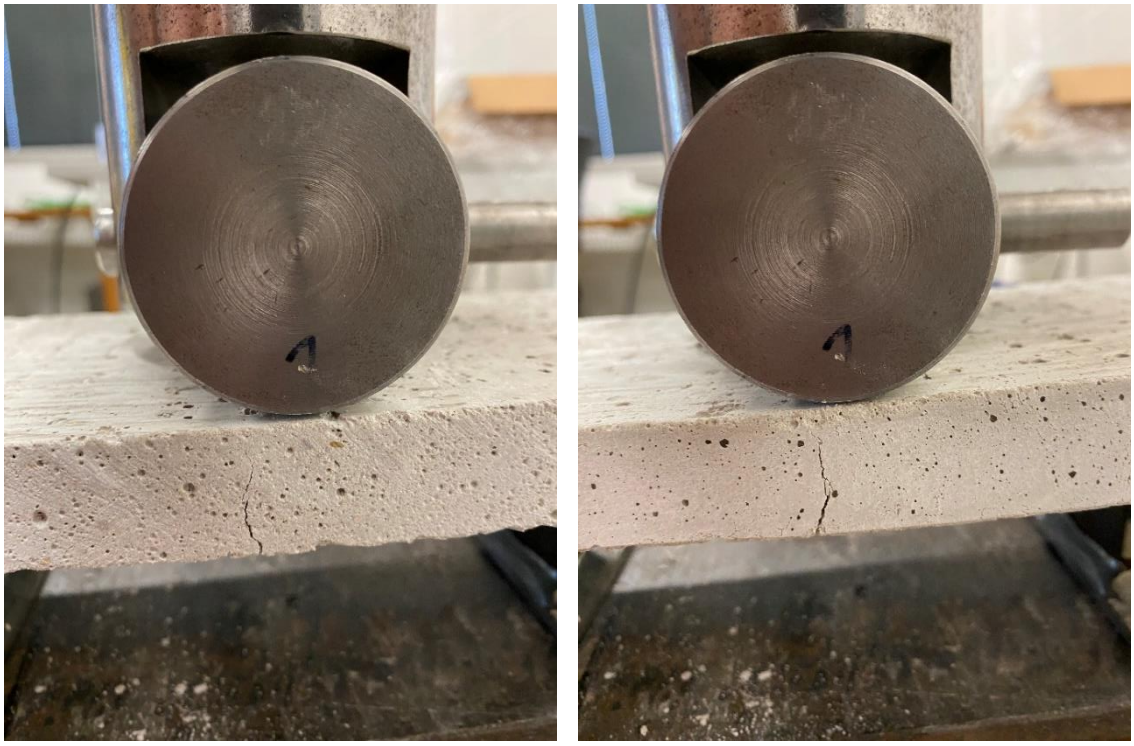

Figure 135: Tensile Flexural Strength Test – Solid slab with GF – Crack

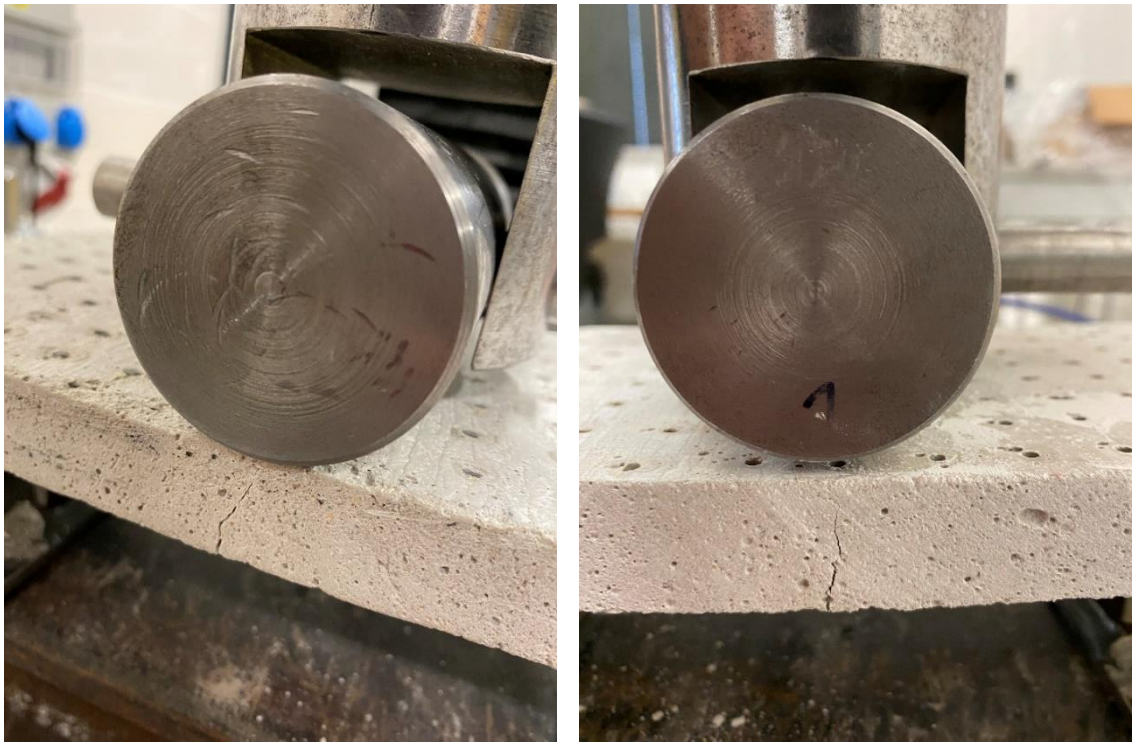

Figure 136: Tensile Flexural Strength Test – Slab with POF a GF - Crack

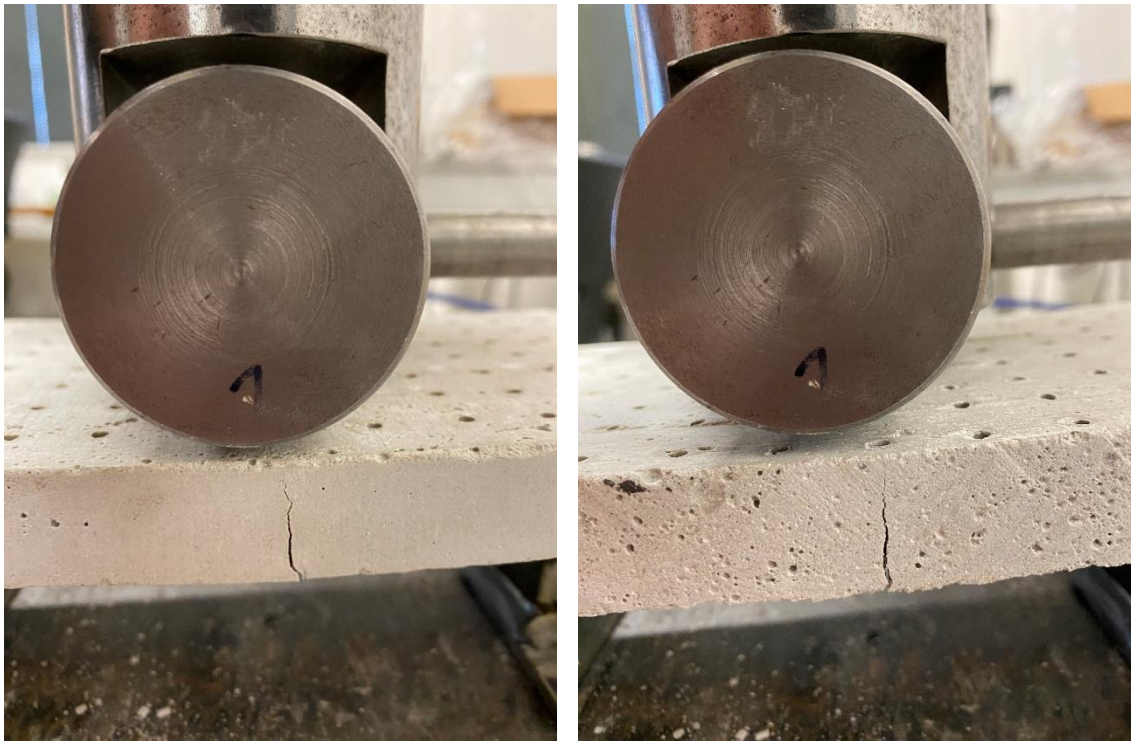

Figure 137: Tensile Flexural Strength Test – Slab with Air holes and GF – Crack

Figure 138: Tensile Flexural Strength Test – Solid slab with GF - Crack

Figure 139: Tensile Flexural Strength Test – Slab with Air holes and GF - Crack

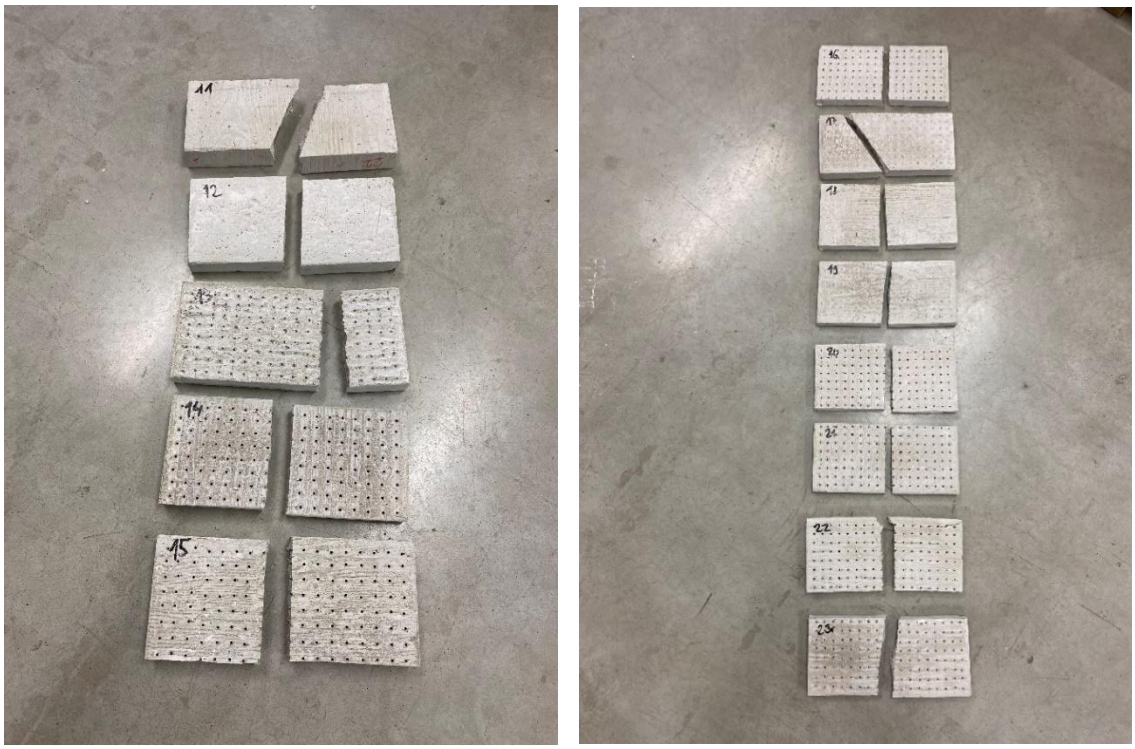

Figure 140: Broken samples after tensile flexural strength test

The failure of the specimens due to loading, including crack formation, can be seen from the Figure 135 to Figure 139. The destroyed samples after three-point bending test and its comparison can be seen from the Figure 140 to Figure 141.

In the following chapter 7.4, I compare the individual slabs with the stone cladding commonly used in the construction industry. The individual properties of the different types of stone slabs and the translucent concrete slabs considered in the experiment are given in Table 21. It can be seen that the tensile flexural strength of LTC slabs is close to those of granite. Contrary, the values compressive strength of LTC slabs is then comparable to travertine. A comparison of the individual strength of materials is shown in the Figure 142 and Figure 143 below.

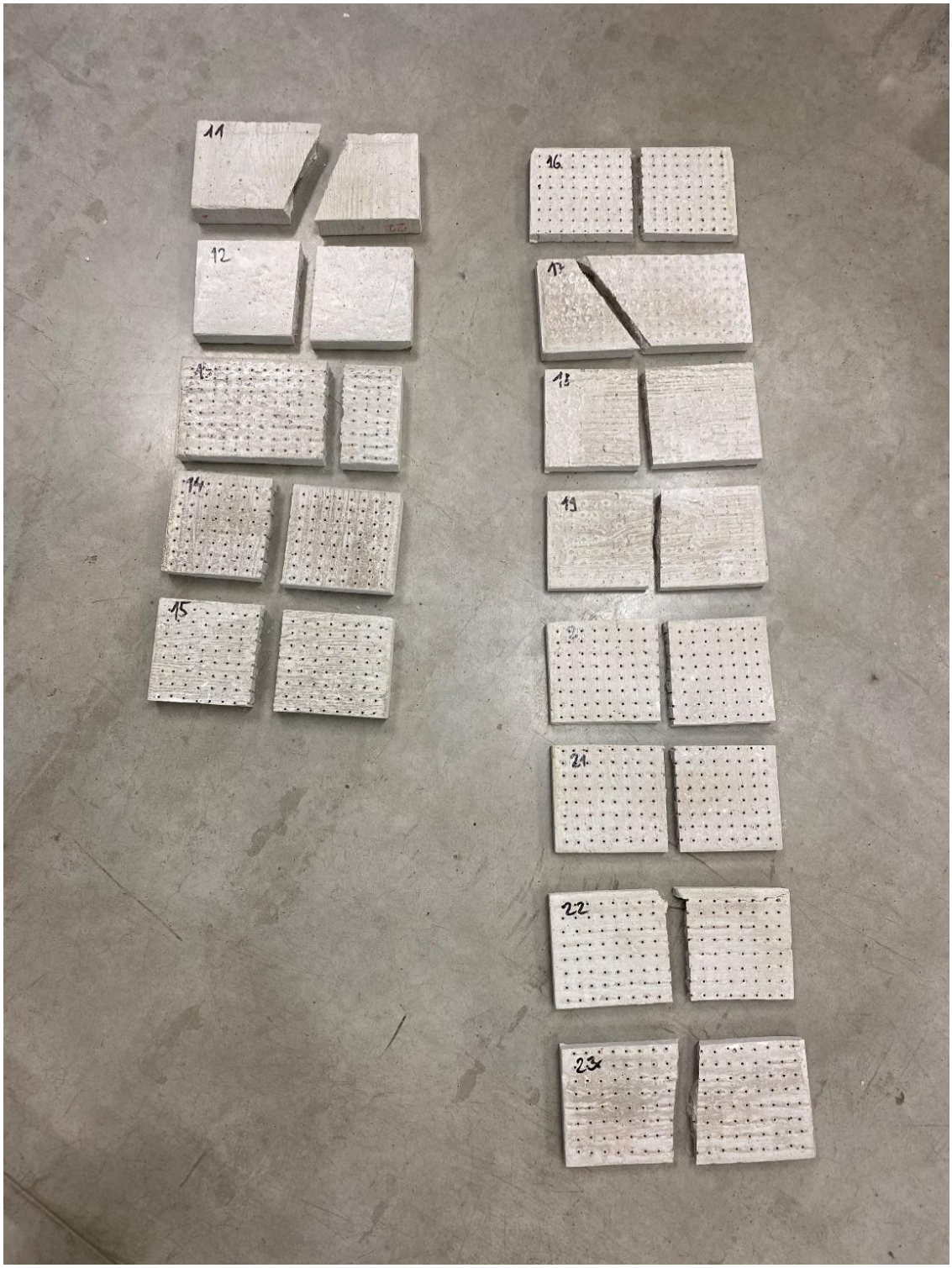

Figure 141: Broken samples after tensile flexural strength test

7.4 Comparison of properties of LTC from HPC+POF+GF and stone

Table 21: Comparison of materials and their strength

Name	Type	Volume Density (kg/m3)	Compressive strength (MPa)	Tensile flexural strength (MPa)
Travertino Romano Classico	Sedimentary	2516	76.10	12.50
Bianco Carrara C - marble	Metamorphic	2694	107.00	17.00
Giallo Veneziano - granite	Volcanic	2630	112.10	9.30
Light transmitting Concrete	POF + GF	1892	59.10	7.80
Light transmitting Concrete	Air Holes + GF	1892	57.20	8.00
High-Performance Concrete	GF	2081	66.00	8.70

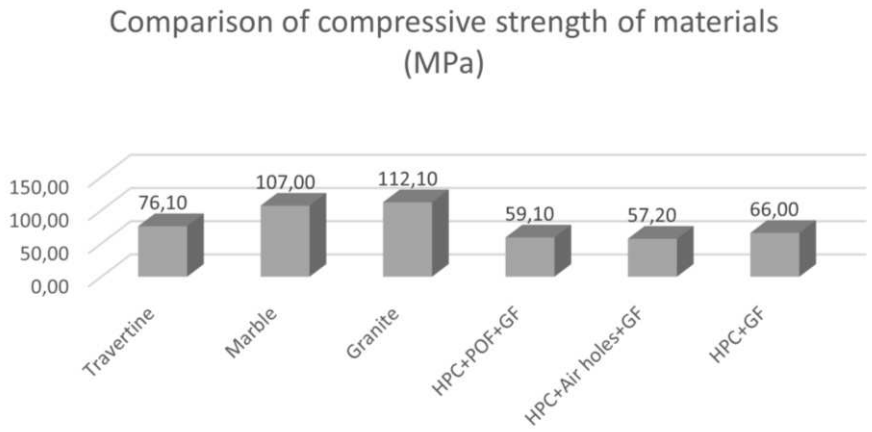

Figure 142: Comparison of compressive strength of materials

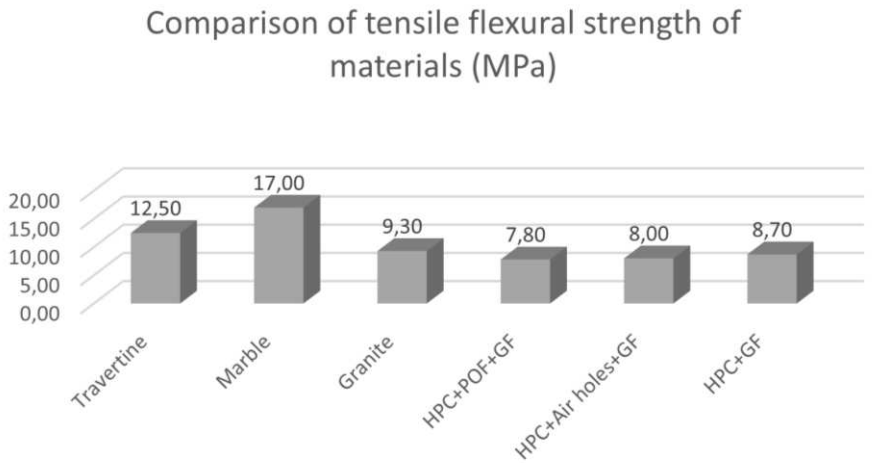

Figure 143: Comparison of tensile flexural strength of materials

8 Experimental Part - Thermal-physical properties

8.1 Measurement of thermal-physical properties

The translucent concrete sample was made of HPC concrete (High performance concrete) with an aggregate fraction of 0-4 mm. POF thicknesses 3 mm are placed in a regular grid of 15x15 mm in a sample of 250x250x20(30) mm. Emphasis was on the workability of the concrete mixture and its vibration. The mixture was poured into the prepared concrete formwork and thoroughly vibrated to get the aggregate fraction between all the optical fibers of the sample. The sample was aged in a dry environment at 22 °C ± 2 °C for 28 days. Before starting the measurement, the sample was cleaned and visually checked to see if the sample was dry, as increased environmental humidity could significantly affect the course of the measurement. Before we turn on the device for measurement, it is important to place the surface measuring probe on the tested material sample. The thickness of the layer of the measured material must be between 20-40 mm, depending on the thermal conductivity of the material, which is fulfilled in this case, since the measured sample has a thickness of 20 and 30 mm. The accuracy of thermal conductivity measurement is 0.001 W/mK. The measurement uncertainty is ± 5 % of the measured value + 0.001 W/mK. The sample measurement itself took place in three repetitions for samples with a thickness of 20 mm and 30 mm. Surface probes for hard materials were used for the measurement. The measurement took place in a dry environment at a temperature of 21°C. The measurement principle is based on the analysis of the time dependence of the temperature response on pulses of heat flow from the probe to the material. The heat flow is generated by the dissipated electrical power in the probe resistance. Its surface is thermally conductively connected to the measured material. The resistance temperature is sensed by a semiconductor sensor. The course of temperature as a function of time is at discrete sample points and these samples are fitted with regression polynomials using the mathematical method of "least squares". The regression polynomial coefficients are then used to calculate thermophysical parameters using analytical relations.

ISOMET 2114 was device used for measure illuminance. It is a luxmeter with a removable receptor head and has the following parameters listed in the Table 22 below:

Table 22: Device for measuring Thermal-physical properties - Isomet 2114

Isomet 2114	
Measuring ranges for the surface sensor IPS 1105 of device	
Thermal conductivity	/0.04-0.3 - 0.04 .. 0.3 W/m.K;
	/0.3-3.0 - 0.30 .. 3.0 W/m.K;
	/3.0-6.0 - 3.0 .. 6.0 W/m.K
Volume heat capacity	/0.04-0.3 - 4.0.104 .. 1.5.106 J/m^3.K;
	/0.3-3.0 - 1.5.106 .. 3.0.106 J/m^3.K;
	/3.0-6.0 - 1.5.106 .. 3.0.106 J/m^3.K
Temperature	-15+50°C
Measurement accuracy ranges of device Isomet 2114	
Therman conductivity	0.015 .. 0.70 W/m.K - 5 % of reading + 0.001 W/m.K
	0.70 .. 6.0 W/m.K - 10 % of reading
Volume heat capacity	4.0.104 .. 3.0.106 J/m^{3}K - 15 % of reading +1.103 J/m^3.K
Temperature	-20 +70 °C 1°C
Measurement reproducibility for the device Isomet 2114	
Thermal conductivity	3 % of reading + 0.001 W/m.K
Volume heat capacity	3 % of reading + 1.103 J/m^3.K

The thermal resistance expresses the area of the structure and the temperature difference across its surfaces that will transfer 1 Watt, or 1 Joule of energy per 1 second. It has the designation *R (m²K/W)*. Thermal resistance is the thermal insulating property of a layer of material. If the value of the thermal conductivity coefficient of the material layer is known and is constant, the surfaces perpendicular to the direction of heat flow are parallel to each other (planar layer) and a uniform heat flow flows through the layer. The thermal resistance is calculated from the relationship in the Equation 9 below:

$$R = \frac{\mathrm{d}}{\lambda} \ (m^2K/W) \tag{9}$$

R_T (m²K/W), the heat transfer resistance of the structure preventing heat exchange between environments separated by a building structure of thermal resistance *R* with adjacent boundary air layers. Where is resistance to heat transfer on the inside of the structure R_{Tsi}(m²K/W), thermal resistance *R* (m²K/W) and resistance to heat transfer on the outside of the structure R_{se} (m²K/W). The heat transfer resistance is defined by the relationship in the Equation 10 below:

$$R_T = R_{si} + R + R_{se} \ (m^2K/W) \tag{10}$$

Transmission heat loss coefficient expresses how much heat escapes through a 1 m^2 structure when the temperature difference of its surfaces is 1 K. The transmission heat loss coefficient, also referred to as $U\ (W/m^2K)$. It indicates the total steady state heat exchange between two environments separated by a building structure of thermal resistance $R\ (m^2K/W)$ with adjacent boundary air layers and includes the effect of any thermal bridges. We need to calculate its value for slabs of light-transmitting concrete so that we can use its value for the design of either exterior or interior structures. The transmission heat loss coefficient is defined by the relationship in the Equation 11 below:

$$U = \frac{1}{R_{si}+R+R_{se}} = \frac{1}{R_T}\ (W/m^2K) \tag{11}$$

The transmission heat loss coefficient $U\ (W/m^2K)$ and the heat transfer resistance R_T (m^2K/W), express the heat transfer through the whole structure. Therefore, it must include the effect of all thermal bridges and other sources of heat flux increase contained in the structure. The influence of thermal bridges in the structure can be neglected if their cumulative effect is less than 5 % of the heat transfer coefficient calculated with the influence of thermal bridges. The individual translucent slabs properties were measured with the device Isomet 2115 and are shown in the Figure 144 and Figure 145.

The transmission heat loss coefficient for a light-transmitting concrete slab was determined by measurement and calculation, and its value is:

$$\mathbf{U = 5,3787\ [W/m^2K]}$$

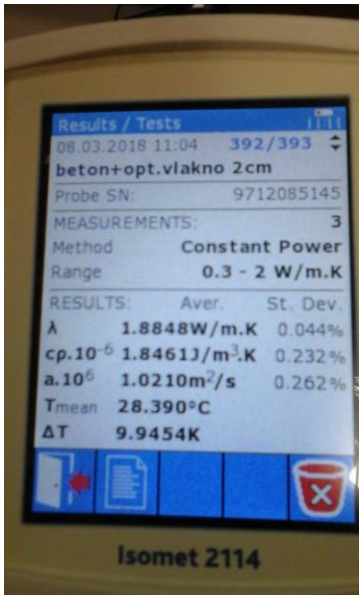

Figure 144: The results of measuring the thermal insulation parameter - Slab with optical fibers 20 mm

Figure 145: The results of measuring the thermal insulation parameter – Slab with optical fibers 30 m

9 Practical Part - Anchoring system for LTC unified slabs

It will be necessary to experimentally demonstrate sufficient resistance to the applied loads of unified slabs of light translucent concrete themselves and of the anchoring system, which must transfer the loads from its own weight, from the blocks, and at the same time resist wind loads.

For safety reasons, we can reinforce the unified façade slabs from 20 mm to 30 mm in thickness with textile mesh and impregnate them with epoxy resin. We could also reinforce them with carbon fiber, but this would be unnecessarily expensive.

Light transmission through the unified slab works with both natural and artificial light. Through the ends of the fibers, which terminate on the side surfaces, it is therefore possible to achieve light effects evenly distributed over virtually the entire side surface of the slab, which alternatively emits light. The advantage is that the light transmitting fibers are completely integrated with the cast material, while the strength of the building block is almost unaffected. Unified slabs create a homogeneous structure with the ability to carry heavy loads.

Fibers conducting electromagnetic radiation (which is light rays) could be glass optical fibers or plastic optical fibers made of transparent plastics. The thickness of the fiber can be on the order of a few tenths of a millimeter to several millimeters.

The light transmission of the building block depends on the number of fibers, but a ratio of about 1:10 is suitable. This means that one tenth of the light emitted on the surface of the slab is emitted by the fibers on the other side of the slab.

9.1 Design of fixing system for stone, artificial or unified slabs of light transmitting concrete

The anchoring system must comply with the main regulations (UNI7965, DIN18516) and European standards. The anchoring system must be designed on the basis of EIS (Etem Integrated Solution). EIS is a set of processes and standards for construction, which aims to design architectural systems with the highest level of safety, best design, and ease of application. The main support profiles, including accessories, are designed to withstand the extreme stresses caused by façade materials weighing more than 90kg/m^2.

9.2 Undercut anchors mounting system (hidden fixing)

The mounting system, which is shown in the Figure 146, was primary designed for the installation of stone cladding slabs but is the best solution for light-transmitting concrete unified slabs. We are applying all the requirements and principles for their installation. It is based on a special technique for fixing and placing stone and lightweight concrete panels respectively. The system offers various fixing options using special individual accessories.

System for fixing façade cladding panels by means of concealed fixing. This is a mechanical fixing technology via undercut or screw anchors on the back of the cladding material. The fixing of light-transmitting slabs in this type of cladding is not externally visible, it helps to create a visually aesthetic compact façade surface. The chosen flush-mounting technology of the undercut anchor allows us an easy, and economical handling with translucent slabs. The shape of the undercut anchor creates an inter-locking and stress-free fixing in the conical undercut mounting hole. Setting the anchor using undercut technology allows us to select the best structural position in the façade panel. This significantly reduces the bending moment of the panel.

This anchor allows higher failure loads compared to common systems. This cladding fixing solution provides us possibility for anchoring heavy façade panels using the carbon fibre-reinforced undercut anchors with flush installation. Slabs are fixed with a consistent drill hole depth aligned to the back of the slab. This type of fixing technology is perfect for our case. It is ideal for calibrated façade panels or for reveal angle installation. The fastening hole is drilled with an absolute anchoring depth. Flush installation of the anchor is carried out with wet diamond drill, at first cylindrical, then conical to create the undercut. Subsequently, it is necessary expanding the undercut anchor by pressing down the washer using the setting tools. Slabs for this method of attachment must be at least 20 mm thick, this also applies for stone slabs and light transmitting concrete slabs or other artificial concrete panels.

The undercut holes on the back of the facade panels should be made ideally under workshop conditions. The undercut hole is produced in one step (cylindrical drilling and undercutting). Correct installation of the undercut anchor is possible only if a precisely undercut hole exists. The hole geometry is regularly monitored with the gauge. We are assessing the insertion depth of the anchor. The hole depth is set by gauge, and all major hole dimensions can be checked efficiently with it. The undercut anchor consists of an anchor sleeve and its hex screw as we can see in the Figure 147. Hole, anchor sleeve and screw length have to be matched to the hole depth required and to the panel bracket chosen. The anchor sleeve, which is compressed in the lower end, is placed in the hole with the specified panel bracket. The screw is screwed in while exerting slight pressure on the panel bracket (to fix the anchor). The locking ratchets of the screw cuts into the panel bracket to secure it. The panel bracket forms a rigid unit with the facade anchor for this type of installation. The anchor sleeve is expanded to its original dimension by inserting the screw to a controlled depth, so that the sleeve sits snugly against the undercut section of the hole in the facade panel. After installation, the anchor sits stress-free in the undercut hole (i.e., the bracket can still be rotated with a certain amount of effort). Expansion of the anchor sleeve controlled by insertion depth requires precise matching of the screw length to the anchor and panel bracket. The screwed-in part must be flush with the anchor sleeve at the front.

This system is also used for fixing cement fiber boards (such as Silbonit, Cembonit, Eternit, Swisspearl), compact boards (such as Fundermax, Trespa, Prodema, Resopal, Kronospan), composite boards (such as bond-based materials), as well as other

façade materials that meet the requirements of national standards as well as manufacturers' regulations and recommendations.

Figure 146: Facade Cladding System – Undercut anchors (hidden fixing) [78]

Figure 147: Undercut anchor mounting system - Fischer anchor [79]

9.3 Stainless steel pins mounting system

The pin's fixing system is designed for the installation of stone, or any artificial slabs and its diagram is shown in the Figure 148. We could use it for light-permeable concrete cladding slabs too, but the best solution for our case is undercut anchors. For this mounting system is necessary thickness of the slabs from 30 mm, which excludes our 20 mm thick slabs.

The support structure is assembled from aluminum profiles. These profiles are subsequently used to form a support grid into which stainless steel pins are mounted. The system is designed for the installation of various cladding slabs with all the necessary requirements and principles. It is based on a stainless steel pins for fixation and placing cladding slabs.

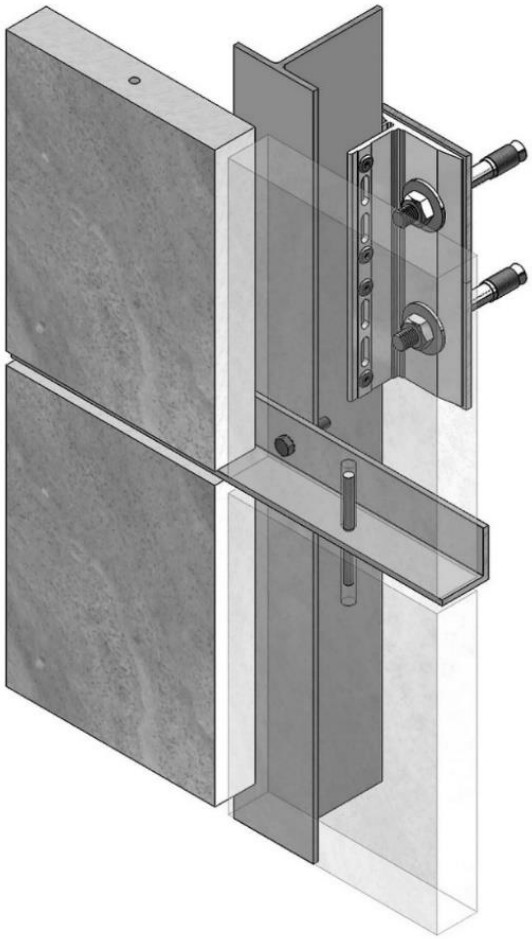

Figure 148: Facade Cladding System – Stainless steel fixing [78]

9.4 Design of a custom LTC slabs mounting system

Due to the complex assessment of the light permeable concrete slabs from their design, production, assessment of their properties and their final installation as a structure, I have proposed in the drawings shown in the Figure 149, Figure 150 and Figure 151 below the functional use and their installation on the facade, including their fixing system using undercut anchors or hidden fixing. The mounting system uses aluminum profiles and creates a sandwich structure with an air gap where an artificial light source can be placed, while the structure meets the thermal technical parameters imposed on the building envelope. The drawings show the attachment of the slabs to the face of the concrete structure and the placement of thermal insulation to prevent thermal loss. In the Figure 152, Figure 153 and Figure 154 below we can see the use of the panels in a raster façade made of aluminum profiles and thermal insulation, using LED lighting to create a light effect on the façade. During the day the structure looks like ordinary concrete and at night it looks like a simple screen.

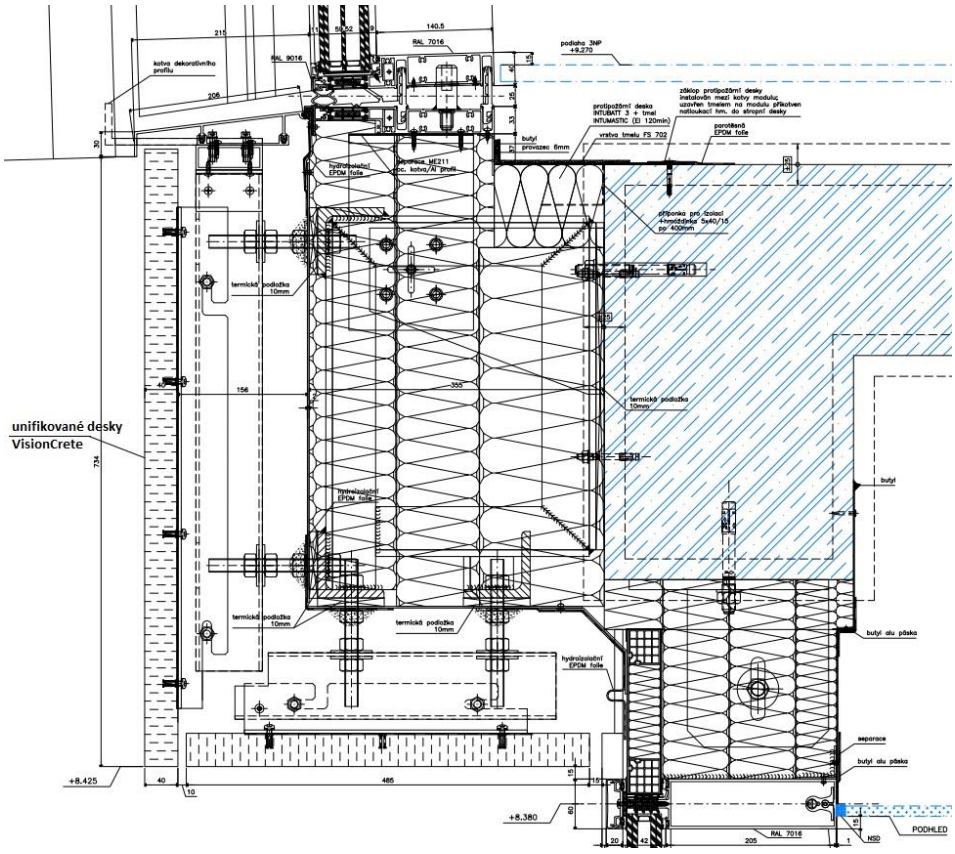

Figure 149: Detail - fixing of the slabs - section in contact with the ceiling slab

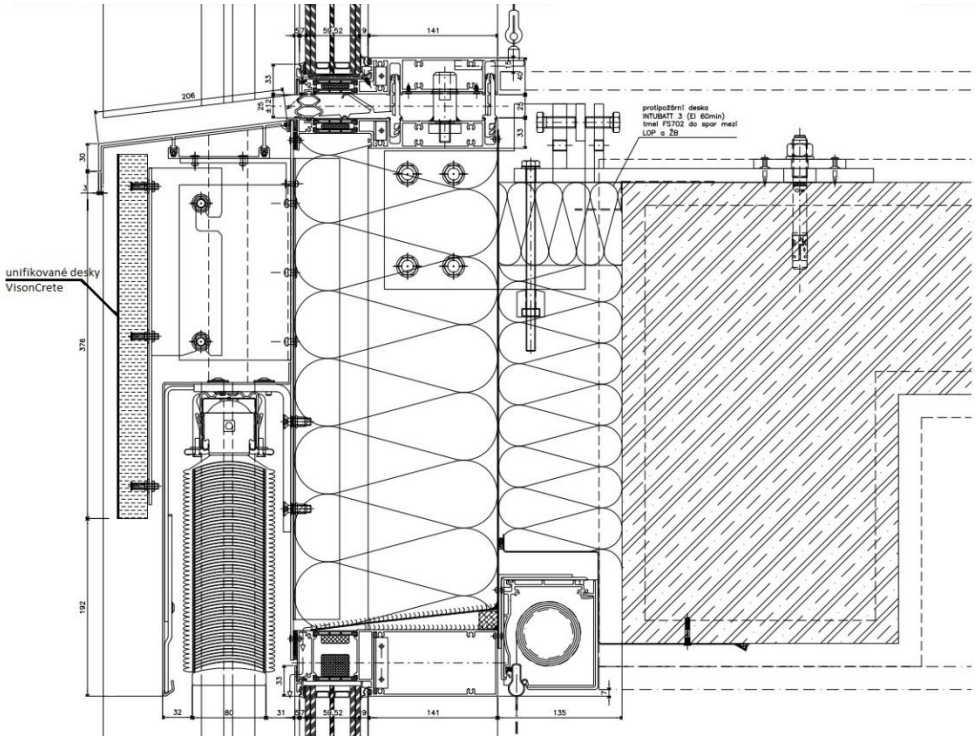

Figure 150: Detail - fixing of the slabs - section in contact with the ceiling slab

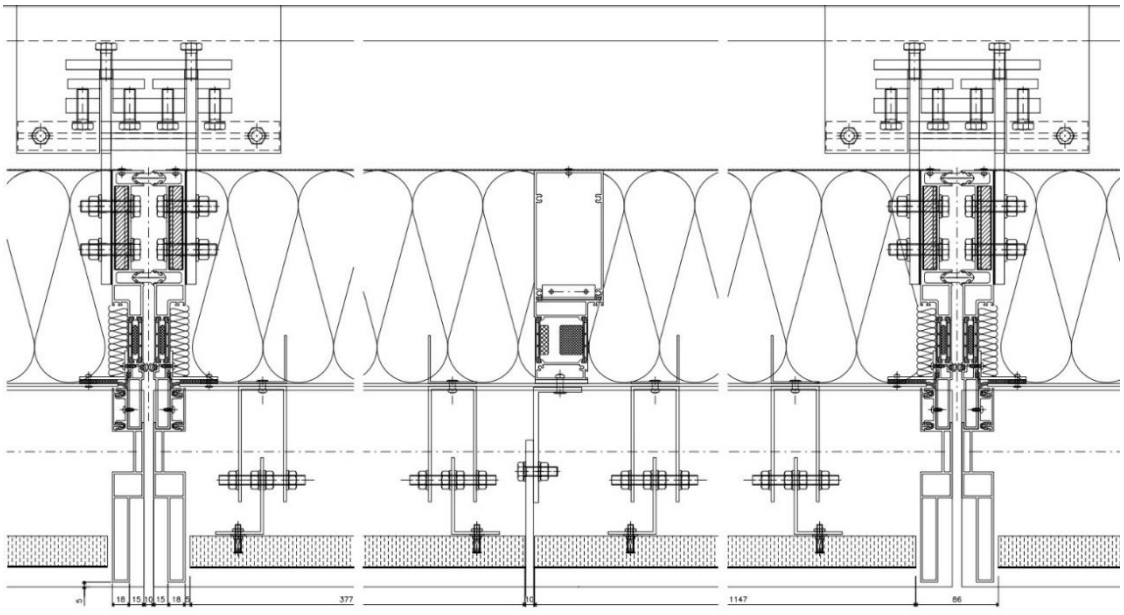

Figure 151: Detail – fixing of the slabs - ground plan

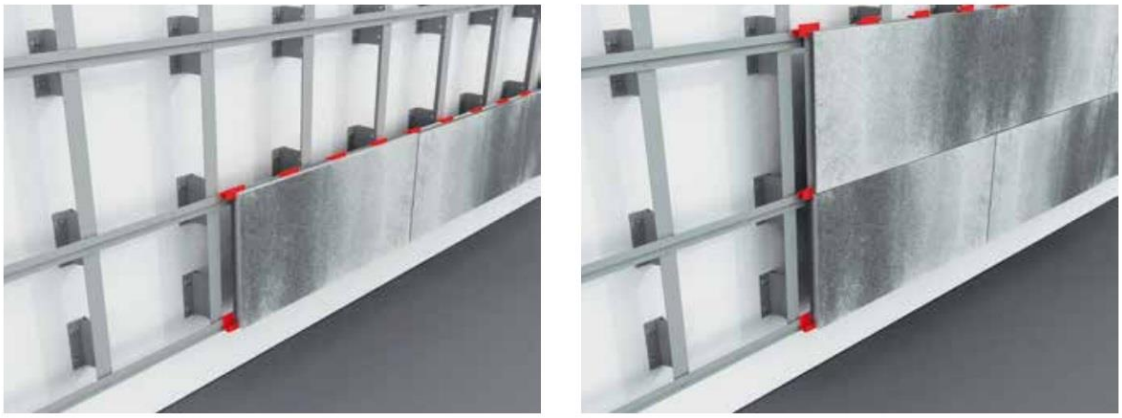

Figure 152: Example of a support grid for unified panels placed on a façade

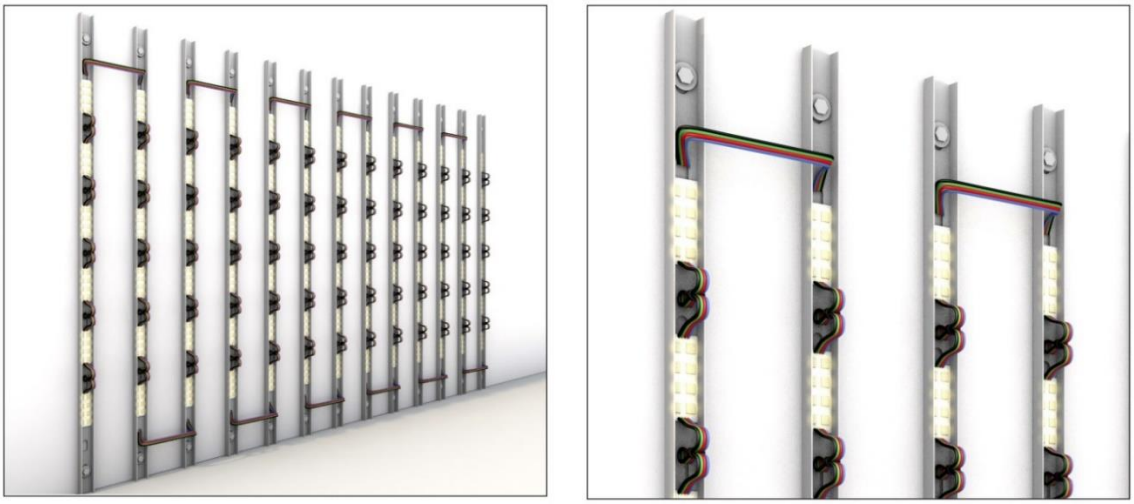

Figure 153: Possibility of illuminating the unified panels on the façade [4]

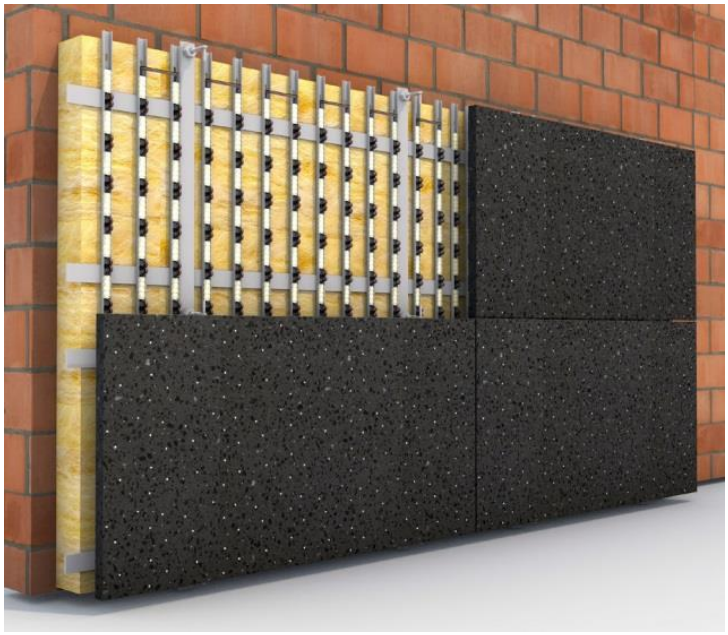

Figure 154: Example of a façade in combination with lighting and the use of uniform slabs of light-transmitting concrete [4]

10 Conclusions

The aim of this research was to determine the positive contributions made by light-transmitting concrete to the light values of building interiors, hence to the betterment of its overall environment. This in turn has a positive effect on the people who live and work in those buildings.

We carried out measurements of the penetration of daylight through structures made of light-permeable concrete and the penetration of electromagnetic radiation from a stationary source through the dividing structure between two spaces. Based on the data from the measurement, it can be said that the use of light translucent concrete does in fact support my supposition that interior light values do improve. It is well-documented that the abundance of light benefits overall human emotional and mental health and for this important reason I wanted to prove the usefulness of this material.

In the communal spaces without access to daylight, the use of a light-transmitting concrete structure will significantly improve the lighting conditions. This is an improvement in units of percent, but in rooms where the level of daylight is at the minimum limit, or in rooms without access to daylight, these are non-negligible values. It can be further determined that the thickness of the walls, partitions, ceiling, etc. does not have a negative effect on the transmission of light information through the optical fibers placed in the light-permeable concrete structure. Regarding the comparison of light penetration through constructions with optical fibers compared to air penetrations, it was found that the daylight factor improved its values 10-fold. The measured values of the daylight factor through the slabs with air holes are on average around 0.03%, in comparison to the values through the slabs with optical fibers are on average around 0.39%. So, if we build the perimeter walls of the rooms from light-permeable concrete we get half the standard values of the daylight factor, which is great for improving the interior space in relation to lighting. This could help indoor spaces in inner city areas in terms of decreasing building setbacks. Structures made of light-transmitting concrete also have a secondary benefit, in the form of their aesthetic contribution to interior design.

In conclusion it is submitted that it would be wise to consider the use of light transmitting concrete in construction to optimize its ability to contribute light information from both the exterior, and between the interior spaces of buildings. Improving the amount of interior lighting, even if the increase is negligible compared to window openings, skylights, etc., has a positive effect on people, both psychologically and physically. In an experimental measurement of the light transmission from an artificial source from one room to another through a vertical partitioning structure, it was found that on average 5% of the light emitted from an artificial source pass through a structure made of light-permeable concrete. However, it is dependent upon the position of the artificial source relative to the optical fibers and the angle of the incident light to the end of the optical fiber. When the angle of incidence light is greater, the less light passes through the structure. The

light transmission decreases proportionally from the center of the circle created by the artificial light source, due to the light scattering on the slab surface. This affect plus the angle of incidence light rays' results in minimal light transmission at the corners of the slab. The optical fibers that are placed perpendicular to the artificial light source transmit the highest amount of light through the slabs.

The reflection factor of my samples of high-performance light transmitting concrete with rough surfaces is around 0.5 and for smooth surfaces around 0.4. For comparison, the reflection factor of the black boards used to create the down-scaled model of rooms is around 0.01, which made them suitable to use for the model as they do not negatively affect the measured values.

Regarding the placement of optical fibers in the concrete mixture, the laboratory results on the samples showed only a minimal deterioration of the compressive and tensile flexural strength. The experiment measured compressive strengths of the concrete, which were in the range of 57.2 MPa for 250x250x20 mm for high-performance light-transmitting concrete slabs, and the compressive strength of the 250x250x30 mm slabs with measured values around 65.9 MPa. For the use of the slabs as a cladding material on the interior structure or on the facade of a building, it was important to measure their tensile flexural strength. Light transmitting concrete slabs measured values of tensile flexural strength are in the range from 7.64 MPa for 20 mm thick slabs to 7.78 MPa for 30 mm thick slabs. By comparison the compressive strength values of typically used cladding materials of stone such as granite and travertine are 112.1 MPa and 76.1 MPa respectively. The tensile flexural strength values are 12.5 MPa for travertine and 9.3 MPa for granite. Based on this we can conclude that their compressive strength values are similar to those of travertine and their tensile flexural strength values are similar to those of granite. It follows that, I can use the regulation requirements for stone cladding material and implement them for light transmitting concrete slabs. Likewise, I am able to use the mounting system, including anchors, that are used for stone cladding. Based on my results I can conclude that the compressive strength values of light transmitting concrete are similar to those of granite. Finally, I can conclude that the use of light-transmitting concrete structures, combining both optical and glass fibers together, will improve the lighting and thermal technical conditions of a building without significantly reducing the strength of the structure itself.

Some questions arose from my research that could be answered in follow-up research works. The strength results of the LTC slabs are satisfactory, but it would be suitable to increase the strength when using the slabs on the building envelope. Further research could look at more complex reinforcement, for example with textile reinforcement (TRC), or other alternative reinforcement for thin-walled structures combined with optical fibers grid. Other work could investigate and resolve the issue of the heat transfer coefficient, which does not meet the regulations. There could be an examination and designing a sandwich slab structure and measuring its properties. Lastly, follow-up research could address the issue of prefabrication and design of a complex element such as a composite corner, not only rectangular but also at different shapes. Its use would be very useful in construction practice.

References

[1] Paul S., & Dutta A., (2013). Translucent Concrete, *International Journal of Scientific and Research Publications 10*, 1-10, https://www.ijsrp.org/research-paper-1013.php?rp=P221895

[2] Valambhiya H. B., Tuvar T. J., & Rayjada P. V. (2017). History and case study on light transmitting concrete, *Journal of Emerging Technology and Innovative Research 4*, https://www.jetir.org/papers/JETIR1701004.pdf

[3] Litracon Bft., Hungary (2004), http://www.litracon.hu/

[4] Lucem GmbH, Germany (2007), http://www.lucem.de/

[5] Luccon Lichtbeton GmbH (A brand of Lucem GmbH), Austria (2006), http://www.luccon.com/

[6] Graveli s.r.o., LiCrete, Czech Republic (2012), https://www.gravelli.com/en/our-concrete/

[7] Nam, H. P., Hai, N. M., Van Huong, N., Quang, P. D., Tuan, N. D., Hai, D. V., Binh, N. T., & Vy, T. Q. (2023). Experimental study on 80 MPa grade light transmitting concrete with high content of optical fibers and eco-friendly raw materials. *Case Studies in Construction Materials*, *18*. https://doi.org/10.1016/j.cscm.2022.e01810

[8] Huang B., Mosalam K. M., & Chiew S. P. (2013). Anidolic Daylight Concentrator of Structural Translucent Concrete Envelope, *Berkeley Education Alliance for Research in Singapore 2013*, https://sinberbest.berkeley.edu/sites/default/files/Anilodic+Daylight+Concentrator+of+Structural+Translucent+Concrete+Envelope__+Baofeng+Huang.pdf

[9] Henriques, T. dos S., Dal Molin, D. C., & Masuero, Â. B. (2020). Optical fibers in cementitious composites (LTCM): Analysis and discussion of their influence when randomly arranged. *Construction and Building Materials*, *244*. https://doi.org/10.1016/j.conbuildmat.2020.118406

[10] Sawant A. B., Jugdar R. V., & Sawant S. G. (2014). Light transmitting concrete by using optical fiber, *Light Transmitting Concrete by using Optical Fiber 3*, 23–28, https://www.ijies.org/wp-content/uploads/papers/v3i1/A0558123114.pdf

[11] Gawatre D. W., Giri S. D., & Bande B. B. (2016). Transparent concrete as an eco-friendly material for building, *International Journal of Engineering Science Invention 5*, 55–62, https://www.ijesi.org/papers/Vol(5)3/Version-2/I050302055062.pdf

[12] Navabi, D., Javidruzi, M., Hafezi, M. R., & Mosavi, A. (2021). The high-performance light transmitting concrete and experimental analysis of using polymethylmethacrylate optical fibers in it. *Journal of Building Engineering*, *38*. https://doi.org/10.1016/j.jobe.2020.102076

[13] Li, Y., Li, J., Wan, Y., & Xu, Z. (2015). Experimental study of light transmitting cement-based material (LTCM). *Construction and Building Materials*, *96*, 319-325. https://doi.org/10.1016/j.conbuildmat.2015.08.055

[14] Dvořáček P. (2005). New Possibilities in Building Industry and Architecture, *Beton 5*, 38-41.

[15] Altlomate, A., Alatshan, F., Mashiri, F., & Jadan, M. (2017). Experimental study of light-transmitting concrete. *International Journal of Sustainable Building Technology and Urban Development*, *7*(3-4), 133-139. https://doi.org/10.1080/2093761X.2016.1237396

[16] Salih S. A., Joni H. H., & Mohamed S. A. (2014). Effect of Plastic Optical Fiber on Some Properties of Translucent Concrete, *Engineering and Technology Journal, 32*, 2846-2861, https://www.researchgate.net/publication/301697305

[17] Li, Y., Zhang, J., Cao, Y., Hu, Q., & Guo, X. (2021). Design and evaluation of light-transmitting concrete (LTC) using waste tempered glass: A novel concrete for future photovoltaic road. *Construction and Building Materials*, *280*. https://doi.org/10.1016/j.conbuildmat.2021.122551

[18] Zielińska, M., & Ciesielski, A. (2017). Analysis of Transparent Concrete as an Innovative Material Used in Civil Engineering. *IOP Conference Series: Materials Science and Engineering*, *245*. https://doi.org/10.1088/1757-899X/245/2/022071

[19] Kim, B. (2017). Light Transmitting Lightweight Concrete with Transparent Plastic Bar. *The Open Civil Engineering Journal*, *11*(1), 615-626. https://doi.org/10.2174/1874149501711010615

[20] Henriques, T. dos S., Dal Molin, D. C., & Masuero, Â. B. (2018). Study of the influence of sorted polymeric optical fibers (POFs) in samples of a light-transmitting cement-based material (LTCM). *Construction and Building Materials*, *161*, 305-315. https://doi.org/10.1016/j.conbuildmat.2017.11.137

[21] Tuaum, A., Shitote, S., Oyawa, W., & Biedebrhan, M. (2019). Structural Performance of Translucent Concrete Façade Panels. *Advances in Civil Engineering*, *2019*, 1-10. https://doi.org/10.1155/2019/4604132

[22] Italcementi S.p.A., i.light, Italy (1864), https://www.italcementi.it/it/ilight

[23] Mainini, A. G., Poli, T., Zinzi, M., & Cangiano, S. (2012). Spectral Light Transmission Measure and Radiance Model Validation of an innovative Transparent Concrete Panel for Façades. *Energy Procedia*, *30*, 1184-1194. https://doi.org/10.1016/j.egypro.2012.11.131

[24] Juan, S., & Zhi, Z. (2019). Preparation and Study of Resin Translucent Concrete Products. *Advances in Civil Engineering*, *2019*, 1-12. https://doi.org/10.1155/2019/8196967

[25] https://lucem.com/projects/

[26] https://www.gravelli.com/cs/projekty/?mgc__41=104/svtlopropustn-beton

[27] http://www.litracon.hu/en/references/

[28] https://www.heidelbergmaterials.com/en/italian-pavilion-shanghai

[29] Li Y., Xu Z., Gu Z., Bao Z. (2011). Preparation of Light Transmitting Cement-Based Material with Optical Fiber Embedded by the Means of Parallel Arrange. *Advanced Materials Research, 391-392*, 677-682. https://doi.org/10.4028/www.scientific.net/AMR.391-392.677

[30] https://prodisplay.com/lcd-led-screens/large-format-led/indoor-led-screen/

[31] https://botland.store/led-strings-chains-matrices/6183-elastic-matrix-16x16-256-led-rgb-ws2812b-5904422374945.html

[32] https://www.3cinno.com/transparent-led-screen-glass-media-facade/

[33] https://www.traiva-shop.cz/bezpecnostni-tabulky

[34] Sasidharan J., Naga Sai Teja A., Sakthivel K., Manickavel D., & Mohan S. K. (2017). Translucent Concrete, *International Journal of Engineering Research and Technology 6*, 782-786, https://www.ijert.org/research/translucent-concrete-IJERTV6IS040596.pdf

[35] Mahto S., & Kujure J. (2017). Light Weight Translucent Concrete, *International Journal of Advances in Mechanical and Civil Engineering 3*, 112-115, https://www.iraj.in/journal/journal_file/journal_pdf/13-373-1503725247112-115.pdf

[36] Arias-Erazo, J., Villaquirán-Caicedo, M. A., & Goyes, C. E. (2021). Ecological light transmiting concrete made from glass waste and acrylic sheets. *Construction and Building Materials*, *304*. https://doi.org/10.1016/j.conbuildmat.2021.124644

[37] Pagliolico, S. L., Verso, V. R. M. L., Torta, A., Giraud, M., Canonico, F., & Ligi, L. (2015). A Preliminary Study on Light Transmittance Properties of Translucent Concrete Panels with Coarse Waste Glass Inclusions. *Energy Procedia*, *78*, 1811-1816. https://doi.org/10.1016/j.egypro.2015.11.317

[38] Hu, H., Zha, X., Li, Z., & Lv, R. (2022). Preparation and performance study of solar pavement panel based on transparent Resin-Concrete. *Sustainable Energy Technologies and Assessments*, *52*. https://doi.org/10.1016/j.seta.2022.102169

[39] Sklocement Beneš s.r.o., Czech Republic (1991), https://www.sklocement.cz/sklenena-vlakna-cem-fil/anti-crak-hp/

[40] Spiesz, P., Rouvas, S., & Brouwers, H. J. H. (2016). Utilization of waste glass in translucent and photocatalytic concrete. *Construction and Building Materials*, *128*, 436-448. https://doi.org/10.1016/j.conbuildmat.2016.10.063

[41] https://www.serraciments.com/en/product/hp-anti-crack-fibreglass-12-mm/

[42] Wikipedia (2001), Optical Fiber, https://en.wikipedia.org/wiki/Optical_fiber

[43] Jiao, P., Huang, Y., Fu, Y., Wang, Y., Wang, J., Du, Y., Zhang, J., & Jia, J. (2022). Design of optical fiber path for tapered optical fiber array and improvement of light transmission uniformity. *Optical Fiber Technology*, *74*. https://doi.org/10.1016/j.yofte.2022.103149

[44] Abdulmajeed, N. S., & Said, S. H. (2022). Compressive characteristics of resin translucent cement mortar (RTCM) used in the external walls to rationalize the energy spent inside the building. *Case Studies in Construction Materials*, *17*. https://doi.org/10.1016/j.cscm.2022.e01687

[45] Li, Y., Li, J., & Guo, H. (2015). Preparation and study of light transmitting properties of sulfoaluminate cement-based materials. *Materials & Design*, *83*, 185-192. https://doi.org/10.1016/j.matdes.2015.06.021

[46] Ayesta, I., Azkune, M., Illarramendi, M. A., Arrospide, E., Zubia, J., & Durana, G. (2023). Fabrication and characterization of active polymer optical fibers with a ring-doped structure. *Optical Fiber Technology*, *75*. https://doi.org/10.1016/j.yofte.2022.103209

[47] Subathra, P., & Sangeetha, S. P. (2021). Study on pellucid concrete incorporating optical fibers–a review. *Materials Today: Proceedings*, *45*, 6682-6686. https://doi.org/10.1016/j.matpr.2020.12.110

[48] Luhar, I., Luhar, S., Savva, P., Theodosiou, A., Petrou, M., & Nicolaides, D. (2021). Light Transmitting Concrete: A Review. *Buildings*, *11*(10). https://doi.org/10.3390/buildings11100480

[49] Kashiyani B. K., Raina V., Pitroda J., & Shah B. K. (2013). A study of Transparent Concrete: A Novel Architectural Material to Explore Construction Sector, *International Journal of Engineering and Innovative Technology 8*, 83-87, https://www.ijeit.com/vol%202/Issue%208/IJEIT1412201302_18.pdf

[50] https://shiningfiber.com/types-of-optical-fiber/

[51] Mleziva, J., Šňupárek, J. (2000). Polymery, Sobotáles, ISBN: 80-85920-72-7

[52] Mleziva, J., Kálal, J. (1986). Základy makromolekulární chemie, *SNTL/Alfa*, ISBN 04-621-86

[53] Kinzlink, J. (2005). Technologie chemických látek, Vutium, ISBN 80-214-2913-5

[54] https://www.mekaglobal.com/en/blog/case-study-alkali-silica-reaction-concrete-cancer

[55] Wikipedia (2001), Air mass, https://en.wikipedia.org/wiki/Air_mass_(solar_energy)

[56] Ahuja, A., Mosalam, K. M., & Zohdi, T. I. (2015). Computational Modeling of Translucent Concrete Panels. *Journal of Architectural Engineering*, *21*(2), B4014008-. https://doi.org/10.1061/(ASCE)AE.1943-5568.0000167

[57] Li Y., Xu Z. Y., Gu Z. W., & Bao Z. Z. (2012). Research on the light transmitting cement mortar, *Advanced Materials Research 450-451*, 397–401, https://citeseerx.ist.psu.edu/document?repid=rep1&type=pdf&doi=f8e23e3abd0b2f93967470a6fd98f8c462aab425

[58] Chiew, S. M., Ibrahim, I. S., Mohd Ariffin, M. A., Lee, H. -S., & Singh, J. K. (2021). Development and properties of light-transmitting concrete (LTC) – A review. *Journal of Cleaner Production*, *284*. https://doi.org/10.1016/j.jclepro.2020.124780

[59] Shenoy, A., Nayak, G., Tantri, A., & Shetty, K. K. (2022). Thermal transmission characteristics of plastic optical fibre embedded light transmitting concrete. *Materials Today: Proceedings*, *65*, 1759-1773. https://doi.org/10.1016/j.matpr.2022.04.798

[60] Ahuja, A., & Mosalam, K. M. (2017). Evaluating energy consumption saving from translucent concrete building envelope. *Energy and Buildings*, *153*, 448-460. https://doi.org/10.1016/j.enbuild.2017.06.062

[61] Su, X., Zhang, L., Liu, Z., Luo, Y., Lian, J., & Liang, P. (2020). Daylighting performance simulation and analysis of translucent concrete building envelopes. *Renewable Energy*, *154*, 754-766. https://doi.org/10.1016/j.renene.2020.03.041

[62] Su, X., Zhang, L., Luo, Y., & Liu, Z. (2022). An energy analysis of translucent concrete embedded with inclined optical fibers. *Energy and Buildings*, *273*. https://doi.org/10.1016/j.enbuild.2022.112409

[63] Huang, B., Wang, Y., Lu, W., & Cheng, M. (2022). Fabrication and energy efficiency of translucent concrete panel for building envelope. *Energy*, *248*. https://doi.org/10.1016/j.energy.2022.123635

[64] Weisová T. (2018). Analýza denního osvětlení v učebnách základních škol – diploma thesis, *Czech Technical University*, https://dspace.cvut.cz/bitstream/handle/10467/78057/F1-DP-2018-Weisova-Tereza-DP_Weisova_2018.pdf?sequence=-1&isAllowed=y

[65] Vychytil, J., & Kaňka, J. (2016). *Stavební světelná technika: přednášky*. České vysoké učení technické. ISBN: 978-80-01-06060-5.

[66] ČSN 730580-2: Denní osvětlení budov: Část 2: Denní osvětlení obytných budov, Úřad pro techniku normalizaci, metrologii a státní zkušebnictví (UNMZ), 2007.

[67] Chiew, S. M., Ibrahim, I. S., Sarbini, N. N., Mohd Ariffin, M. A., Lee, H. S., & Singh, J. K. (2021). Development of light-transmitting concrete – A review. *Materials Today: Proceedings*, *39*, 1046-1050. https://doi.org/10.1016/j.matpr.2020.05.166

[68] Su, X., Zhang, L., Liu, Z., Luo, Y., Liang, P., & Lian, J. (2022). An optical and thermal analysis of translucent concrete considering its dynamic transmittance. *Journal of Cleaner Production*, *364*. https://doi.org/10.1016/j.jclepro.2022.132588

[69] Mei Chiew, S., Syahrizal Ibrahim, I., Azreen Mohd Ariffin, M., Lee, H. -S., & Kumar Singh, J. (2022). Evaluation of light transmittance performance of light-transmitting concrete with optical fibre. *Construction and Building Materials*, *351*. https://doi.org/10.1016/j.conbuildmat.2022.128949

[70] Palanisamy, C., Krishnaswami, N., kumar Velusamy, S., Krishnamurthy, H., kumaar Velmurugan, H., & Udhayakumar, H. (2022). Transparent concrete by using optical fibre. *Materials Today: Proceedings*, *65*, 1774-1778. https://doi.org/10.1016/j.matpr.2022.04.799

[71] Raut Z. P., Dhanke S. S., Lanjewar V. R., Mahadule A., & Kolte M. (2020). Light Transfer through Concrete by using Optical Fiber, *International Journal of Innovative Research in Technology 7*, 305-309, https://ijirt.org/master/publishedpaper/IJIRT150070__PAPER.pdf

[72] ČSN EN 12390-3: Zkoušení ztvrdlého betonu: Část 3: Pevnost v tlaku zkušebních těles, Úřad pro techniku normalizaci, metrologii a statni zkušebnictví (UNMZ), 2009.

[73] ČSN EN 12390-5: Zkoušení ztvrdlého betonu: Část 5: Stanovení pevnosti v tahu ohybem zkušebních těles, Úřad pro techniku normalizaci, metrologii a státní zkušebnictví (UNMZ), 2009.

[74] Said, S. H. (2020). State-of-the-art developments in light transmitting concrete. *Materials Today: Proceedings*, *33*, 1967-1973. https://doi.org/10.1016/j.matpr.2020.06.128

[75] Tahwia, A. M., Abdel-Raheem, A., Abdel-Aziz, N., & Amin, M. (2021). Light transmittance performance of sustainable translucent self-compacting concrete. *Journal of Building Engineering*, *38*. https://doi.org/10.1016/j.jobe.2021.102178

[76] Tahwia, A. M., Abdelaziz, N., Samy, M., & Amin, M. (2022). Mechanical and light transmittance properties of high-performance translucent concrete. *Case Studies in Construction Materials*, *17*. https://doi.org/10.1016/j.cscm.2022.e01260

[77] https://www.brachot.com/

[78] https://www.iltegro.cz/forte-uchyceni-kamennych-desek

[79] https://www.fischer-international.com/en/products/facade-systems/zykon-panel-anchors/zykon-panel-anchor-fzp-ii

[80] ČSN 730580-1: Denní osvětlení budov: Část 1: Základní požadavky, Úřad pro techniku normalizaci, metrologii a státní zkušebnictví (UNMZ), 2007.

[81] ČSN 730580-1 ZMĚNA Z1: Denní osvětlení budov: Část 1: Základní požadavky, Úřad pro techniku normalizaci, metrologii a státní zkušebnictví (UNMZ), 2011.

[82] ČSN 730580-1 ZMĚNA Z2: Denní osvětlení budov: Část 1: Základní požadavky, Úřad pro techniku normalizaci, metrologii a státní zkušebnictví (UNMZ), 2017.

List of Figures

List of Tables